SPIN FLUCTUATIONS IN ELIASHBERG THEORY

By

Peter J. Williams, B.Sc., M.Sc.

A Thesis

Submitted to the School of Graduate Studies

in Partial Fulfilment of the Requirements

for the Degree

Doctor of Philosophy

McMaster University

July 1990

SPIN FLUCTUATIONS IN ELIASHBERG THEORY

DOCTOR OF PHILOSOPHY (1990) McMASTER UNIVERSITY
(PHYSICS) Hamilton, Ontario

TITLE: Spin Fluctuations in Eliashberg Theory

AUTHOR: Peter J. Williams, B.Sc. (McMaster University)
M.Sc. (McMaster University)

SUPERVISOR: Dr. J.P. Carbotte

NUMBER OF PAGES: vi, 148

ABSTRACT

In this thesis, we have studied the properties of a superconductor in which there are two competing dynamical interactions. One of the interactions promotes the pairing, while the other is pair breaking. We have studied the model in the framework of Eliashberg theory for the complete range of coupling strengths, from weak coupling (BCS) to the extreme strong coupling limit. We find that there are distinctive signatures in the specific heat results that are not found in a model with no dynamical pair breaking.

The work was motivated by the fact that the parent compounds of most of the high-T_c superconductors are antiferromagnetic insulators. In the superconducting state, spin fluctuations have been observed, at least in LaSrCuO and YBaCuO. For an s-wave superconductor, spin fluctuations are pair breaking. The observed thermodynamic data are consistent with the model that we have studied.

ACKNOWLEDGEMENTS

I acknowledge financial support from the Natural Sciences and Engineering Research Council (NSERC) of Canada, the Harry Lyman Hooker, Desmond G. Burns, and Clifton W. Sherman scholarships.

The administrative staff of the physics department, Marg Wilby, Jackie Collin, Jane Hammingh, and Wendy Malarek have all been extremely helpful and kind. I also thank Jane as my squash partner.

I would like to thank all of the physics faculty at McMaster for the stimulation that they have provided in the form of courses, seminars, and discussion. I would also like to thank Dr. D.A. Goodings and Dr. C.V. Stager for stimulating teaching assistantship work.

My fellow students, post-doctoral fellows, and visitors have all contributed a great deal to my work and my stay at McMaster. Frank Marsiglio was extremely helpful in all aspects. Elisabeth Nicol has assisted in many ways. Her keen eye as a proof reader, and her invaluable help after I left McMaster are greatly appreciated. Ewald Schachinger has provided invaluable assistance with computing. John Benjamins has kept the computer system running, and has also provided a great amount of technical assistance. I have enjoyed stimulating discussions with Micheal Prohammer. Abdalla H. Abdalla has provided stimulation, both intellectualy and socially, and enriched my stay immensely.

All of the work in this thesis has been done in collaboration with Jules Carbotte. I could not ask for a better supervisor, and I thank him deeply.

Acknowledgements

My family and friends have all been supportive of my endevours, and I thank them.

Alex Peace has been infinitely patient, loving, kind and supportive. Thank you.

Table of Contents

Chapter 1

Introduction

1.1 GENERAL BACKGROUND

Superconductivity was first observed in Hg by K. Onnes[1] in 1911. Since the initial discovery, many more materials have been observed to superconduct. Recently, great excitement has been generated by the discovery of superconductivity in various metallic oxides, with transition temperatures of the order of 100K [2].

Superconductors exhibit some beautiful behavior. They are named for the property that below their transition temperature, T_c, they have no DC electrical resistance. Their AC electrical resistance is zero for frequencies below a certain threshold, at which point it becomes finite. This behavior is shown in Figures 1.1 and 1.2. Figure 1.1 shows the temperature dependence of the DC resistivity of a high T_c material. There is a sudden drop of the

resistivity to zero, with an onset of about 95 K. Figure 1.2 shows the frequency dependence of the optical conductivity of a typical normal metal and a superconductor.

The optical results shown were calculated using Drude theory for the normal state, and the theory of Mattis and Bardeen[4] for the superconducting state. Optical conductivity is typically measured using far-infrared techniques.

Superconductors also exhibit some unusual magnetic properties, which were discovered in 1933 by Meissner and Ochsenfeld[5]. As a superconductor is cooled through T_c, it begins to expel magnetic flux from itself. Whether the flux exclusion is complete or not will depend upon the details of the individual material. A type I material will expel the flux completely, and will be perfectly diamagnetic for applied fields less than the thermodynamic critical field, $H_c(T)$. For applied fields in excess of $H_c(T)$, the material reverts to the normal state.

A type II superconductor is perfectly diagmagnetic for applied fields less than $H_{c1}(T)$, the lower critical field. As the applied field is increased beyond this value, flux begins to penetrate the sample. When the applied field reaches $H_{c2}(T)$, the upper critical field, the material goes into the normal state. Figure 1.3 show magnetization curves for type I and type II superconductors. It is important to note that this magnetic behavior is not simply a consequence of the zero electrical resistance. A material with zero electrical resistance will freeze in whatever flux was present when it makes the transition to the zero resistance state. It will not expel flux.

Measurement of $H_c(T)$, the thermodynamic critical field, gives one the free energy difference between the normal and superconducting states

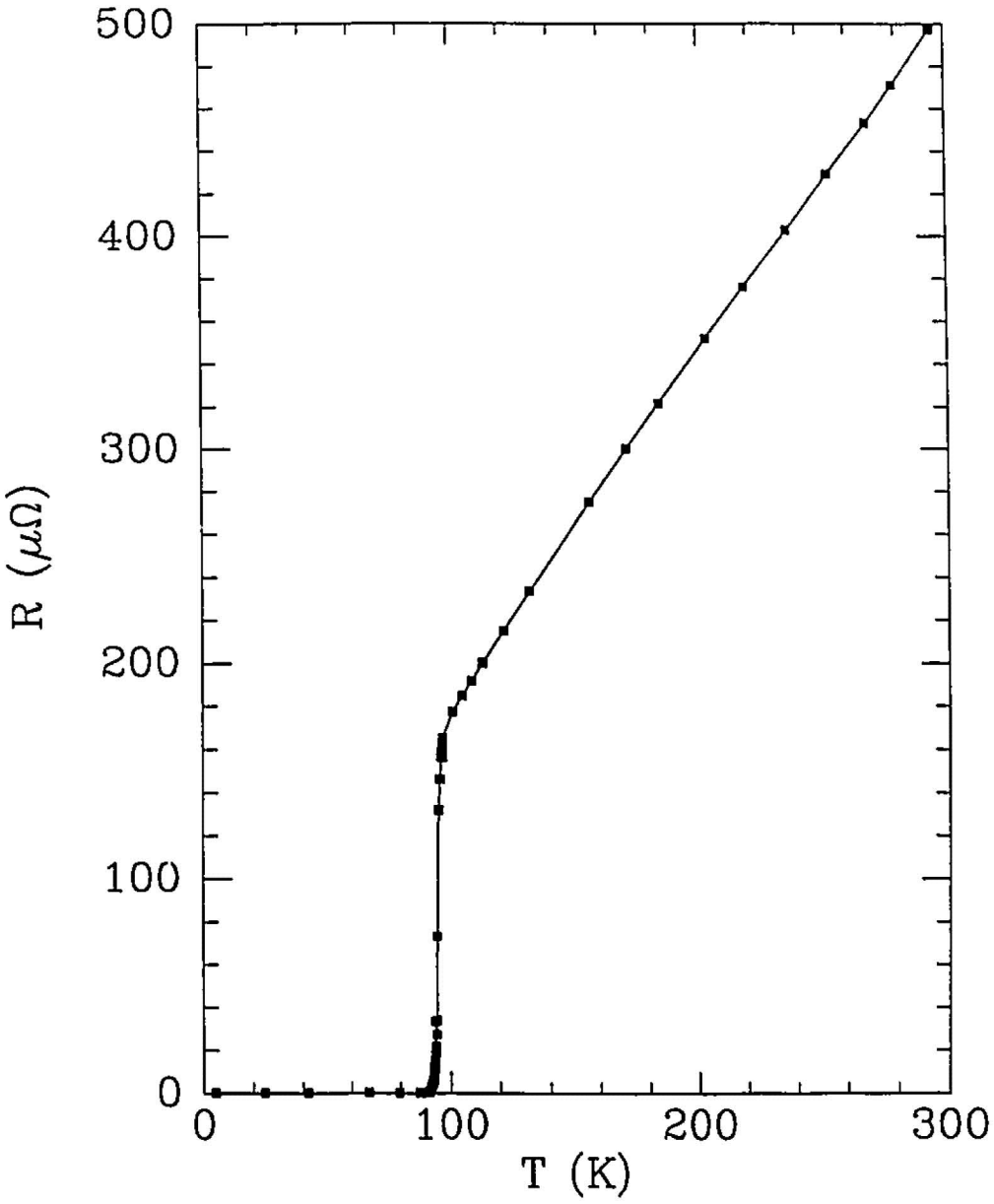

Figure 1.1-Resistance versus temperature for a sample of $YBa_2Cu_3O_{6.8}$[3]. Note the dramatic drop in resistance, starting at approximately 95 K. The zero resistance state is fully developed at approximately 91 K.

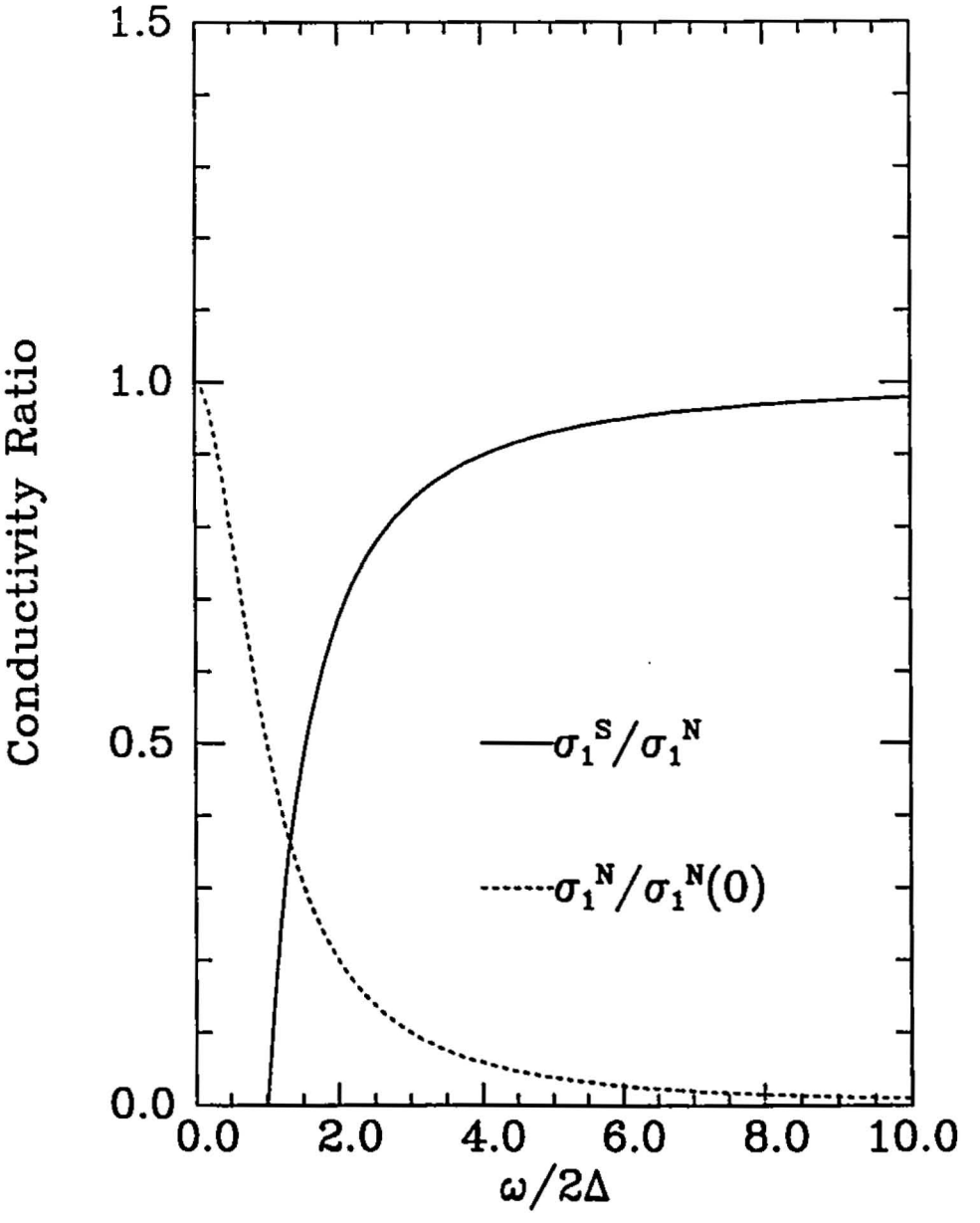

Figure 1.2-Real part of the optical conductivity of a superconductor and a Drude metal. Note the zero optical conductivity for the superconductor up to twice the gap edge. There is a delta function at the origin which gives the zero DC resistivity. The superconducting conductivity was calculated using the results of Mattis and Bardeen[4].

through the relation

$$F_N - F_S \equiv \Delta F = \frac{H_c^2(T)}{8\pi}, \tag{1.1}$$

where F_N is the free energy of the normal state and F_S is the free energy of the superconducting state, per unit volume.

The specific heat of a superconductor exhibits a discontinuity at the transition temperature. This type of behavior is characteristic of a second order phase transition. At low temperatures the specific heat vanishes exponentially, which indicates that there is a gap in the excitation spectrum. Figure 1.4 shows the specific heat of aluminum as a function of temperature. The normal state data was obtained by applying a magnetic field of sufficient strength to drive the sample into the normal state.

There are many other physical properties of superconductors which are too numerous to discuss in detail. One property which has received a great deal of attention within the context of the high T_c oxide superconductors is the isotope effect. For most conventional superconductors, the transition temperature $T_c \propto \frac{1}{M^\alpha}$, $\alpha \lesssim \frac{1}{2}$, where M is the ionic mass. This is one of the indications that lattice vibrations are related to the superconductivity. In the oxide superconductors, the isotope effect is generally small[6], and this is sometimes interpreted as an indication that lattice vibrations are not responsible for the superconductivity in these materials.

The theoretical explanation of superconductivity was a problem that challenged physicists for nearly half a century. It was not until 1957 that a successful microscopic theory of the phenomena was formulated. Various phenomenological theories were proposed prior to 1957 which met with some success.

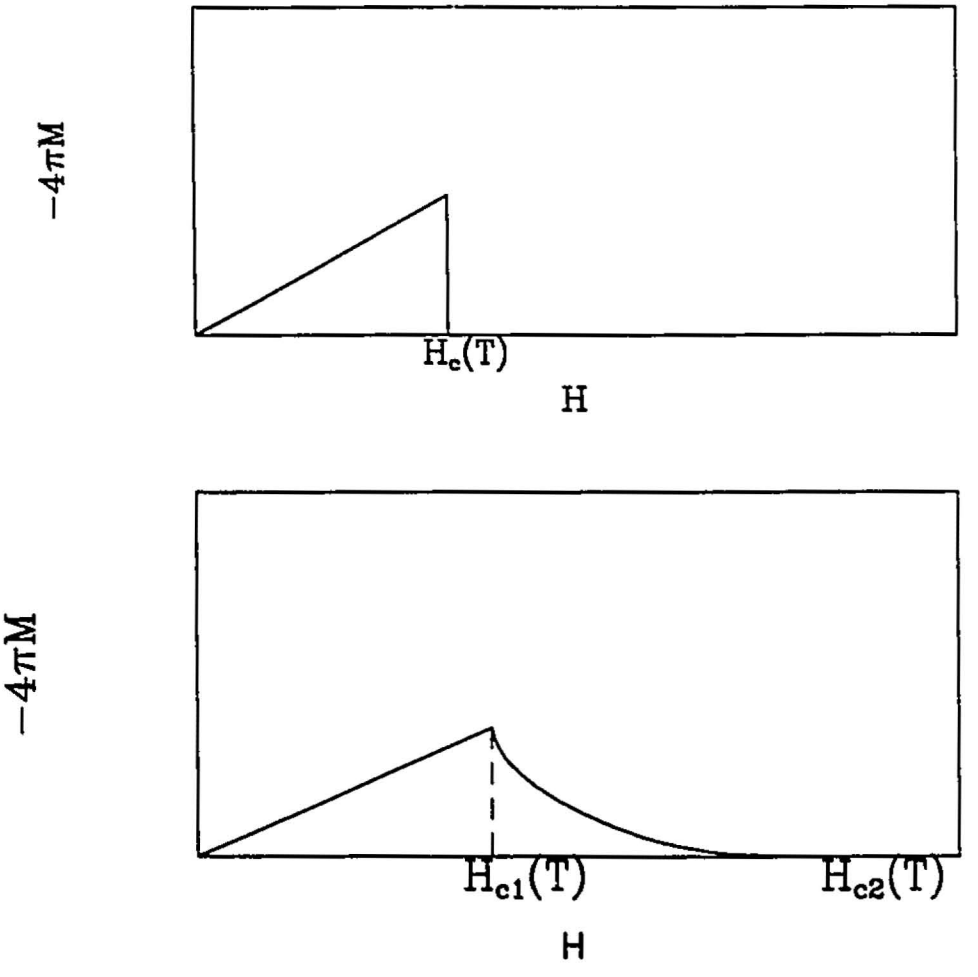

Figure 1.3-Magnetization versus applied field for type I (upper) and type II (lower) superconductors. Both types are diamagnetic until the applied field reaches $H_c(T)$ or $H_{c1}(T)$. At this point the type I material goes normal, while the type II material enters a mixed state, eventually going normal at $H_{c2}(T)$.

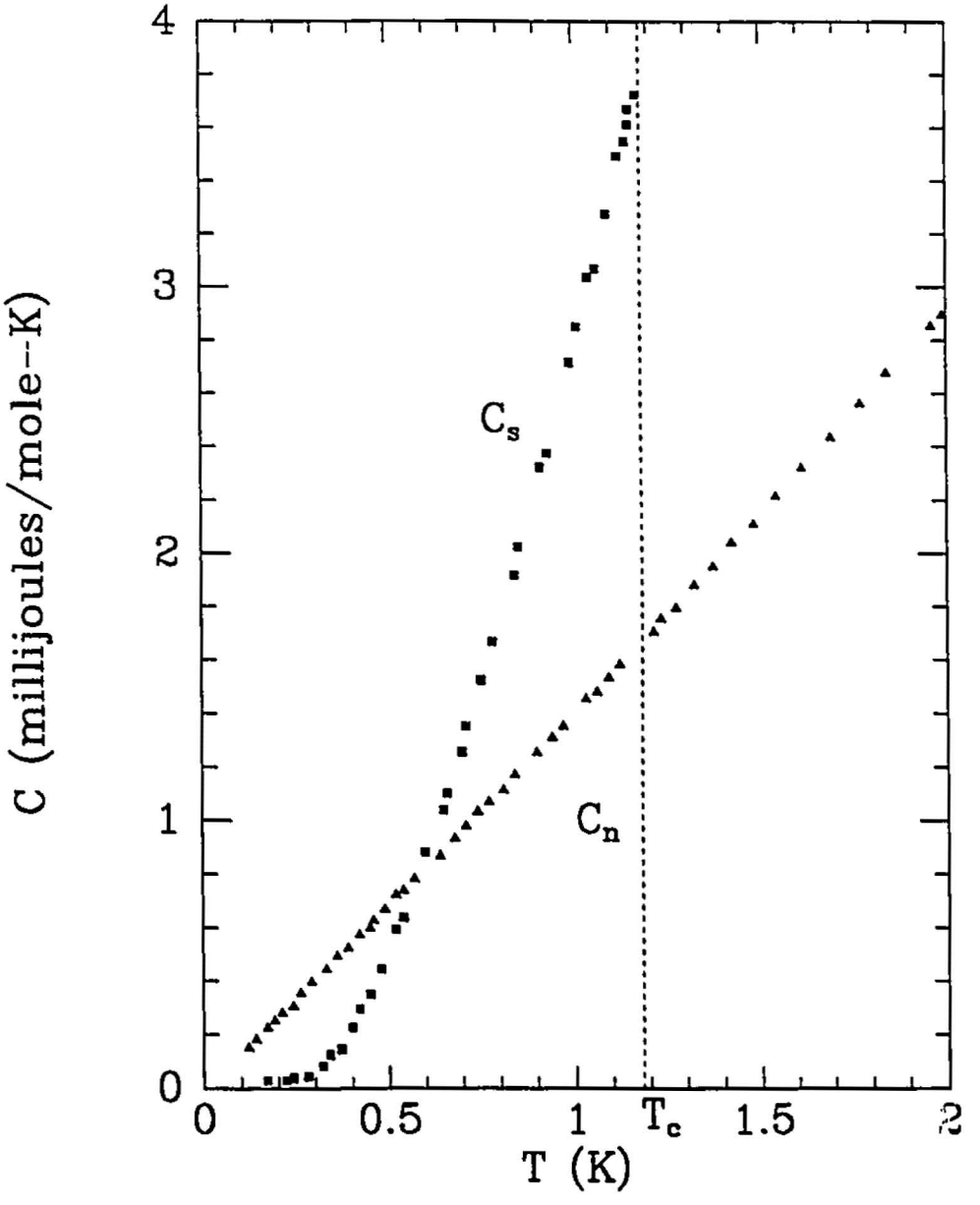

Figure 1.4-The specific heat of Al^{86} in the normal and superconducting states. Note the jump at T_c. Also note the exponential behaviour at low T, indicative of an energy gap in the excitation spectrum. The normal state data was measured by applying a magnetic field to drive the sample normal.

In 1934, Gorter and Casimir[7] proposed a two fluid model which was reasonably successful in describing the thermodynamic properties of superconductors. In 1935, F. and H. London[8] developed a theory for the electrodynamics of superconductors, based upon the two fluid model. This model was very successful. In 1953, Pippard[9] generalized the London theory to include non-local effects. In 1950, Ginzburg and Landau[10] were able to extend the London model by taking into account spatial variations of the superfluid density. This theory was able to successfully describe the magnetic behavior of both type I and type II superconductors.

The development of the microscopic theory started with Fröhlich's[11] proposal that it is the electron-phonon interaction that is responsible for superconductivity. It is interesting to note that Fröhlich was unaware of the isotope effect when he made this proposal, although the publication of that discovery[12] preceded the publication of Fröhlich's work. In 1956, L. N. Cooper[13] considered the problem of a pair of electrons interacting only with each other in the presence of a filled Fermi sea. The attractive interaction was assumed to arise from the electron-phonon interaction, and was restricted to act between states within ω_D, a characteristic phonon energy, of the Fermi surface. He found that a bound state existed for the pair of electrons when both their spin and momentum were equal and opposite. This suggested that the Fermi sea is unstable to the formation of these pairs, usually referred to as Cooper pairs.

In 1957, Bardeen, Cooper and Schrieffer (BCS)[14] proposed a wave function for a superconductor which incorporated the ideas of Cooper. Using this wave function, they were able to successfully describe the features of the superconducting state. Their theory requires one parameter, and once

this is specified, one is able to calculate all the superconducting properties of the material. However, the theory is not able to describe all materials. In particular, the BCS theory makes predictions for the ratios of various quantities which are completely independent of any material parameters. These ratios are observed to vary from material to material. This is due to the simplifying approximations made with respect to the nature of the electron-phonon interaction. The BCS theory treats the effective electron-electron interaction as a constant for energy transfers less than ω_D, and zero for energy transfers greater than ω_D. In reality, the interaction is not a constant, and reflects various details of the material, such as the lattice structure, the electronic structure and the coupling strength between the electrons and the phonons.

In 1960, Eliashberg[15] developed a theory of superconductivity based upon the BCS theory which takes into account the full energy dependence of the electron-phonon interaction. Using the Eliashberg formalism, it is possible to explain the deviations from the BCS theory in most materials[16], with the possible exceptions of organic superconductors, heavy fermion superconductors, and the high T_c oxide superconductors.

1.2 OUTLINE

In metals, there are excitations other than phonons to which the electrons can couple. Berk and Schrieffer[101] pointed out that by considering the effects of ferromagnetic spin fluctuations, they were able to understand why some of the transition metals had reduced effective pairing potentials. The spin fluctuations suppress the superconductivity in these systems.

Whether an excitation promotes or suppresses superconductivity is related to the symmetry of the interaction. If the interaction Hamiltonian for the excitation preserves the symmetry of the superconducting state, then the excitation enhances the superconductivity. If on the other hand, the perturbation breaks the symmetry of the superconducting state, then the excitation suppresses the superconductivity. Indeed, the symmetry of the superconducting state is determined by the symmetry of the interaction which leads to the superconductivity.

Conventional electron-phonon superconductors are believed to be s-wave, spin singlet superconductors. The spin fluctuations break this symmetry by introducing the possibility of spin flip scattering, and hence suppress the superconductivity in these systems.

In the heavy fermion superconductors, there is considerable evidence that the superconducting state is not an s-wave state. For example, the low temperature specific heat of UBe_{13} does not vanish exponentially as one would expect for an s-wave superconductor[104]. The ultra-sonic attenuation of this material also exhibits features which are not consistent with s-wave superconductivity[105].

For a d-wave state, spin fluctuations can lead to pairing. Antiferromagnetic spin fluctuations are observed in the heavy fermion materials[108]. Hence, it has been proposed that in the heavy fermion materials, the superconducting state is a d-state that is stabilized by antiferromagnetic spin fluctuations[106]. This suggestion has some rather appealing features. It produces the large masses that are observed in the heavy fermion superconductors. In addition, it predicts that the mass enhancement is proportional to the

magnetic susceptibility, which is observed[111]. Norman[107] has performed calculations for several of the heavy fermion superconductors, based upon this proposal, using the Eliashberg formalism. He has found reasonable agreement with experiment for the critical temperature and the specific heat data.

D-wave superconductivity has also been considered for the high T_c superconductors. The resistivity of these materials is linear right down to the transition temperature. This would indicate that there is a great deal of low frequency scattering. It was suggested that this low frequency scattering would be pair-breaking[113], and that T_c would be suppressed. However, Bergmann and Reiner[24] have previously shown that for s-wave superconductors, scattering at any frequency does not lead to pair-breaking. In searching for a model in which the low frequency scattering is pair-breaking, Millis *et al.* [19] considered a d-wave state due to antiferromagnetic spin fluctuations. For such a state, they found that the high frequency modes promoted pairing, while the low frequency modes were pair-breaking. However, they concluded that such a model would not produce high critical temperatures. D-wave solutions have also been considered by Rieck *et al.* [114]. Using an isotropic electron-phonon interaction in addition to a non-phonon anisotropic interaction, they find reasonable agreement with the tunnelling density of states.

It is now believed that the superconducting state in the high T_c materials is an s-wave, singlet state[112]. However, it is questioned whether the electron-phonon interaction can produce such high critical temperatures. The BCS theory predicts that

$$k_B T_c = 1.13 \omega_D e^{\frac{-1}{N(0)V}}, \tag{1.2}$$

where $N(0)$ is the electronic density of states at the Fermi surface and V is the effective electron-electron interaction. For materials where the BCS formalism is appropriate, $N(0)V$ is typically of the order of 0.2, and Debye frequencies are typically in the range of $10 \sim 40$ meV. These values produce critical temperatures in the range of $.1 \sim 10$ K. Strong coupling effects, which are described by the Eliashberg formalism, tend to raise the critical temperatures. In fact, the Eliashberg theory places no formal limit upon the value of T_c. One can obtain any value one desires by simply increasing the strength of the electron-phonon interaction. However, if the electron-phonon interaction becomes too strong, it is expected that a lattice instability will result[17]. The BCS result of equation 1.2 suggests that if one could increase the characteristic frequency of the interaction, high critical temperatures would be attainable. This has led to the consideration of alternate mechanisms of superconductivity, with the pairing mediated by excitons[18] for example. Theories of pairing by mechanisms of electronic origin suffer from the difficulty that many of the simplifying approximations that one is able to make for the electron-phonon case do not appear to be valid[98]. Spin fluctuations are also observed in the high T_c materials[40,41]. In such a case, one would expect the spin fluctuations to be suppressing the superconductivity.

There has been proposed a model of the high T_c materials which is motivated by the normal state properties[21]. An ansatz is made about the polarizability, from which follows, among other properties, the linear resistivity, the tunneling conductance, and the nuclear relaxation rate. The model is referred to as a marginal Fermi liquid model, as while the quasi-particle lifetime remains infinite on the Fermi surface, there is only a logarithmic singularity in the momentum distribution. The superconducting state may,

to a first approximation, be described by the Eliashberg theory. There is coupling via both charge and spin degrees of freedom, and hence there is pair-breaking in this model.

There is another school of thought which suggests that these materials are not well described by a Fermi liquid approach[20]. This belief is motivated by the fact that the parent compounds of these materials are all antiferromagnetic insulators.

In this work, we have adopted the viewpoint that the Fermi liquid approach is appropriate, and that the superconducting state may be described within the context of the Eliashberg formalism. We have studied a system where there are two competing dynamical mechanisms, one which promotes the superconductivity, and one which suppresses the superconductivity. We do not specify what the attractive interaction is, but assume that it exists. We will mainly consider the repulsive interaction to be due to spin fluctuations. However, our equations are similar to the d-state considered by Millis *et al.* [19]. In that case, the superconductivity is due to the antiferromagnetic spin fluctuations, which are attractive at high frequencies, but repulsive at low frequencies. We have also done calculations for the marginal Fermi liquid model, which also exhibits pair-breaking at low frequencies.

In Chapter 2 we give an introduction to the basic ideas underlying the theory of conventional superconductors and we present the Eliashberg equations. We also describe some of the techniques that are employed throughout the rest of the thesis.

In Chapter 3 we introduce and motivate the particular models that we have studied, and present results for the case where the frequency dependence of the pairing and depairing interactions is the same. We also discuss the

marginal Fermi liquid model, and give some results for that model at the end of Chapter 3. In Chapter 4 we treat the case where the two interactions have different frequency dependencies, such as one might expect in an s-wave superconductor in which there are also spin fluctuations.

Chapter 5 deals with the model of Chapter 3 in the limit of the pairing interaction being extremely large. We have also studied this limit for models in which there is no pair breaking. As the remainder of the thesis deals exclusively with models in which there is pair breaking, it was decided to present these results in Appendices 2 and 3 rather than in the main body of the thesis.

Chapter 6 contains a summary of our theoretical results. Where possible we have compared our results to experiment. Appendix 1 contains some mathematical details relating to Chapter 3.

Chapter 2

Eliashberg Equations

In this chapter we will present the formalism which is used in the rest of the thesis - the Eliashberg equations. Unfortunately, they are a rather complicated set of equations, for which one resorts to numerical solutions for any realistic case. As such, it seems appropriate to include a discussion of the basic ideas underlying the theory before presenting the equations themselves.

It is believed that the electron-phonon interaction is responsible for causing superconductivity in conventional superconductors. By conventional, we mean not heavy fermion, organic, or high temperature superconductors. The basic idea is that a net attractive electron-electron interaction, which leads to the formation of Cooper pairs, can come about due to the electron-phonon interaction. Of course, the electrons are charged, and hence interact with one another via the Coulomb interaction. The electron-phonon interaction must be sufficiently strong to overcome the Coulomb repulsion in order

for a material to be a superconductor. How does this net attractive interaction come about?

A simple way of visualizing this effect is to consider an electron travelling through a lattice of positively charged ions. An attractive force exists between the electrons and the ions, and the lattice tends to be polarized along the path of the electron. This polarized region will appear to be slightly more positive than the rest of the lattice, and hence a second electron will be attracted to this region. An essential feature of this interaction is the fact that it is retarded in time. The electrons travel through the metal at the Fermi velocity, $v_F \sim 10^8 cms^{-1}$. Lattice vibrational frequencies are typically of the order of 10~100 meV. If we treat the lattice vibrations as simple harmonic oscillators, then $u(t)$, the excursion of an ion from its equilibrium position is given by $u(t) = u_o \sin(\omega t)$, where u_o is the maximum displacement. Maximum displacement, and hence maximum lattice polarization, will occur at a time t such that $\omega t = \frac{\pi}{2}$. In this time the electron will have travelled a distance

$$d = v_F t = \frac{v_F \pi}{2\omega} \sim 1000\mathring{A} \tag{2.1}$$

The electron which initially polarized the lattice has travelled a significant distance by the time the lattice is fully polarized. It is this retardation effect which is essential.

BCS[14] proposed a wave function of the form

$$\Psi = \prod_k (u_k + v_k c^\dagger_{k,\uparrow} c^\dagger_{-k,\downarrow})|0\rangle \,. \tag{2.2}$$

u_k and v_k are variational parameters, and $c^\dagger_{k,\uparrow}$ creates an electron of momentum k, spin $\uparrow$. In the presence of a net attractive interaction, they were able to find a solution with lower energy than the free electron ground state. The

electrons form Cooper pairs, of the form $c^{\dagger}_{k,\uparrow}c^{\dagger}_{-k,\downarrow}$. Associated with the formation of these pairs is an energy, $\Delta(T)$, referred to as the energy gap. The BCS solution is an s-wave singlet solution, and the energy gap forms over the entire Fermi surface. It is this feature which is responsible for, among other things, the exponential behaviour at low temperature in the specific heat. It should be noted that the Cooper pairs do not form in real space but rather in momentum space. As such, the pairs are quite large, and there is a significant amount of overlap between pairs in real space..

The isotropic Eliashberg equations written on the imaginary axis are[80]

$$Z(i\omega_n)\Delta(i\omega_n) = \pi T \sum_{m=-\infty}^{\infty} [\lambda(m-n) - \mu^*] \frac{\Delta(i\omega_m)}{\sqrt{\Delta^2(i\omega_m) + \omega_m^2}}, \tag{2.3a}$$

$$Z(i\omega_n)\omega_n = \omega_n + \pi T \sum_{m=-\infty}^{\infty} \lambda(m-n) \frac{\omega_m}{\sqrt{\Delta^2(i\omega_m) + \omega_m^2}}. \tag{2.3b}$$

The $\Delta(i\omega_n)$ are the energy gap functions, evaluated at the Matsubara frequencies, $i\omega_n = i\pi T(2n-1)$, $n \epsilon I$, $(\hbar = k_B = 1)$. $Z(i\omega_n)$ is the renormalization function. μ^* is the Coulomb pseudo-potential[27], which mimics the effect of the Coulomb repulsion between the electrons. In order to calculate the energy gap, it is necessary to analytically continue the gap function to the real axis where it is given by

$$\Re\Delta(\omega = \Delta_o) = \Delta_o \tag{2.4}$$

All the details of the electron-phonon interaction enter Eliashberg theory via

$$\lambda(m-n) = 2\int_0^{\infty} \frac{\omega\, \alpha^2 F(\omega)}{\omega^2 + (\omega_m - \omega_n)^2} d\omega. \tag{2.5}$$

where $\alpha^2 F(\omega)$, the electron-phonon spectral density function, is given by

$$\alpha^2 F(\omega) = [\frac{\Omega_a}{(2\pi)^3}]^2 \frac{1}{N(0)\hbar} \sum_j \int d^3\vec{k}\delta(\epsilon_{\vec{k}}) \int d^3\vec{k}'\delta(\epsilon_{\vec{k}'}) \mid g_{\vec{k},\vec{k}',j} \mid^2 \delta(\omega - \omega_j(\vec{k} - \vec{k}')) \tag{2.5a}$$

$$g_{\vec{k},\vec{k}',j} = \sqrt{\frac{\hbar}{2M\omega_j(\vec{k} - \vec{k}')}} \langle \psi_{\vec{k}} | \epsilon^j(\vec{k} - \vec{k}') \cdot \nabla V | \psi_{\vec{k}'} \rangle . \tag{2.5b}$$

Ω_a is the unit cell volume, $N(0)$ is the electronic density of states at the Fermi surface, $\epsilon_{\vec{k}}$ are the energies of the electronic states $\psi_{\vec{k}}$, and $\epsilon^j(\vec{k})$ are the polarization vectors of the phonon modes, with branch index j and energy $\omega_j(\vec{k})$. M is the ionic mass and V is the electron-ion potential.

In deriving the Eliashberg equations, an assumption has been made that vertex corrections are small. This is known as Migdal's theorem[109], which asserts that the corrections are of order $\frac{\omega_D}{\epsilon_F}$, with ω_D being the Debye frequency and ϵ_F is the Fermi energy. It seems to be valid for the electron-phonon interaction, but may not be valid for all interactions.

It is possible, but formidable, to calculate $\alpha^2 F(\omega)$ from first principles[22]. It is more usual to obtain $\alpha^2 F(\omega)$ from inversion of tunnelling data[23] through the use of the Eliashberg equations themselves. Using such a procedure, one is able to predict structure in the tunnelling data, due to multi-phonon processes, which occurs beyond the range of the data used in the inversion process. One is also able to calculate other superconducting properties using a tunnelling derived $\alpha^2 F(\omega)$, and the agreement with experiment is generally quite good.

In figure 2.1 we show two $\alpha^2 F(\omega)$ spectra, one for Al, and one for Pb. Al is a material whose superconducting properties are well described by the BCS theory. Pb, however, exhibits significant deviations from BCS behavior.

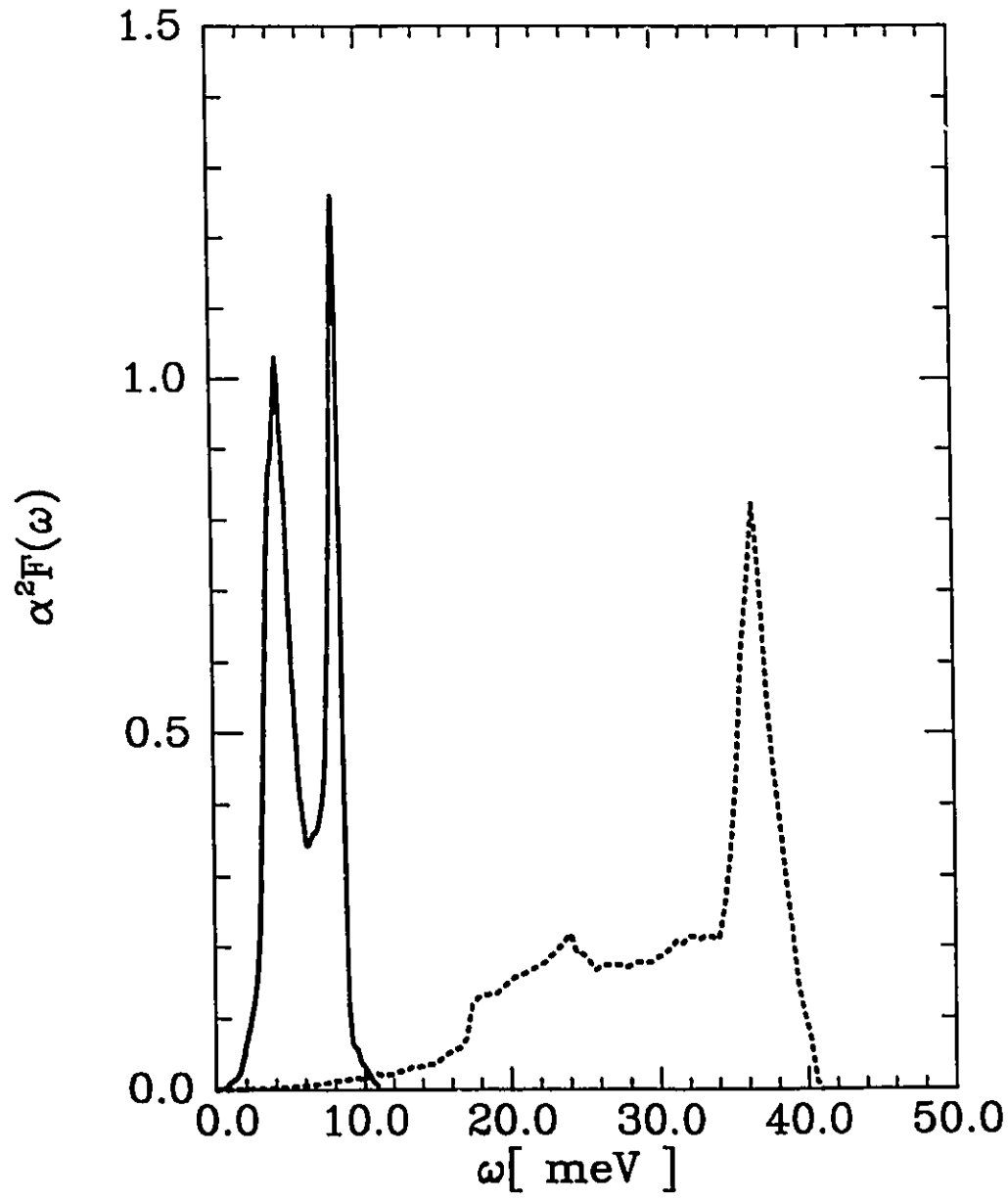

Figure 2.1-Electron-phonon spectral densities, $\alpha^2F(\omega)$, for Pb (solid) and Al (dashed). The Pb spectrum was obtained from tunnelling inversion [88]. The Al spectrum was calculated[89]. The superconducting properties of Al are well described by the BCS theory. Pb exhibits significant deviations from the BCS results, but is well described by Eliashberg theory.

Unfortunately, it is not always obvious what superconducting properties will result from a given $\alpha^2F(\omega)$. In order to gain some more insight into the dependence of the superconducting properties upon the frequency distribution of $\alpha^2F(\omega)$, one can employ functional derivative techniques [24].

In general, any superconducting property, Q, is a functional of $\alpha^2F(\omega)$, denoted $Q[\alpha^2F(\omega)]$. If one wishes to know how Q will change in response to a change in $\alpha^2F(\omega)$ at some ω, one can calculate the functional derivative of Q with respect to $\alpha^2F(\omega)$, defined as

$$\frac{\delta Q}{\delta \alpha^2F(\omega_o)} = \lim_{\epsilon \to 0} \frac{Q[\alpha^2F(\omega) + \epsilon\delta(\omega - \omega_o)] - Q[\alpha^2F(\omega)]}{\epsilon} \tag{2.6}$$

In figure 2.2 we show the functional derivative of the critical temperature with respect to $\alpha^2F(\omega)$ for the weak coupling (BCS) limit of Eliashberg theory [25]. The function goes to zero at both low and high frequencies and is peaked at $\frac{\omega}{T_c} \sim 10$. This peak reflects the retarded nature of the electron-phonon interaction. Phonons with very low frequencies will be fully polarized long after the first electron has subsequently scattered. Phonons with high frequencies will be fully polarized while the first electron is still in the vicinity, and the Coulomb repulsion will dominate. Those phonons whose frequency allows the electron to travel far enough to reduce the Coulomb interaction, but not so far that it has scattered again, are most effective for T_c. The derivative is everywhere positive definite, which means that no phonons reduce T_c, regardless of their frequency.

It is found that the functional derivatives of most superconducting properties have their maxima at some finite frequency. This suggests that

one would be able to obtain extreme values for that quantity by placing all of the spectral weight at the optimum frequency.

An $\alpha^2F(\omega)$ spectrum with all of its spectral weight at one frequency corresponds to an Einstein phonon model. By using such spectra, one is able to compare the range of values produced with experiment in order to determine if the Eliashberg description is appropriate [26].

Since all superconducting properties are functionals of $\alpha^2F(\omega)$, it is tempting to try to identify a functional of $\alpha^2F(\omega)$ which would allow one to predict the properties of a superconductor without solving the Eliashberg equations. Many attempts have been made to find such a parameter. Perhaps the most common electron-phonon parameter is λ, the electron mass enhancement factor, given by

$$\lambda = 2\int_0^\infty \frac{\alpha^2F(\omega)}{\omega}d\omega\,. \tag{2.7}$$

In 1962, Morel and Anderson[27] derived a T_c equation from the microscopic theory of the form

$$T_c = 1.13\omega_D e^{\frac{-1}{\lambda-\mu^*}} \tag{2.8}$$

where μ^* is the Coulomb pseudopotential. A perhaps more famous equation for T_c, derived by McMillan[28] is

$$T_c = \frac{\Theta_D}{1.45}e^{\frac{-1.04(1+\lambda)}{\lambda-\mu^*(1+0.62\lambda)}} \tag{2.9}$$

The McMillan equation works well for some materials, but fails for others. It also implies that there is a maximum T_c attainable from the Eliashberg theory which is not true[29]. An excellent discussion of T_c is given by Allen and Mitrović[30].

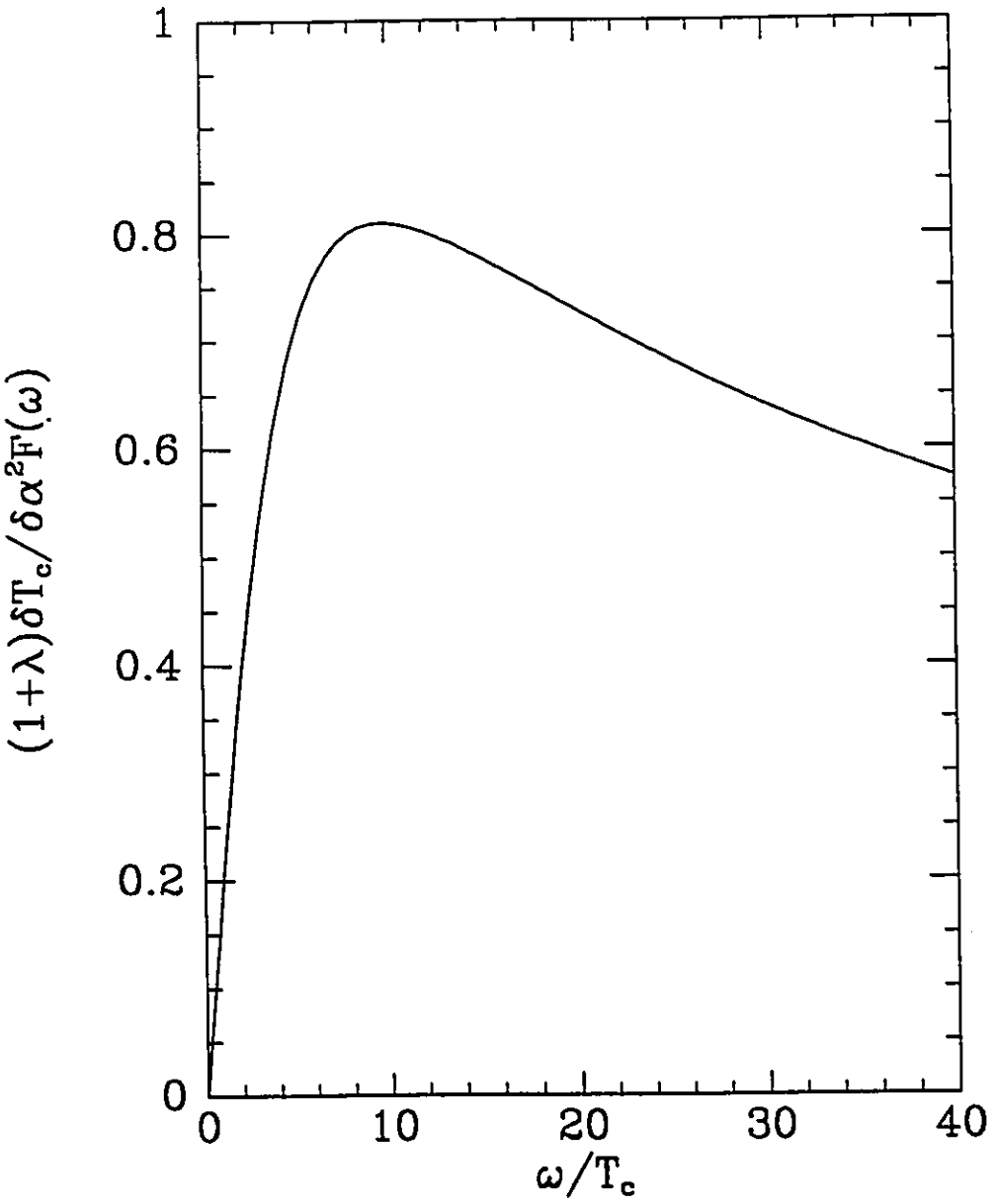

Figure 2.2-Functional derivative of the critical temperature with respect to the electron-phonon spectral density, $\frac{\delta T_c}{\delta \alpha^2 F(\omega_o)}$. The derivative was calculated using the square-well model. The derivative is everywhere positive, and is peaked for $\frac{\omega}{T_c} \sim 10$.

A single quantity which seems to characterize a spectrum well is $\frac{T_c}{\omega_{ln}}$, where ω_{ln} is defined as[29]

$$\omega_{ln} \equiv exp\left[\frac{2}{\lambda}\int_0^\infty \frac{\alpha^2 F(\omega)}{\omega}\ln(\omega)\, d\omega\right] \tag{2.10}$$

In the BCS approximation, in which the Eliashberg equations can be solved analytically, $\frac{T_c}{\omega_{ln}} = 0$. In this limit, many ratios are predicted to be universal numbers, independent of any material parameters. For example, BCS predicts

$$\frac{2\Delta_o}{k_B T_c} = 3.53 \tag{2.11}$$

where Δ_o is the zero temperature gap edge. This relationship does not hold for all materials. It is however possible to expand the Eliashberg equations in powers of $\frac{T_c}{\omega_{ln}}$, in order to calculate the corrections to the BCS values. Mitrović *et al.* [31] have calculated such an expression for the gap ratio. Their result is

$$\frac{2\Delta_o}{k_B T_c} = 3.53[1 + a(\frac{T_c}{\omega_{ln}})^2 \ln(\frac{\omega_{ln}}{bT_c})] \tag{2.12}$$

with $a = 12$ and $b = 2$. a and b are in fact determined by various moments of $\alpha^2 F(\omega)$, but Mitrović *et al.* have determined a and b from fitting to gap ratios which were obtained from full numerical solutions of the Eliashberg equations. The values of a and b so obtained are in fairly reasonable agreement with values which one would obtain for delta function spectral densities. Their results are shown in Figure 2.3 along with values obtained from full numerical solutions. One can see that the agreement between the expansion and the calculated values is quite good. Similar expansions for other superconducting properties have also been performed[32], and the same level of agreement is also achieved. Therefore, it seems that $\frac{T_c}{\omega_{ln}}$ is a good parameter

for characterizing spectral densities. In this work, we make extensive use of the parameter $\frac{T_c}{\omega_{ln}}$. We also use primarily Einstein spectral functions of the form

$$\alpha^2 F(\omega) = A\delta(\omega - \omega_E)\,, \tag{2.13}$$

and for such spectral functions $\omega_{ln} = \omega_E$.

In order to calculate any thermodynamic properties one needs an expression for the free energy difference between the normal and superconducting states. There are two common expressions available in the literature. One, due to Wada[87], is

$$\begin{aligned}\frac{F_N - F_S}{N(0)} = 2\pi T \sum_{n=-\infty}^{\infty} \omega_n \Big[\frac{\tilde{\omega}(i\omega_n)}{\sqrt{\tilde{\Delta}^2(i\omega_n) + \tilde{\omega}^2(i\omega_n)}} - sign\omega_n\Big] + (\pi T)^2 X \\ \sum_{n=-\infty}^{\infty}\sum_{m=-\infty}^{\infty} \Bigg\{ \Big[\frac{\tilde{\omega}(i\omega_n)}{\sqrt{\tilde{\Delta}^2(i\omega_n) + \tilde{\omega}^2(i\omega_n)}} \frac{\tilde{\omega}(i\omega_m)}{\sqrt{\tilde{\Delta}^2(i\omega_m) + \tilde{\omega}^2(i\omega_m)}} - sign\omega_n\omega_m\Big]\lambda(m-n) \\ + \frac{\tilde{\Delta}(i\omega_n)}{\sqrt{\tilde{\Delta}^2(i\omega_n) + \tilde{\omega}^2(i\omega_n)}} \frac{\tilde{\Delta}(i\omega_m)}{\sqrt{\tilde{\Delta}^2(i\omega_m) + \tilde{\omega}^2(i\omega_m)}} \Big[\lambda(m-n) - \mu^*\Big] \Bigg\}\end{aligned} \tag{2.14}$$

This form has the extremely useful property that it is stationary with respect to variations in any $\tilde{\Delta}(i\omega_n)$ and $\tilde{\omega}(i\omega_n)$ which are solutions to the Eliashberg equations. As a result, one can immediately calculate functional derivatives of thermodynamic properties from this expression by noting that[33]

$$\frac{\delta\,\Delta F}{\delta\,\alpha^2 F(\omega_o)} = \frac{\partial \Delta F}{\partial \lambda(m-n)} \frac{\delta\,\lambda(m-n)}{\delta\,\alpha^2 F(\omega_o)}\,. \tag{2.15}$$

Another expression for the free energy difference, which can be obtained from the Wada expression by substituting (2.3a) and (2.3b) into

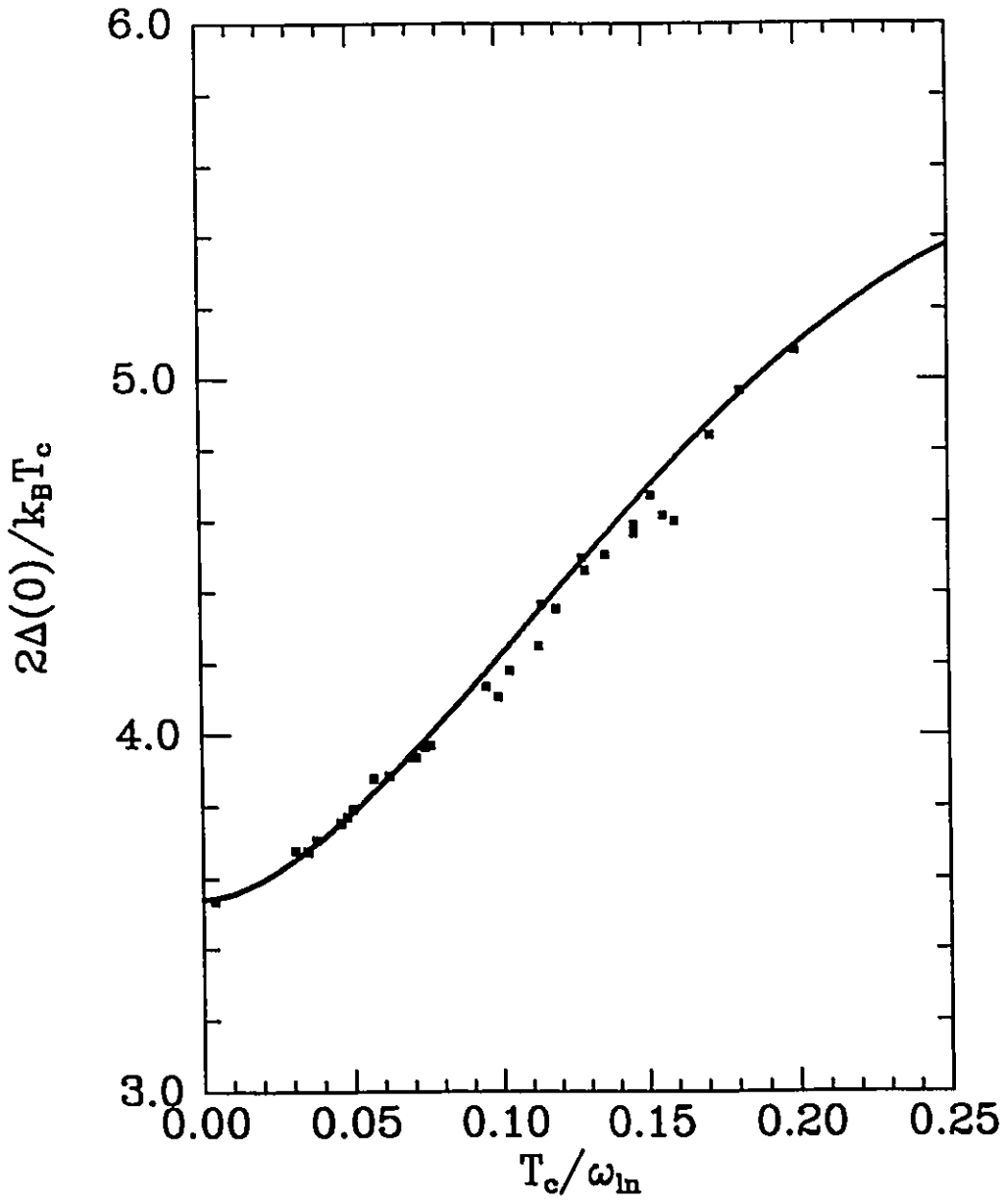

Figure 2.3-Zero temperature gap ratio versus $\frac{T_c}{\omega_{ln}}$. The points are from full numerical solution, and the curve is the analytic form of equation 2.12. The parameter $\frac{T_c}{\omega_{ln}}$ is useful for characterizing an $\alpha^2F(\omega)$ spectrum.

(2.14), is[34]

$$F_N - F_S = N(0)\pi T \sum_{m=-\infty}^{\infty} \left[\sqrt{\tilde{\Delta}^2(i\omega_m) + \tilde{\omega}^2(i\omega_m)} - |\,\tilde{\omega}(i\omega_m)\,| \right] \left[1 - \frac{|\,\tilde{\omega}^\circ(i\omega_m)\,|}{\sqrt{\tilde{\Delta}^2(i\omega_m) + \tilde{\omega}^2(i\omega_m)}} \right]$$

$$\tilde{\omega}^\circ(i\omega_n) \equiv \omega_n + \pi T \sum_{m=-\infty}^{\infty} \lambda(m-n)\, sign\omega_m \tag{2.16}$$

Both (2.14) and (2.16) give the same results, and the use of one over the other is dictated by the type of calculation one wishes to perform.

Once an expression for the free energy difference is obtained, one can readily determine the specific heat jump. This quantity is usually normalized to the normal state specific heat at T_c, $C_N(T_c) = \gamma T_c$.

$$\frac{\Delta C}{\gamma T_c} = \frac{C_S - C_N}{\gamma T_c} = -\frac{T}{\gamma T_c} \frac{\partial^2 (F_S - F_N)}{\partial T^2}\,. \tag{2.17}$$

This quantity is then independent of the electronic density of states at the Fermi surface. For materials with low critical temperatures,

$$\gamma = \frac{2}{3}\pi^2 N(0)(1+\lambda)\,. \tag{2.18}$$

For materials with higher critical temperatures, it is necessary to modify this expression to correctly account for the temperature dependence of the electron phonon interaction. We must replace λ with $\lambda(T)$, which is given by[35]

$$\lambda(T) = 2\int_0^\infty \frac{\alpha^2 F(\omega)}{\omega} G(\frac{\hbar\omega}{k_B T})\, d\omega\,, \qquad G(y) = \int_{-\infty}^{\infty} \frac{\partial f(t)}{\partial t} \frac{y^2}{t^2 - y^2}\, dt \tag{2.19}$$

and f is the Fermi function.

One final set of equations is needed for the work in this thesis. They are the equations for the upper critical field $H_{c2}(T)$. First given by Schossmann and Schachinger[36], they are

$$\Delta(i\omega_n)Z_s(i\omega_n) = \pi T \sum_{m=-\infty}^{\infty} [\lambda^-(m-n) - \mu^*] \frac{\tilde{\Delta}(i\omega_m)}{\mathcal{X}^{-1}(\tilde{\omega}(i\omega_m))}, \tag{2.20a}$$

and

$$\mathcal{X}(\tilde{\omega}(i\omega_m)) = \frac{2}{\sqrt{\alpha}} \int_0^{\infty} dq e^{-q^2} \tan^{-1} \frac{q\sqrt{\alpha}}{|\tilde{\omega}(i\omega_m)|} \tag{2.20b}$$

where $\alpha \equiv \frac{1}{2} e H_{c2}(T) v_F^2$. Here e is the electronic charge and v_F is the Fermi velocity. One can avoid the need to specify v_F by considering the reduced upper critical field which is defined as

$$h_{c2}(t) \equiv \frac{H_{c2}(T)}{T_c \mid \frac{dH_{c2}(T)}{dT} \mid_{T_c}}. \tag{2.21}$$

In this expression $t \equiv \frac{T}{T_c}$ is the reduced temperature.

Chapter 3

Spin Fluctuations in Superconductivity

3.1 INTRODUCTION

To this point we have limited our discussion to the case where there is only an attractive component to the electron-electron interaction, due to phonons. There are other interactions in metals to which the electrons couple. We now consider what effect these other interactions have on the superconducting state.

From equation 2.2 for the BCS wave function we see that the superconducting state is symmetric under exchange of momentum and spin. This symmetry is referred to as time-reversal symmetry[49]. In the case of static impurities, Anderson[91] has shown that if the perturbation does not break the time-reversal symmetry, the thermodynamic properties of the superconducting state are unaltered. This is nicely illustrated by the effects of non-magnetic and magnetic impurities. Non-magnetic impurities do not

break time-reversal symmetry, and have little effect on the thermodynamic properties of a superconductor. Their principal effect is to cause a change in the density of states at the Fermi surface, and hence a change in the pairing strength, N(0)V.

Magnetic impurities do break time-reversal symmetry as they introduce the possibility of spin-flip scattering. This leads to a strong suppression of T_c which has been observed experimentally[92]. This problem has been successfully treated theoretically[93,94], and an excellent summary of such work is given by Maki[19].

If one considers dynamic interactions, a similar picture emerges. Excitations which couple via charge, such as excitons, are attractive, while excitations which couple via spin, such as spin fluctuations, are repulsive. In searching for mechanisms to produce higher critical temperatures, various interactions have been proposed, such as excitons[74,76] and plasmons[76]. The attractive feature of such mechanisms is that their characteristic frequencies are high, and from a simple BCS approach

$$T_c \propto \Omega e^{-\frac{1}{N(0)V}}, \tag{3.1}$$

where Ω is the characteristic energy of the excitation. The alternate route of increasing T_c by increasing the coupling strength of the interaction is argued to lead to an instability, either of the lattice in the case of the electron-phonon interaction[17], or of the electronic system itself[95]. Models of superconductivity of electronic origin have been studied extensively (see for example 95, 96, 97, 98). The main difficulty lies in treating the Coulomb interaction in a suitable fashion.

In the electron-phonon case, Migdal's theorem allows one to neglect vertex corrections. However, this is only valid when the characteristic energy of the excitations is much less than the Fermi energy. For excitations of electronic origin, this approximation does not appear to be valid[98].

There are also repulsive interactions and in particular we wish to consider the effects of spin fluctuations on superconductivity. Spin fluctuations arise in a metal due to the Coulomb repulsion that exists between the electrons. These effects are particularly pronounced in materials that are well described by a tight binding approach, in which the electrons form narrow bands. Hubbard[99] pointed out that for such materials, the dominant term due to Coulomb effects would be of the form

$$H_I = U \sum_{i,\sigma,\sigma'} n_{i,\sigma} n_{i,\sigma'} \tag{3.2}$$

where $n_{i,\sigma}$ is the density operator for an electron of spin σ at the ith site of the lattice, and

$$U = \int d^3x_1 d^3x_2 \Psi^*(x_1)\Psi^*(x_2) V_{sc}(x_1 - x_2)\Psi(x_1)\Psi(x_2) \tag{3.3}$$

where V_{sc} is a screened Coulomb interaction and the Ψ are the tight-binding wave functions. H_I of equation 3.2 can be rewritten as

$$H_I = UN + U \sum_i n_{i,\uparrow} n_{i,\downarrow} \tag{3.4}$$

where we have used $n_{i,\sigma}^2 = n_{i,\sigma}$. We can then see from 3.4 that depending upon the sign of U, there will be a tendency for the electronic system to favour ferromagnetic (U > 0) or antiferromagnetic (U < 0) order. Prior to the onset of long range magnetic order, there may be some fluctuations in the spin density, referred to as spin fluctuations.

The standard textbook approach to this problem studies the linear response of the electron gas to an external perturbation[100]. The perturbing Hamiltonian is given as

$$H_{int} = -\int \vec{\mathcal{H}}(x,t)\cdot\vec{\sigma}(x)d^3x \tag{3.5}$$

where $\vec{\mathcal{H}}(x,t)$ is the external magnetic field, and $\vec{\sigma}(x)$ is the spin density operator.

$$\vec{\sigma}(x) = \sum_{electrons} \delta(x - x_{electron})\vec{\sigma}_{electron} \tag{3.6}$$

To first order in $\vec{\mathcal{H}}(x,t)$, one finds

$$\langle\sigma_i(x,t)\rangle = \langle\sigma_i(x,t)\rangle_{\mathcal{H}=0} + \sum_j \int dt' \int dx' \chi_{i,j}(x-x',t-t')\mathcal{H}_i(x,t) \tag{3.7a}$$

where

$$\chi_{i,j}(x-x',t-t') = i\theta(t-t')\langle[\sigma_i(x,t),\sigma_j(x',t')]\rangle \tag{3.7b}$$

is referred to as the susceptibility tensor. The subscripts i and j refer to Cartesian components. In practice one solves for the transverse susceptibility

$$\begin{aligned}\chi^{-+}(x-x',t-t') &= i\theta(t-t')\langle[\sigma^-(x,t),\sigma^+(x',t')]\rangle \\ \sigma^{\pm} &= \frac{1}{2}(\sigma_x \pm i\sigma_y)\end{aligned} \tag{3.7c}$$

and χ_{zz}. One can calculate χ^{-+} in the random phase approximation to find, after Fourier transforming in space and time,

$$\begin{aligned}\chi^{-+}(\vec{q},\omega) &= \frac{\Gamma^{-+}(\vec{q},\omega)}{1 - U\Gamma^{-+}(\vec{q},\omega)} \\ \Gamma^{-+}(\vec{q},\omega) &= \frac{1}{N}\sum_{\vec{p}} \frac{f_{\vec{p},\uparrow} - f_{\vec{p}+\vec{q},\downarrow}}{\omega - (\tilde{\epsilon}_{\vec{p},\downarrow} - \tilde{\epsilon}_{\vec{p}+\vec{q},\uparrow}) + i\eta}\end{aligned} \tag{3.8}$$

where $f_{\vec{p},\uparrow}$ is the Fermi function and $\tilde{\epsilon}_{\vec{p},\downarrow}$ are the electronic energies. $\chi^{-+}(\vec{q},\omega)$ diverges when

$$U\Gamma^{-+}(\vec{q},\omega) = 1 \tag{3.9}$$

which is the signature of the transition to the magnetically ordered phase. As one approaches this point, the susceptibility will be enhanced.

Berk and Schrieffer[101] pointed out that in the transition metals with enhanced susceptibilities, the BCS pairing interaction V was sharply reduced compared to those transition metals without enhanced susceptibilities. They proposed that this was due to the spin fluctuations in these systems. For the case of ferromagnetic correlations, this is fairly easy to picture. Any electron will tend to be surrounded by a spin-polarized cloud of electrons, all having the same spin. Another electron of opposite spin trying to take advantage of the lattice polarization produced by the first electron will be repelled by the polarized cloud. This repulsion only occurs for pairing between electrons of opposite spin, as in the s-wave singlet case.

Berk and Schrieffer were able to show that spin fluctuations did indeed suppress T_c in s-wave superconductors. They also pointed out that liquid He^3 has an enhanced susceptibility and that perhaps the superfluidity in this system was being suppressed by spin fluctuations. Doniach and Englesberg[102] and Brinkman and Englesberg[103] analyzed this effect in He^3, and the results agreed well with the experiment. They predicted rather large effective masses and non-linear behavior in the low temperature specific heat.

Large effective masses and anomalous low temperature specific heats are observed in the heavy fermion superconductors[104]. This behaviour in conjunction with other unusual behaviour, ultrasonic attenuation for example[105], led to speculation that the superconducting state in these materials was not an s-wave state. In such a state, spin fluctuations can be attractive, and it has been suggested that the superconductivity in the heavy fermion materials is due to antiferromagnetic spin fluctuations in a d-wave state[106]. Norman[107]

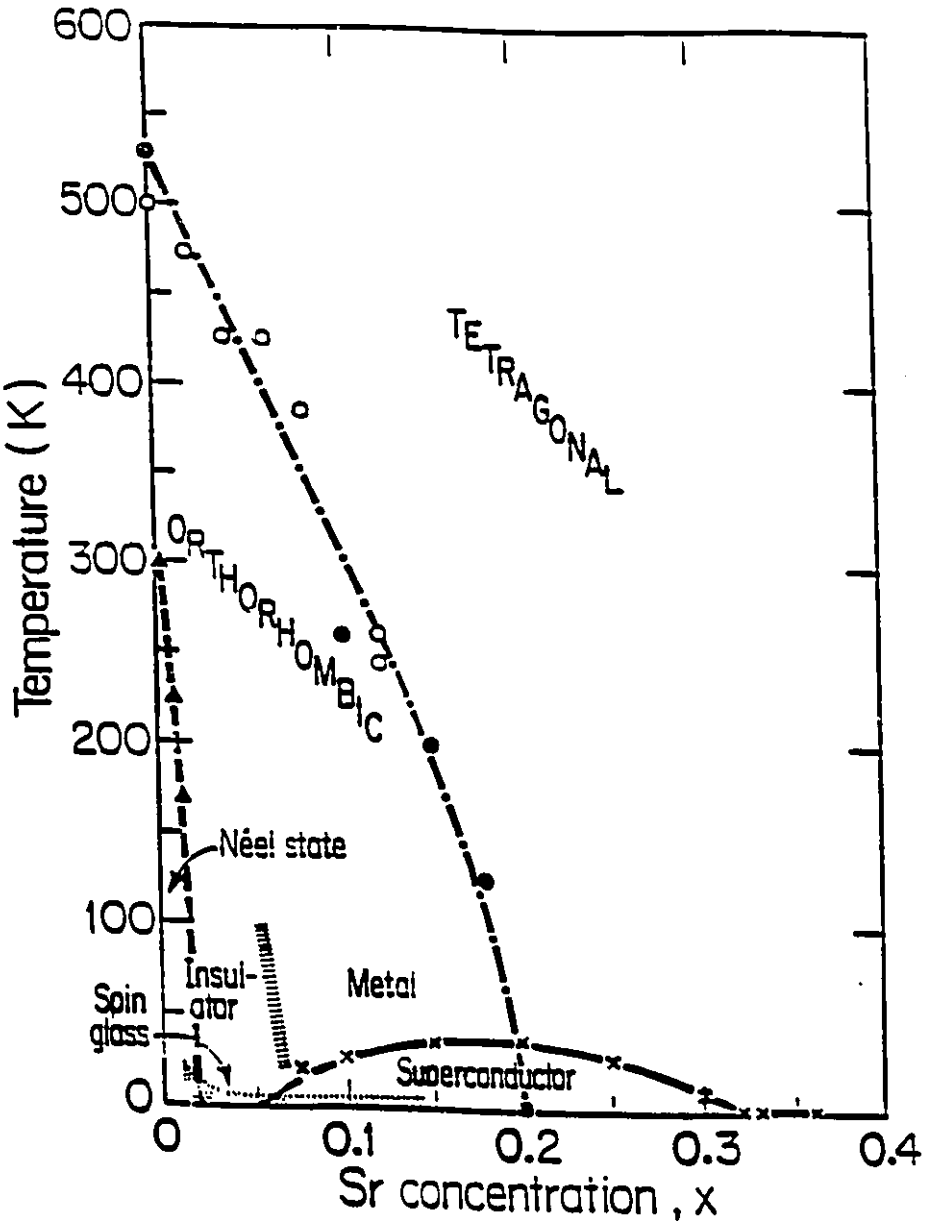

Figure 3.1-Phase diagram for $La_{2-x}Sr_xCuO_4$. For small x, the systems orders antiferromagnetically. As x is increased, the long range antiferromagnetic order is lost, but the total moment is preserved, and there are spin fluctuations in the superconducting regime.

has calculated some of the superconducting properties of UPt_3 and UBe_{13} using this approach in Eliashberg formalism. He found reasonable agreement with experiment for the transition temperatures and the specific heat data.

Spin fluctuations are also observed in the high temperature superconductors. Figure 3.1 is a phase diagram for $La_{2-x}Sr_xCuO_4$, a high T_c oxide superconductor[37]. Plotted are the relevant temperatures versus x. The temperatures of interest are T_N, the Néel temperature, below which the sample orders antiferromagnetically, and T_c, the superconducting transition temperature. While we are showing a phase diagram for a particular material, the features that we are interested in are similar for other high T_c materials. For small values of x, the system orders antiferromagnetically (AF). As x increases, the Néel temperature decreases going to zero at x~0.02. As x reaches 0.05, a superconducting phase is entered. T_c is initially quite small, rising to a maximum for x~0.18 and falling to zero at x~0.32. There are some experiments indicating that there is co-existence of AF order and superconductivity in both LaSrCuO[38] and YBaCuO[39]. More importantly, in both LaSrCuO[40] and YBaCuO[41], AF spin fluctuations have been observed using neutron scattering techniques. These fluctuations persist in the superconducting state, even though there is no long range AF order.

3.2 FORMALISM

For a material in which there are excitations which couple to both charge and spin, Millis *et al.* [19] have derived the following Eliashberg equations

$$Z(\vec{k},\omega_m)\Delta(\vec{k},\omega_n) = \pi T \int_{SF} \frac{dS_p}{|\vec{v}_p|} \sum_{m=-\infty}^{\infty} K^-(m-n,\vec{k}-\vec{p}) \frac{\Delta(\vec{p},\omega_m)}{\sqrt{\Delta^2(\vec{p},\omega_m)+\omega_m^2}} \quad (3.10a)$$

$$Z(\vec{k},\omega_n) = 1 + \frac{\pi T}{\omega_n}\int_{SF}\frac{dS_p}{|\vec{v}_p|}\sum_{m=-\infty}^{\infty} K^+(m-n,\vec{k}-\vec{p})\frac{\omega_m}{\sqrt{\Delta^2(\vec{p},\omega_m)+\omega_m^2}} \quad (3.10b)$$

The integrals are over the Fermi surface and $\vec{v}_p$ is the Fermi velocity. The kernels are given by

$$K^{\pm}(m,\vec{p}) = \alpha^2 D(\vec{p},\omega_m) \pm I^2\chi_2(\vec{p},\omega_m) \quad (3.11)$$

with $D(\vec{p},\omega_m)$ and α being the propagator and the coupling for the bosons which couple to the electron density. They considered spin fluctuations as the excitation which couples to the spin density. Thus, $\chi_2(\vec{p},\omega_m) = ImTr\chi_{i,j}(\vec{p},\omega_m)$ and I is a phenomenological coupling constant. In the derivation of these equations, Millis *et al.* assumed that the Migdal theorem was valid for both the attractive and repulsive interactions. This may not be valid for all excitations. In the case of excitations of electronic origin, it seems that the Migdal theorem is not valid[98]. However, it may be reasonable to assume that the Eliashberg equations are a reasonable starting point. They also neglected to include a term for the static Coulomb repulsion. They were primarily interested in investigating a d-wave solution, which would not be affected by an isotropic Coulomb term. For the rest of this chapter, we have also neglected μ^*.

We can recover the isotropic Eliashberg equations for a phonon superconductor by the following procedure. We set $I^2\chi_2 = 0$, and assume that $\alpha^2 D(\vec{p},\omega_m)$, which would describe the coupling to phonons, is independent of $\vec{p}$. With these assumptions, the right hand sides of equations 3.10 become independent of $\vec{k}$. As a result, $Z(\vec{k},\omega_n) = Z(\omega_n)$, and $\Delta(\vec{k},\omega_n) = \Delta(\omega_n)$. Employing a spectral representation

$$N(0)\alpha^2 D(\omega_n) = \int_0^{\infty}\frac{2\omega\alpha^2 F(\omega)d\omega}{\omega^2+\omega_n^2} \quad (3.12)$$

with

$$N(0) = \int_{SF} \frac{dS_p}{|\vec{v}_p|} \tag{3.12a}$$

one readily obtains 2.3a and 2.3b with $\mu^* = 0$.

One obtains the isotropic Eliashberg equations including spin fluctuations from 3.10 by assuming that both $\alpha^2 D(\vec{p},\omega_m)$ and $I^2\chi_2(\vec{p},\omega_m)$ are independent of $\vec{p}$. Employing a spectral representation for the susceptibility of the form

$$N(0)I^2\chi_2(\omega_n) = \int_0^\infty \frac{2\omega P(\omega)d\omega}{\omega^2 + \omega_n^2} \tag{3.13}$$

one then obtains

$$\Delta(i\omega_n)Z_s(i\omega_n) = \pi T \sum_{m=-\infty}^{\infty} \lambda^-(m-n)\frac{\Delta(i\omega_m)}{\sqrt{\Delta^2(i\omega_m) + \omega_m^2}} \tag{3.14a}$$

and

$$\omega_n Z_s(i\omega_n) = \omega_n + \pi T \sum_{m=-\infty}^{\infty} \lambda^+(m-n)\frac{\omega_m}{\sqrt{\Delta^2(i\omega_m) + \omega_m^2}} \tag{3.14b}$$

with

$$\lambda^{\pm}(m-n) = 2\int_0^\infty \frac{\omega[E(\omega) \pm P(\omega)]d\omega}{\omega^2 + (\omega_n - \omega_m)^2} \tag{3.14c}$$

We have denoted the spectral density for the attractive portion of the interaction by $E(\omega)$. We are primarily interested in the effects of spin fluctuations in suppressing superconductivity. As such, we assume that there is an attractive interaction, due to some boson exchange, and we will denote the spectral density of that interaction by $E(\omega)$. We present calculations for this model in Chapter 4.

As mentioned previously, Millis *et al.* were interested in d-wave solutions. We will now discuss their model. They assume that $\chi_2(\vec{p},\omega_m)$ may be written in the separable form

$$\chi_2(\vec{p},\omega_m) = \chi_o(\vec{p})\Phi(\omega_m) \tag{3.15}$$

where $\mathcal{X}_o$ is the static susceptibility and they employ a spectral representation for $\Phi(\omega_m)$

$$N(0)I^2\Phi(\omega_m) = \int_0^\infty \frac{2\omega A(\omega)}{\omega^2+\omega_m^2}d\omega \tag{3.16}$$

That the susceptibility may be written this way was motivated by experiments in the heavy fermion superconductors. Neutron scattering data has been fit with such a separable form for UPt_3[108]. Norman[107] has also used such a form in his calculations for this material, and he obtained reasonable agreement with experiment.

Millis *et al.* consider a case where $D(\vec{p},\omega_m) = 0$ and they assume the following for the susceptibility

$$I^2\mathcal{X}_o(\vec{p}) = J_0 - J_1\gamma(\vec{p}) \tag{3.17}$$

with

$$\gamma(\vec{p}) = 2(cosp_xa + cosp_ya + cosp_za) \tag{3.18}$$

They also assume a separable form for the gap functions

$$\Delta(\vec{p},\omega_m) = \Delta(\omega_m)\eta(\vec{p}) \tag{3.19}$$

They assume that $\eta(\vec{p})$ is a function with d symmetry. One explicit form for $\eta(\vec{p})$ that they consider is

$$\eta(\vec{p}) = \sqrt{6}(cosp_xa - cosp_ya) \tag{3.20}$$

However, it suffices to impose the following conditions upon $\eta(\vec{p})$

$$\begin{aligned}\int_{SF}\frac{dS_p}{|\vec{v}_p|}\eta(\vec{p}) &= 0\\ \int_{SF}\frac{dS_p}{|\vec{v}_p|}\eta^2(\vec{p}) &= 1\end{aligned} \tag{3.21}$$

Putting these assumptions into equations 3.10, one arrives at the following equations for a d-wave superconductor

$$Z(i\omega_n)\Delta(\omega_n) = g\pi T \sum_{m=-\infty}^{\infty} \lambda(m-n)\frac{\Delta(i\omega_m)}{\sqrt{\Delta^2(i\omega_m)+\omega_m^2}} \tag{3.22a}$$

and

$$Z(i\omega_n) = 1 + \frac{\pi T}{\omega_n} \sum_{m=-\infty}^{\infty} \lambda(m-n)\frac{\omega_m}{\sqrt{\Delta^2(i\omega_m)+\omega_m^2}} \tag{3.22b}$$

where

$$g = \frac{\int \frac{dS_p}{|\vec{v}_p|}\frac{dS_k}{|\vec{v}_k|}\eta(\vec{p})\eta(\vec{k})I^2\mathcal{X}_0(\vec{p}-\vec{k})}{\int \frac{dS_p}{|\vec{v}_p|}\frac{dS_k}{|\vec{v}_k|}I^2\mathcal{X}_0(\vec{p}-\vec{k})} \tag{3.22c}$$

and

$$\lambda(m) = 2\int_0^{\infty} \frac{\omega A(\omega)}{\omega^2+\omega_m^2}d\omega \tag{3.22d}$$

In arriving at this result, it is necessary to neglect the momentum dependence in the square root denominators. As a result, we would only expect these equations to be valid for $T = T_c$

Returning to equations 3.13, we note that if the functions $E(\omega)$ and $P(\omega)$ have the same frequency dependence, then 3.13 are of the same form as 3.22.

In this chapter we consider the case in which the frequency dependence of $E(\omega)$ and $P(\omega)$ is the same, but the strength of the interactions are different. This form has the advantage that one can readily obtain analytical results for limiting cases. The equations which we will now study are

$$\Delta(i\omega_n)Z_s(i\omega_n) = g\pi T \sum_{m=-\infty}^{\infty} \lambda(m-n)\frac{\Delta(i\omega_m)}{\sqrt{\Delta^2(i\omega_m)+\omega_m^2}} \tag{3.23a}$$

$$\omega_n Z_s(i\omega_n) = \omega_n + \pi T \sum_{m=-\infty}^{\infty} \lambda(m-n)\frac{\omega_m}{\sqrt{\Delta^2(i\omega_m)+\omega_m^2}} \tag{3.23b}$$

$$\lambda(m-n) = 2\int_0^{\infty} \frac{\omega\, A_2(\omega)}{\omega^2+(\omega_m-\omega_n)^2}d\omega \tag{3.23c}$$

In this case, the parameter g is given by

$$\begin{aligned} E(\omega) + P(\omega) &= A(\omega) \\ E(\omega) - P(\omega) &= gA(\omega) \end{aligned}, \qquad (3.23d)$$

and it is a measure of the relative strengths of the two interactions, with $g = 1$ being the purely attractive case, and $g = -1$ being the purely repulsive case.

3.3 CRITICAL TEMPERATURE

We start by considering the limit in which $\frac{T_c}{\omega_{ln}} - 0$, which is referred to as the weak coupling or BCS limit. In this limit one can make a square-well approximation for the $\lambda(m-n)$[25]

$$\lambda(m-n) = \begin{cases} \lambda(0), if & |\omega_n|, |\omega_m| < \omega_c; \\ 0, & |\omega_n|, |\omega_m| > \omega_c, \end{cases} \qquad (3.24)$$

where ω_c is some maximum frequency. In the BCS theory, ω_c is taken to be ω_D, the Debye frequency. Using this model in equation 3.23b one obtains

$$Z(i\omega_n) = 1 + \lambda \qquad (3.25)$$

Substituting this result in 3.23a and using the approximation for the $\lambda(m-n)$, one obtains

$$\Delta(T) = \pi T \frac{g\lambda}{1+\lambda} \sum_{m=-N_c}^{N_c} \frac{\Delta(T)}{\sqrt{\Delta^2(T) + \omega_m^2}} \qquad (3.26)$$

This equation can be solved for T_c to give

$$k_B T_c = \hbar\omega_c 1.13 e^{-\frac{1+\lambda}{g\lambda}} \qquad (3.27)$$

This form illustrates the suppression of T_c as we increase the coupling to the spin fluctuations. This can be seen more clearly by considering the functional derivative of the critical temperature with respect to the spectral density

function. The calculation is presented in some detail, as it is fairly straightforward, and offers some insight into the relationship between the Eliashberg formalism and the BCS results. We will also obtain equation 3.27, the T_c equation.

The functional derivative is calculated by adding an infinitesimal piece to $A(\omega)$ and calculating the change, to first order, in the quantity of interest. Hence, we set

$$\begin{aligned} A(\omega) &\rightarrow A(\omega) + \epsilon\delta(\omega - \omega_o) \\ \lambda(m-n) &\rightarrow \lambda(m-n) + \epsilon \frac{2\omega_o}{\omega_o^2 + (\omega_m - \omega_n)^2} \end{aligned} \tag{3.28}$$

We perform our calculations at T_c, where all of the Δ_n are zero. Hence, we need only consider the linearized versions of 3.23a and 3.23b. Putting 3.28 into 3.23b, and using the model of 3.24 for $\lambda(m-n)$, one obtains

$$Z(i\omega_n)|\omega_n| = |\omega_n|(1+\lambda) + \epsilon\pi T \sum_{m=-\infty}^{\infty} \frac{2\omega_o}{\omega_o^2 + (\omega_m - \omega_n)^2} sign(\omega_n\omega_m) \tag{3.29}$$

From 3.23a, we obtain, to first order in ϵ,

$$\begin{aligned} \tilde{\Delta}(i\omega_n) = \pi T \frac{g\lambda}{1+\lambda} \sum_{m=-N_c}^{N_c} \frac{\tilde{\Delta}(i\omega_m)}{|\omega_m|} - \epsilon(\pi T)\frac{g\lambda}{(1+\lambda)^2} \sum_{m=-N_c}^{N_c} \frac{\tilde{\Delta}(i\omega_m) f_m}{\omega_m^2} \\ + \epsilon \frac{g\pi T}{1+\lambda} \sum_{m=-N_c}^{N_c} \frac{2\omega_o}{\omega_o^2 + (\omega_m - \omega_n)^2} \frac{\tilde{\Delta}(i\omega_m)}{|\omega_m|} \end{aligned} \tag{3.30}$$

where $f_m \equiv \pi T \sum_{m'=-\infty}^{\infty} \frac{2\omega_o}{\omega_o^2 + (\omega_m - \omega_{m'})^2} sign(\omega_m\omega_{m'})$ and $\tilde{\Delta}(i\omega_n) \equiv Z(i\omega_n)\Delta(i\omega_n)$.

All of the n dependence in the right-hand side of 3.30 is contained in the infinitesimal piece. Therefore, we write,

$$\tilde{\Delta}(i\omega_n) = \Delta + \epsilon\delta_n$$

where,

$$\Delta = \pi T \frac{g\lambda}{1+\lambda} \sum_{m=-N_c}^{N_c} \frac{\tilde{\Delta}(i\omega_m)}{|\omega_m|},$$

$$\delta_n \equiv -\pi T \frac{g\lambda}{(1+\lambda)^2} \sum_{m=-N_c}^{N_c} \frac{\tilde{\Delta}(i\omega_m) f_m}{\omega_m^2} + \frac{g\pi T}{1+\lambda} \sum_{m=-N_c}^{N_c} \frac{2\omega_o}{\omega_o^2 + (\omega_m - \omega_n)^2} \frac{\tilde{\Delta}(i\omega_m)}{|\omega_m|} \tag{3.31}$$

Substituting 3.31 into 3.30 and canceling Δ, one obtains

$$\begin{aligned} \frac{1+\lambda}{g\lambda} = \pi T \sum_{m=-N_c}^{N_c} \frac{1}{|\omega_m|} - \epsilon(\pi T)^2 \frac{g\lambda}{(1+\lambda)^2} \sum_{m=-N_c}^{N_c} \sum_{m'=-N_c}^{N_c} \frac{f_m}{|\omega_m|^2} \frac{1}{|\omega_{m'}|} \\ + \epsilon g \frac{(\pi T)^2}{1+\lambda} \sum_{m=-N_c}^{N_c} \sum_{m'=-N_c}^{N_c} \frac{1}{|\omega_m|} \frac{1}{|\omega_{m'}|} \frac{2\omega_o}{\omega_o^2 + (\omega_m - \omega_{m'})^2} \end{aligned} \tag{3.32}$$

To obtain the unperturbed critical temperature, we set $\epsilon = 0$. Then

$$\begin{aligned} \frac{1+\lambda}{g\lambda} = \pi T \sum_{m=-N_c}^{N_c} \frac{1}{|\omega_m|} = \psi(N_c + \frac{1}{2}) - \psi(\frac{1}{2}) \simeq \ln(\frac{2e^{\gamma}\omega_c}{\pi T_c}) \\ k_B T_c = 1.13 \hbar \omega_c e^{(-\frac{1+\lambda}{g\lambda})} \end{aligned} \tag{3.33}$$

In 3.33, ψ is the digamma function, and for large x, $\psi(x) \simeq \ln(x)$.

We can now use the result of 3.33 in 3.32 to get

$$\begin{aligned} \ln(\frac{T_c + \delta T_c}{T_c}) \simeq \frac{\delta T_c}{T_c} = \epsilon g \frac{(\pi T_c)^2}{1+\lambda} \sum_{m=-N_c}^{N_c} \sum_{m'=-N_c}^{N_c} [\frac{1}{|\omega_m|} \frac{1}{|\omega_{m'}|} \frac{2\omega_o}{\omega_o^2 + (\omega_m - \omega_{m'})^2} \\ - \frac{g\lambda}{1+\lambda} \sum_{m''=-N_c}^{N_c} \frac{1}{|\omega_m|^2} \frac{1}{|\omega_{m'}|} \frac{2\omega_o sign(\omega_m \omega_{m''})}{\omega_o^2 + (\omega_m + \omega_{m''})^2}] \\ = \frac{\epsilon}{1+\lambda} \sum_{m=-N_c}^{N_c} \sum_{m'=-N_c}^{N_c} \frac{1}{|2m-1|} \frac{2\omega_o}{\omega_o^2 + (\omega_m - \omega_{m'})^2} \\ [\frac{g}{|2m'-1|} - \frac{sign(\omega_m \omega_{m''})}{|2m-1|}] \end{aligned} \tag{3.34}$$

This then yields the functional derivative as

$$\begin{aligned} \frac{\delta T_c}{\partial A(\bar{\omega})} = \frac{1}{1+\lambda} G(\bar{\omega}) \quad , \quad \bar{\omega} \equiv \frac{\omega_o}{T_c} \\ G(\bar{\omega}) = \sum_{m=-\infty}^{\infty} \sum_{m'=-\infty}^{\infty} \frac{1}{|2m-1|} \frac{2\bar{\omega}}{\bar{\omega}^2 + 4\pi^2(m-m')^2} [\frac{g}{|2m'-1|} - \frac{siyn(\omega_m \omega_{m'})}{|2m-1|}] \end{aligned} \tag{3.35}$$

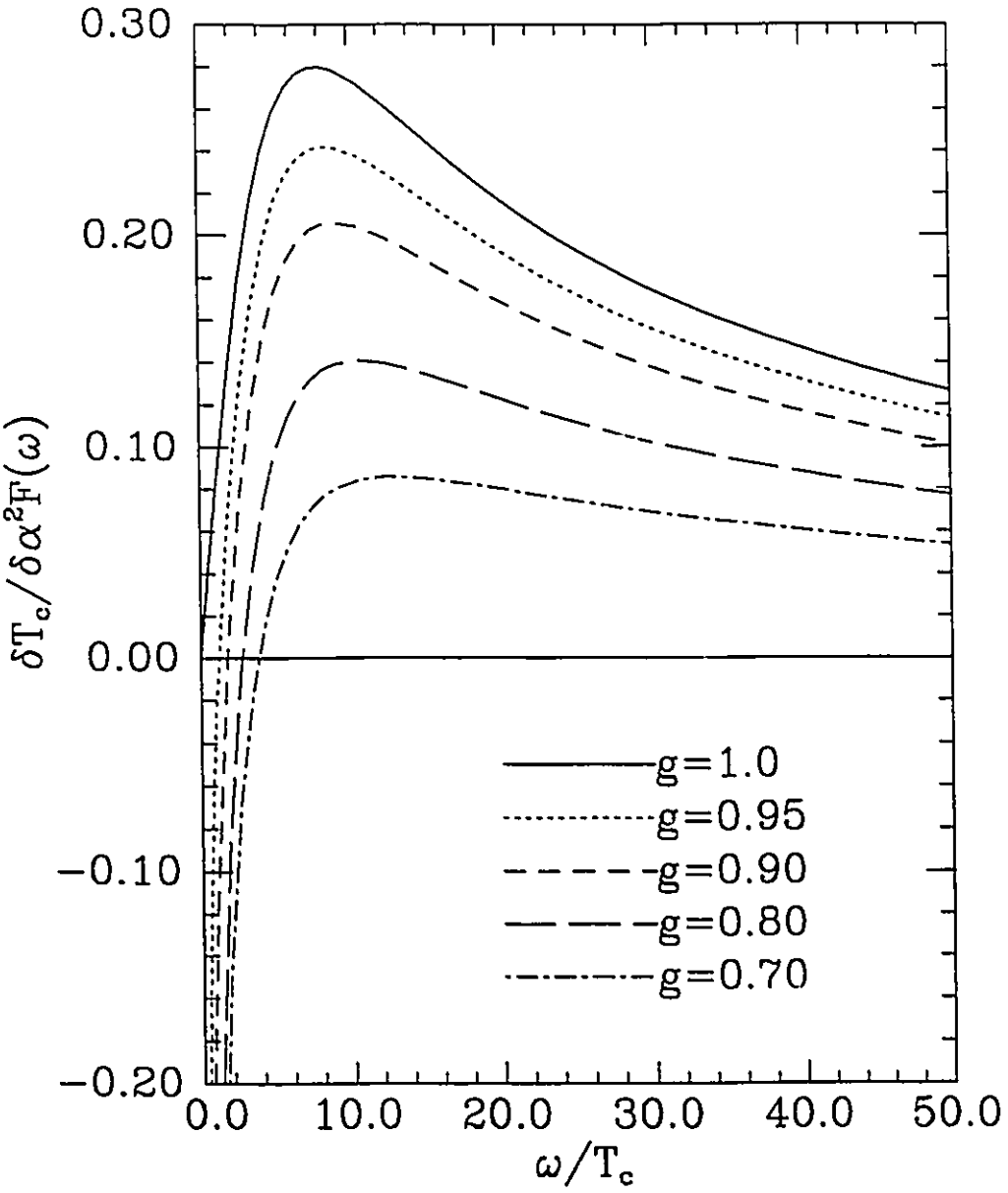

Figure 3.2-The functional derivative of the critical temperature with respect to the electron-boson spectral density, $\frac{\delta T_c}{\partial A(\omega)}$, as given by equation 3.35. For g≠1, there is a negative divergence at low frequencies. For $g = 1$, the curve is everywhere positive definite.

We have relaxed the cutoffs in our sums since they no longer diverge. This also gives the functional derivative as a material independent function $G(\bar{\omega}, g)$, times a prefactor $\frac{1}{1+\lambda}$. If we set g = 1, we recover the result for a superconductor with only attractive interactions[25].

In Figure 3.2, we plot $G(\bar{\omega}, g)$ for various values of g. For g = 1, the curve is everywhere positive, as discussed previously. For g≠1, the curves exhibit a zero crossing at some frequency, ω_{zc}, and diverge negatively as $\omega \to 0$.

The negative divergence of functional derivatives tells us that the low frequency modes are pair breaking. In the case of the d-wave model, it is the same excitations which appear in both the particle-particle channel and the particle-hole channel, although the coupling is weaker in the particle-particle channel. Within this context, the same excitations which bring about the superconductivity are pair breaking at low frequencies. This is distinctly different from the conventional phonon case, given by g = 1.

We also note that as g gets smaller, ω_{zc} gets larger. Numerical work[8] has shown that for g sufficiently small, $\ln\frac{\omega_{zc}}{T_c} \propto \frac{1}{g}$. This relation restricts the values of $\frac{T_c}{\omega_{ln}}$ which one can obtain within this model. As $g \to 0$, $\ln\frac{\omega_{zc}}{T_c} \to \infty$. If we wish to obtain a finite T_c, we must put most of our spectral weight above ω_{zc}. This drives $\frac{T_c}{\omega_{ln}} \to 0$. For example, for g = 0.15, the largest value of $\frac{T_c}{\omega_{ln}}$ we could obtain numerically was 0.001. This brings us very close to the BCS regime.

3.4 THERMODYNAMICS

We now consider the thermodynamics of this system. We will first show that near T_c, the free energy difference is independent of g in the BCS limit. Again,

we will show the calculation in some detail as it is illustrative of subsequent calculations, particularly the strong coupling corrections.

The approach that one takes to calculate the free energy difference, near T_c, is to expand the Eliashberg equations and the free energy difference in powers of $\frac{\Delta_n}{\omega_n}$. The free energy difference goes to zero at T_c as $(\frac{\Delta_n}{\omega_n})^4$. In order to calculate any thermodynamics at T_c, it suffices to determine $(\frac{\Delta_n}{\omega_n})$ to lowest order. We therefore expand 3.23 to obtain

$$\begin{aligned}\tilde{\Delta}(i\omega_n) &= g\pi T \sum_{m=-\infty}^{\infty} \lambda(m-n)\frac{\tilde{\Delta}(i\omega_m)}{|\tilde{\omega}(i\omega_m)|}[1 - \frac{1}{2}(\frac{\tilde{\Delta}(i\omega_m)}{\tilde{\omega}(i\omega_m)})^2 + \quad \ldots \quad] \\ \tilde{\omega}(i\omega_n) &= \omega_m + \pi T \sum_{m=-\infty}^{\infty} \lambda(m-n)sign(\omega_m)[1 - \frac{1}{2}(\frac{\tilde{\Delta}(i\omega_m)}{\tilde{\omega}(i\omega_m)})^2 + \quad \ldots \quad]\end{aligned} \tag{3.36}$$

We now apply the $\lambda^{\theta\theta}$ model (equation 3.24) to 3.36, giving

$$1 = A(T) - C(T)\Delta^2(T) \tag{3.37a}$$

$$A(T) = g\pi T\frac{\lambda}{1+\lambda}\sum_{m=-N_c}^{N_c}\frac{1}{|\omega_m|} \approx g\frac{\lambda}{1+\lambda}\ln(\frac{1.13\omega_c}{k_BT}) \tag{3.37b}$$

$$C(T) = g\frac{\pi T}{2}\frac{\lambda}{1+\lambda}\sum_{m=-\infty}^{\infty}\frac{1}{|\omega_m|^3} = g\frac{7}{8}\frac{\lambda}{1+\lambda}\frac{\zeta(3)}{(\pi T)^2} \tag{3.37c}$$

At $T = T_c$, $\Delta(T_c) = 0$, and we obtain our previous result, 3.12.

We now consider the free energy. For this calculation we will use the Bardeen-Stephen formula, 2.16. We expand to lowest order in $(\frac{\Delta_n}{\omega_m})$, treating Δ_n as a constant, to obtain

$$\begin{aligned}\frac{\Delta F}{N(0)} &= \frac{1}{4}\frac{1}{(1+\lambda)^3}\frac{\Delta^4}{(\pi T)^2}\sum_{m=-N_c}^{N_c}\frac{1}{|2m-1|^3} \\ &= \frac{7}{16}\frac{\zeta(3)}{(1+\lambda)^3}\frac{\Delta^4}{(\pi T)^2} \\ &= \frac{1}{2g\lambda}C(T)\Delta^4(T)\end{aligned} \tag{3.38}$$

We now solve for Δ^2 in 3.37, to obtain

$$\Delta^2(T) = -(T-T_c)\frac{\frac{dA}{dT}}{C} \tag{3.39}$$

Putting this result into 3.38 one finds

$$\frac{\Delta F}{N(0)} = \frac{4}{7}(1+\lambda)\frac{\pi^2}{\zeta(3)}(T-T_c)^2 \tag{3.40}$$

which has no explicit g dependence. One can calculate the specific heat jump in this limit, and obtain $\frac{\Delta C}{\gamma T_c}$=1.43. As we shall see later, our numerical work verifies the g independence of the BCS limit.

3.5 SPECIFIC HEAT JUMP

We will now consider how strong coupling effects will alter the specific heat jump. In order to do this, we perform expansions about the BCS limit, using $\frac{T_c}{\omega_c}$ as our expansion parameter. We employ a model for Δ_n and $Z_S(\omega_m)$[32]

$$\begin{aligned} \Delta(i\omega_n) &= \begin{cases} \Delta_o(T), & \text{if } |\omega_n| < \omega_o; \\ \Delta_\infty, & \text{if } |\omega_n| > \omega_o. \end{cases} \\ Z_S(\omega_n) &= \begin{cases} Z_o(T), & \text{if } |\omega_n| < \omega_o; \\ 1, & \text{if } |\omega_n| > \omega_o. \end{cases} \end{aligned} \tag{3.41}$$

These expansions are rather long and tedious. A sketch of the calculation will be given here with details provided in appendix A. Expansion of equations 3.23a and 3.23b yields for $\Delta_o(T)$

$$1 = F(T) + \Delta_o^2(T)G(T) + \Delta_o^4 J(T) \tag{3.42}$$

where

$$\begin{aligned} F(T) &= \frac{g\lambda}{1+\lambda}\ln\left(\frac{1.13\omega_o}{k_B T}\right) - \frac{g\bar{\lambda}}{1+\lambda} - g\frac{(\pi T)^2}{1+\lambda}\left(\bar{a}(T) - \frac{4}{3}\bar{b}\right) \\ G(T) &= -\frac{g\lambda}{1+\lambda}\frac{7}{8}\frac{\zeta(3)}{(\pi T)^2} + \frac{\bar{b}}{1+\lambda}\left(\frac{7}{8}\zeta(3)g - \frac{1}{2}\right) + \frac{\bar{a}(T)}{1+\lambda}\left(1+\frac{g}{2}\right) \\ J(T) &= \frac{g\lambda}{1+\lambda}\frac{93}{128}\frac{\zeta(5)}{(\pi T)^2} - \frac{\zeta(3)}{(\pi T)^2}\frac{\bar{b}}{1+\lambda}\frac{21}{16}\left(1+\frac{g}{2}\right) - \frac{g}{1+\lambda}\frac{93}{128}\frac{\zeta(5)\bar{b}}{(\pi T)^2} \end{aligned} \tag{3.43}$$

These results reduce to the BCS limits if we set $\bar{\lambda}$, $\bar{a}(T)$, and $\bar{b}$ to zero. which are defined by

$$\bar{\lambda} = 2\int_0^\infty d\omega \frac{A(\omega)}{\omega}\ln(1+\frac{\omega_o}{\omega}) \tag{3.44a}$$

$$\bar{a}(T) = 2\int_0^\infty d\omega \frac{A(\omega)}{\omega}\ln(\frac{1.13\omega}{k_B T}) \tag{3.44b}$$

$$\bar{b} = 2\int_0^\infty d\omega \frac{A(\omega)}{\omega^3} \tag{3.44c}$$

In order to calculate the specific heat jump, it is necessary to obtain an expression for the free energy difference. We expand equation 2.16 to find

$$\frac{\Delta F}{N(0)} = \frac{1}{2}\frac{(1+\lambda)^2}{g\lambda}[\Delta_o^4 K(T) + \frac{4}{3}\Delta_o^6 L(T)] \tag{3.45}$$

where

$$K(T) = G_o(T) - \frac{TF_o'(T)}{1+\lambda}[\bar{c}(T) - \bar{a}(T) + \frac{\bar{b}}{4}] \tag{3.46}$$

and

$$L(T) = J_o(T) + \frac{3}{2}\frac{G_o(T)}{1+\lambda}[\bar{a}(T) - \frac{\bar{b}}{2}] \tag{3.47}$$

The subscript "o" is employed to indicate that there are no strong coupling corrections, ie.

$$G_o(T) = -\frac{g\lambda}{1+\lambda}\frac{7}{8}\frac{\zeta(3)}{(\pi T)^2} \tag{3.48}$$

The prime is used to denote differentiation with respect to temperature, T. We have also introduced another moment of the spectral density function $\bar{c}(T)$, given by

$$\bar{c}(T) = 2\int_0^\infty d\omega \frac{A(\omega)}{\omega^3}\ln^2(\frac{1.13\omega}{k_B T}) \tag{3.49}$$

Putting the solution of 3.42 into 3.45, and using 2.17 and 2.18, we obtain the following expression for the specific heat jump

$$\frac{\Delta C}{\gamma T_c} = p - (1-t)q, \quad t = \frac{T}{T_c} \tag{3.50a}$$

$$p = 1.43[1 + a_1(\frac{T_c}{\omega_{ln}})^2 \ln(\frac{\omega_{ln}}{b_1 T_c})] \tag{3.50b}$$

$$q = 3.77[1 + a_2(\frac{T_c}{\omega_{ln}})^2 \ln(\frac{\omega_{ln}}{b_2 T_c})] \tag{3.50c}$$

The coefficients a_i and b_i are functions of g and are given in Appendix A. They are of the form

$$\begin{aligned} a_i &= \alpha_i + \frac{\beta_i}{g} \\ b_i &= e^{\frac{\gamma_i + \frac{\delta_i}{g}}{a_i}} \end{aligned} \tag{3.51}$$

If we set g = 1, these expressions reduce to the results which have been obtained previously by other authors[32]. The α_i, β_i, γ_i, and δ_i, are functions of the $\bar{a}(T)$, $\bar{b}$, $\bar{c}(T)$ which take on definite values for a given spectral density. In our numerical work, we have used delta function spectral densities, in which case these coefficients are readily determined. If we use these specific values in our expression, we do not get particularly good agreement with our numerical results. If we try to fit one of the curves, we are not able to reproduce all of the curves with the same set of parameters. However, we are able to reproduce the trends that are seen in the numerical results. That is, that $\frac{\Delta C}{\gamma T_c}$ gets larger than the BCS value of 1.43 as $\frac{T_c}{\omega_{ln}}$ increases. This occurs for any value of g. In addition, as g is decreased from 1, for a fixed $\frac{T_c}{\omega_{ln}}$, $\frac{\Delta C}{\gamma T_c}$ increases. We show our numerical results in Figure 3.3a, and the anaiytic results in Figure 3.3b. The numerical results were obtained using spectral density functions of the form

$$A(\omega) = A\delta(\omega - \omega_E) \tag{3.52}$$

The calculations were performed by choosing a T_c and an ω_E, and calculating A. We only show results for g relatively close to 1. Our reason for doing this

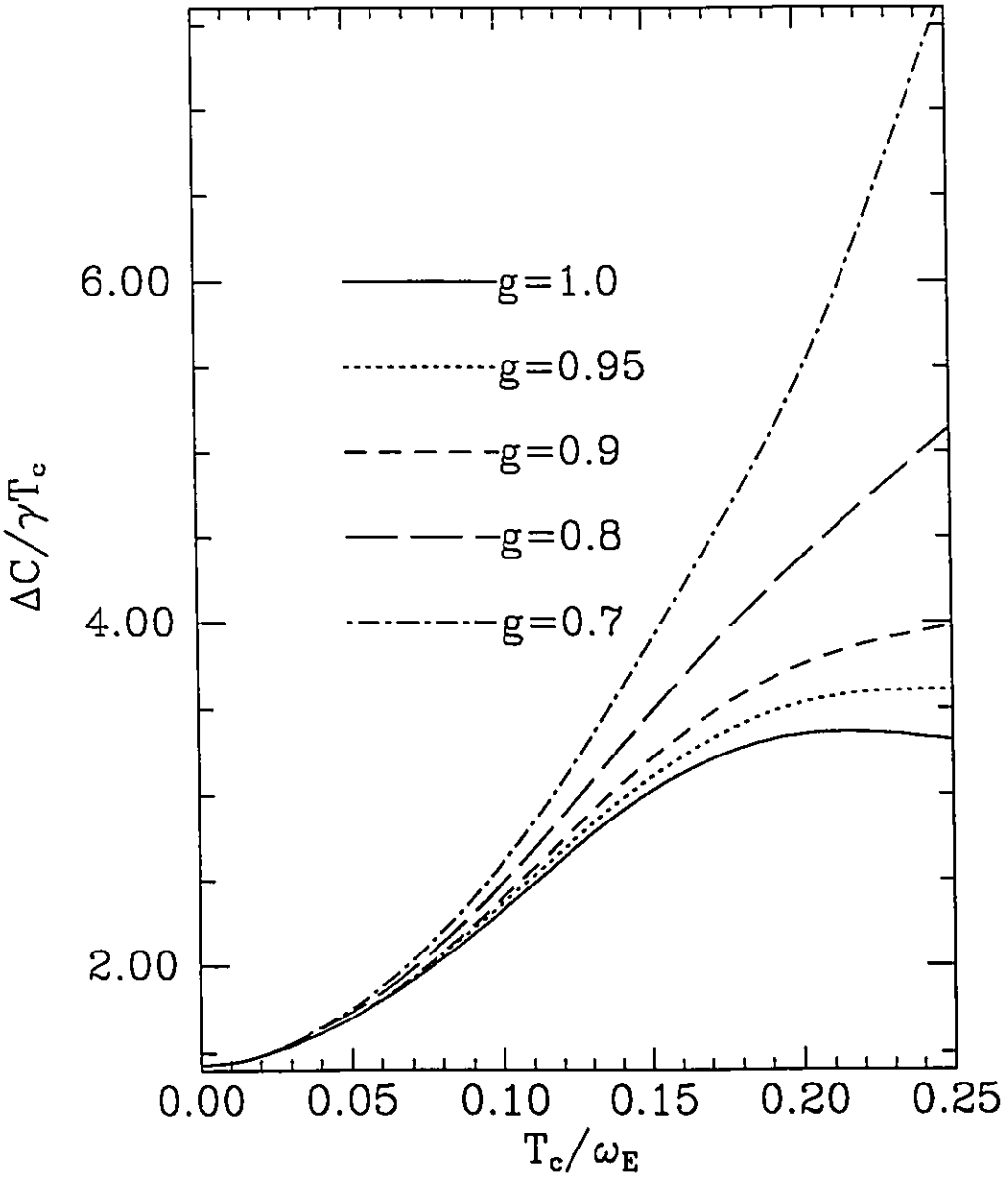

Figure 3.3a-Numerical results for $\frac{\Delta C}{\gamma T_c}$, the specific heat jump, versus $\frac{T_c}{\omega_E}$, for various values of g. Note the strong enhancement of the jump for $g < 1$. Also note the independence of g in the BCS limit, $\frac{T_c}{\omega_E} = 0$.

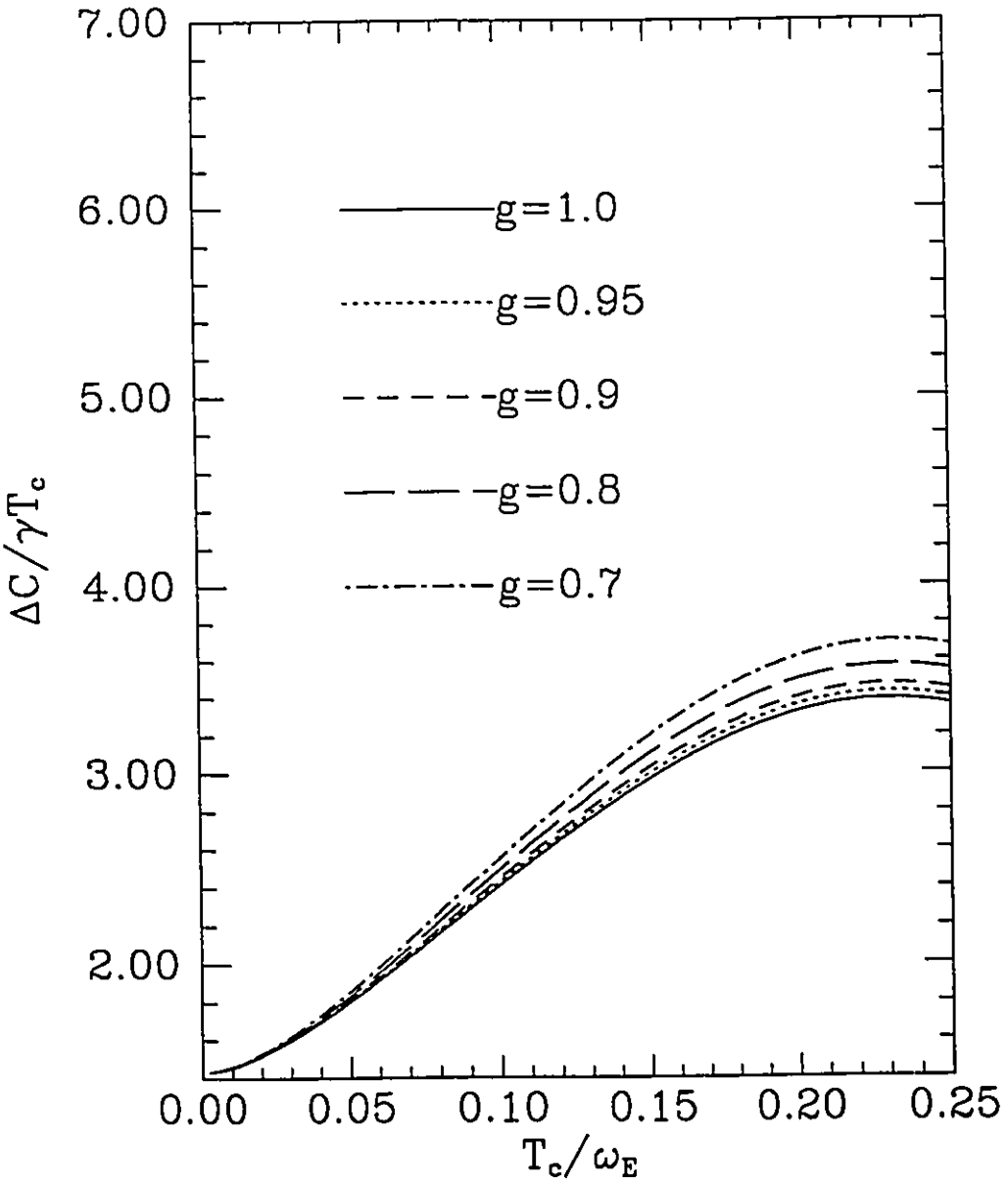

Figure 3.3b-Analytic results for the specific heat jump, $\frac{\Delta C}{\gamma T_c}$, versus $\frac{T_c}{\omega_E}$. We note that the trends of the numerical results are reproduced reasonably well for small $\frac{T_c}{\omega_E}$, but the disagreement becomes more pronounced as $\frac{T_c}{\omega_E}$ increases.

as g gets small, our programs converge much less rapidly. However, we have been able to obtain convergence for g as small as 0.15.

We observe in Figure 3.3a that as $\frac{T_c}{\omega_E} \to 0$, the BCS limit, all of the curves tend to 1.43, the BCS value. This verifies our calculation that the thermodynamics are independent of g in this limit.

From the numerical results, we see that as $\frac{T_c}{\omega_E}$ increases, the curves begin to exhibit some g dependence. When $g = 1$, we obtain the curve for a superconductor in which there are only attractive interactions. This curve steadily increases, has a broad maximum for $\frac{T_c}{\omega_E} \approx 0.2$, and then begins to decrease. The maximum value is ≈ 3.4. Blezius and Carbotte[26] have demonstrated that the maximum value attainable for $\frac{\Delta C}{\gamma T_c}$, where there is no dynamic pair breaking, is ≈ 3.4 for $\mu^* = 0$. As μ^* increases, $\frac{\Delta C}{\gamma T_c}$ also increases slightly, reaching 3.9 for $\mu^* = 0.3$.

As g is decreased from 1, there is a dramatic departure from this behaviour. There is an enhancement of the specific heat jump which becomes more pronounced as $\frac{T_c}{\omega_E}$ increases. For example, with g=0.7, $\frac{T_c}{\omega_E} = 0.26$, we obtain a value of 8.46 for the specific heat jump. We were unable to obtain convergence with g=0.7 and $\frac{T_c}{\omega_E} = 0.27$. This is due to the relation for the zero crossing, ω_{zc}, of the T_c functional derivative, given as

$$\ln\frac{\omega_{zc}}{T_c} \quad \propto \quad \frac{1}{g} \qquad (3.53)$$

This condition restricts the range of $\frac{T_c}{\omega_E}$ for a fixed g. If $\omega_E < \omega_{zc}$, then all of the spectral weight (for an Einstein spectrum) is placed in the frequency regime that is pair-breaking, and no T_c is obtainable.

It is this same effect which controls the maximum value that we are able to obtain for $\frac{\Delta C}{\gamma T_c}$. From figure 3.3a, one might conclude that almost any

value desired could be obtained by either making g quite small, or $\frac{T_c}{\omega_E}$ large. This is not the case. For g=0.6, the largest value of $\frac{T_c}{\omega_E}$ for which our programs converged was 0.18. This yielded a value of 6.12 for $\frac{\Delta C}{\gamma T_c}$, which is less than the maximum value obtained for g=0.7. A rough search gave a maximum value of $\frac{\Delta C}{\gamma T_c} = 9.1$ for g=0.75 and $\frac{T_c}{\omega_E} = 0.31$.

These results are distinctly different from those obtained by Blezius and Carbotte, and would be a clear signature of a system in which there are two competing dynamical mechanisms.

When we compare our analytic form of 3.50 with the numerical results, we see that for small $\frac{T_c}{\omega_E}$, the trends are reproduced quite well. As $\frac{T_c}{\omega_E}$ gets larger however, we see greater disagreement. In fact, the numerical results continue to grow, while the analytic form starts to turn over. It would seem that our expansion is starting to fail in this regime.

In order to gain more insight into the enhancement of the specific heat jump, we will now consider the functional derivative of $\frac{\Delta C}{\gamma T_c}$. We would expect the derivative to be large and positive at low frequencies, reflecting the large enhancements observed for large $\frac{T_c}{\omega_{ln}}$.

The quantity that we will consider is

$$\frac{1}{\gamma}\frac{\delta}{\partial A(\omega)}\frac{\Delta C}{\gamma T_c} \tag{3.54}$$

We have removed the $\frac{1}{\gamma}$ factor from the derivative, as it diverges negatively at low frequencies. An explicit formula for the specific heat functional derivative has been given by Marsiglio *et al.* [42]. In deriving their expression, they have use the fact that the Wada expression, equation 2.14, is stationary with

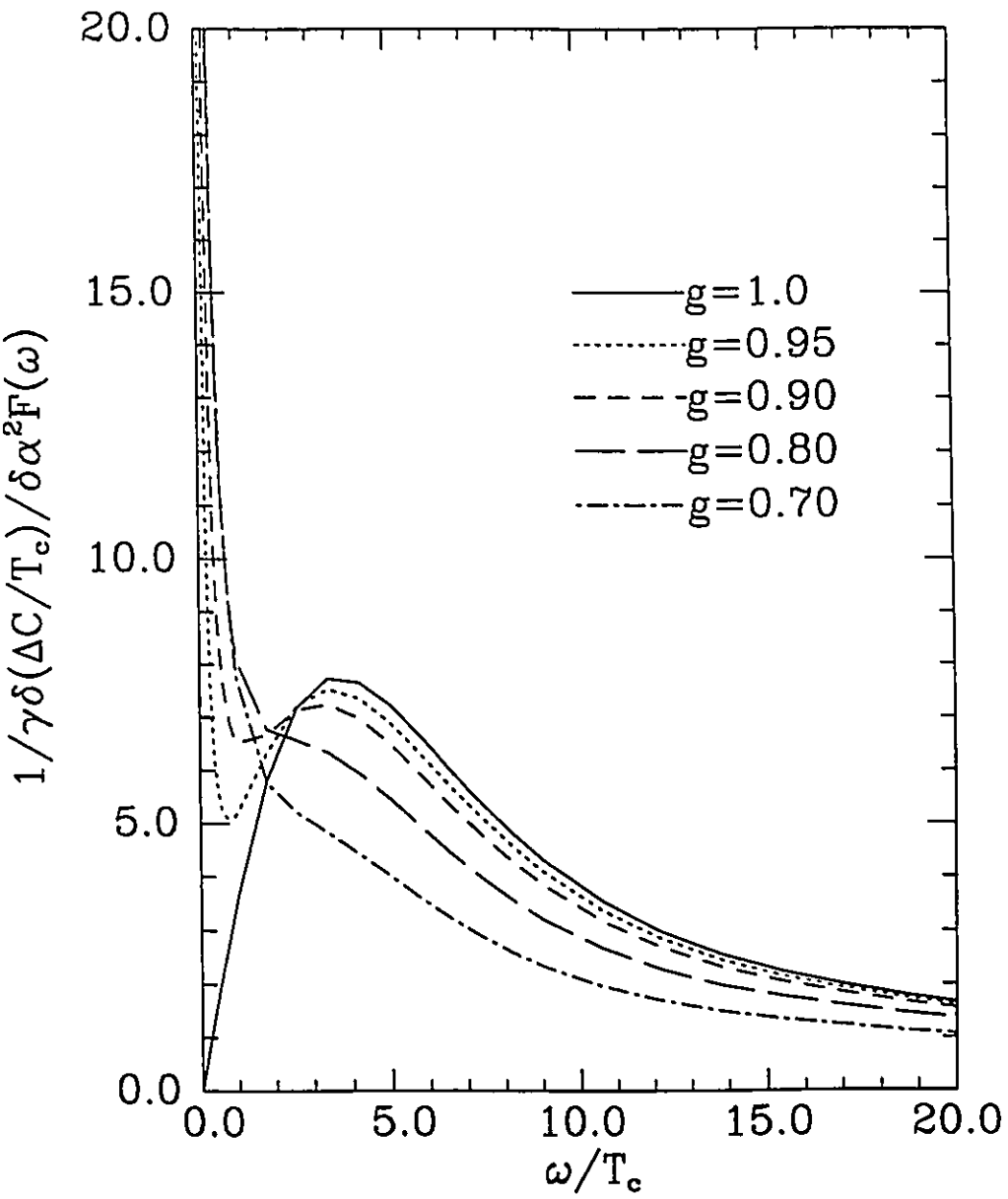

Figure 3.4-Functional derivative of the specific heat jump. For g<1, the curves diverge positively at low frequencies. This is related to the enhancement of the specific heat observed in figure 3.3a. The onset of the divergence shifts to larger frequency as g becomes smaller.

respect to variations in both $\tilde{\Delta}(i\omega_n)$ and $\tilde{\omega}(i\omega_n)$. We have generalized their result to include the competing interactions. The resulting expression is[43]

$$\frac{1}{\gamma}\frac{\delta\frac{\Delta C}{T_c}}{\partial A(\omega)} = -\frac{N(0)}{\gamma}\frac{T}{T_c}\frac{d^2}{dT^2} \times \Big[(\pi T)^2 \sum_{n=-\infty}^{\infty}\sum_{m=-\infty}^{\infty}\Big[\frac{\tilde{\omega}(i\omega_n)}{\sqrt{\tilde{\Delta}^2(i\omega_n)+\tilde{\omega}^2(i\omega_n)}}\frac{\tilde{\omega}(i\omega_m)}{\sqrt{\tilde{\Delta}^2(i\omega_m)+\tilde{\omega}^2(i\omega_m)}} - sign(\omega_n\omega_m) + g\frac{\tilde{\Delta}(i\omega_n)}{\sqrt{\tilde{\Delta}^2(i\omega_n)+\tilde{\omega}^2(i\omega_n)}}\frac{\tilde{\Delta}(i\omega_m)}{\sqrt{\tilde{\Delta}^2(i\omega_m)+\tilde{\omega}^2(i\omega_m)}}\Big] \times \Big[\frac{2\omega_o}{\omega_o^2+(\omega_n-\omega_m)^2} - \frac{2}{T_c}(\omega_n-\omega_m)^2\frac{\delta T_c}{\partial A(\omega)} \times \int_0^\infty \frac{2\omega' A(\omega')\,d\omega'}{[\omega'^2+(\omega_n-\omega_m)^2]^2}\Big]\Big] \tag{3.55}$$

In order to evaluate this expression, we also need the T_c functional derivative, which we have already discussed. We have solved 2.3a and 2.3b numerically, and used the results in 3.55. We show in figure 3.4 the results for the same set of g values as in figure 3.3a.

The solid curve, corresponding to $g = 1$, goes to zero at both low and high frequencies, and displays a maximum at $\frac{\omega}{T_c} \approx 4.0$. This corresponds to $\frac{T_c}{\omega} \approx 0.25$, which is close to the position of the maximum value of $\frac{\Delta C}{\gamma T_c}$ in figure 3.3 for the $g = 1$ case. We note that the maximum of the specific heat jump derivative occurs at a lower frequency than the maximum of the T_c derivative. Therefore, it is not possible to maximize these two quantities simultaneously.

As g is decreased from 1, we see that there is a positive divergence at low frequencies in the derivative. This implies that low frequency modes strongly enhance the normalized specific heat jump. This is the opposite to what was found in the T_c functional derivative. For g= 0.95, we note that

as $\frac{\omega}{T_c}$ decreases, there is a local maximum at some finite frequency, a local minimum, and then the curve diverges once we are sufficiently close to zero frequency. As g is decreased, the local minimum begins to disappear, and the local maximum tends to be swamped by the divergence. This would be consistent with the onset of the divergence shifting to higher frequencies as g is decreased, as was found for the derivative of the critical temperature.

For larger values of $\frac{\omega}{T_c}$, we note that the derivative decreases in magnitude as g decreases. This would seem to be at variance with the fact that as g decreases, $\frac{\Delta C}{\gamma T_c}$ increases. However, it is felt that as the jump is increased as a result of decreasing g, it is tending to its maximum possible value, and it is becoming difficult to increase it further. An analogous situation occurs in the functional derivatives of $\frac{\Delta C}{\gamma T_c}$ for systems with paramagnetic impurities[44]. As the concentration of paramagnetic impurities is increased, $\frac{\Delta C}{\gamma T_c}$ decreases. However, the functional derivative of $\frac{\Delta C}{\gamma T_c}$ is enhanced.

3.6 SLOPE OF THE SPECIFIC HEAT JUMP

Unfortunately, it is very difficult to determine $\frac{\Delta C}{\gamma T_c}$ experimentally. One of the reasons for this difficulty is that γ, the coefficient of the linear term in the normal state specific heat, is not well known. As such, it would be desirable to calculate a quantity related to the specific heat that is independent of γ. We have calculated the slope of the specific heat at T_c, normalized to the jump itself

$$T_c \frac{\frac{d\Delta C}{dT}}{\Delta C} \tag{3.56}$$

We have multiplied by T_c in order to obtain a dimensionless quantity.

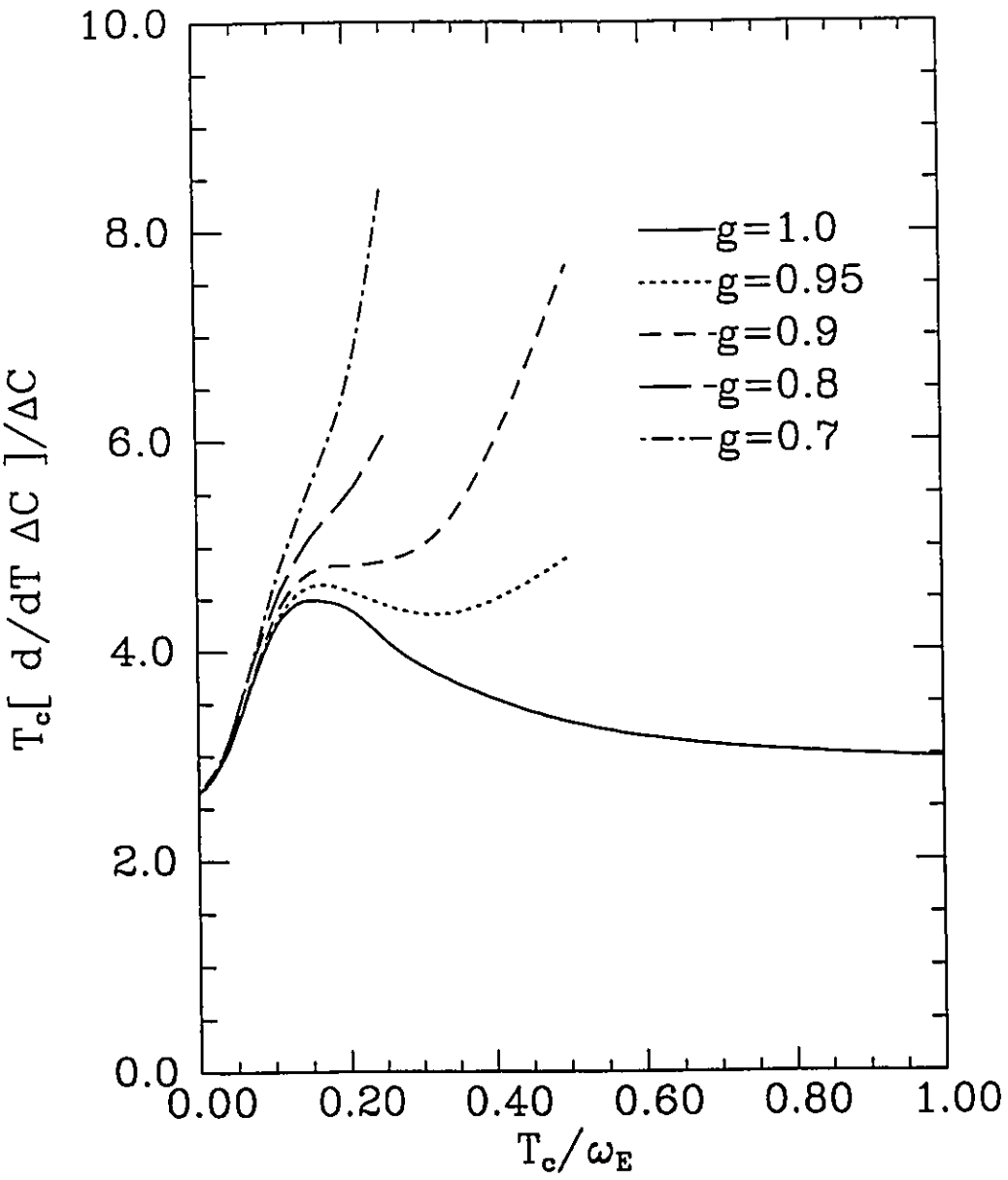

Figure 3.5-Numerical results for normalized slope of the specific heat jump versus $\frac{T_c}{\omega_E}$. For g<1, there is significant enhancement over the $g = 1$ results. This quantity is independent of γ, the normal state specific heat parameter.

We will present only numerical results for this quantity. Although we did obtain analytic expression for both of the quantities needed for this ratio in our strong coupling calculations, we feel that the ratio of the two would be particularly sensitive to the fitted parameters. Since we were only able to obtain qualitative agreement between the analytic expressions and the numerical results, it would seem that the ratio of the analytic expressions would be of dubious merit.

In figure 3.5 we show our numerical results for the normalized slope versus $\frac{T_c}{\omega_E}$ for the same set of g values as in the two previous figures. The solid curve is the $g = 1$ case. It starts out at the BCS value of 2.64 at $\frac{T_c}{\omega_E} = 0$. It increases fairly rapidly to a maximum value of$\approx$ 4.5 for $\frac{T_c}{\omega_E} \approx 0.18$, and then decreases, falling slightly below 3 at $\frac{T_c}{\omega_E} = 1.0$. The $g = 1$ case has been studied by Akis and Carbotte[45], who have also included μ^* in their calculations. We have set μ^* to zero in all of our work. For $\mu^* = 0$, Akis and Carbotte obtain a maximum value of 4.6 for the normalized slope. This increases to approximately 5.0 for $\mu^* = 0.4$. When g$\neq$1, we again see significant departure from the $g = 1$ behaviour. For $\frac{T_c}{\omega_E} = 0$, all the curves converge to the BCS value, as expected. As $\frac{T_c}{\omega_E}$ increases however, we see an enhancement of the normalized slope. As g is decreased, the normalized slope is enhanced quite significantly above the $g = 1$ values. The largest value that we achieved, again without an exhaustive search, occurred for $g = 0.78$ and $\frac{T_c}{\omega_E} = 0.344$. For these parameters, we found $T_c\frac{\Delta C'}{\Delta C} = 9.75$, which is more than twice the maximum observed with $g = 1$. We point out that it is not possible to increase this quantity indefinitely, for the same reasons that were outlined in our discussion of the specific heat jump itself.

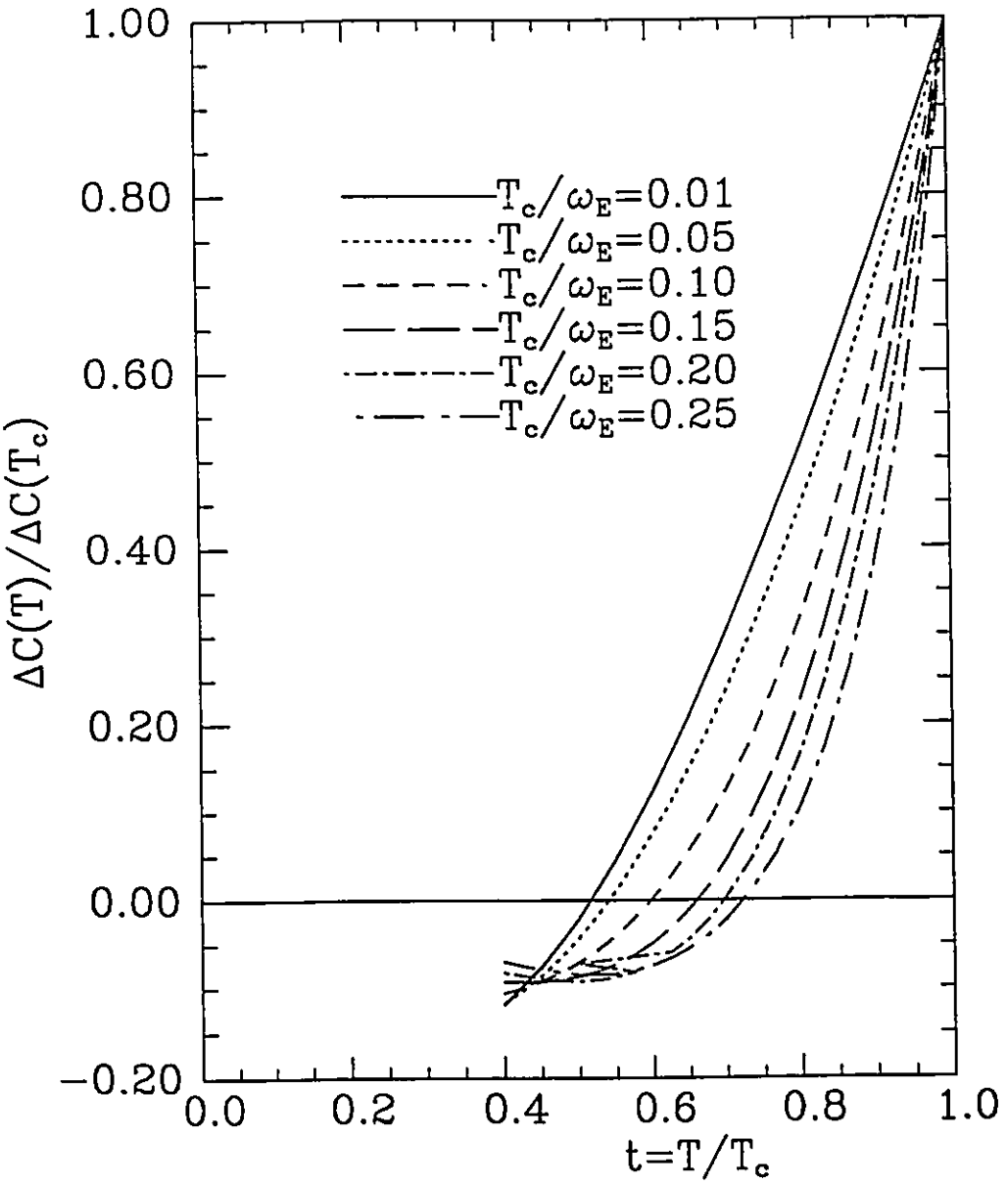

Figure 3.6-Numerical results for the normalized specific heat difference $\frac{\Delta C(T)}{\Delta C(T_c)}$ versus reduced temperature t. For all the curves, g=0.7. As $\frac{T_c}{\omega_E}$ increases, the slope below T_c becomes steeper, and the zero crossing shifts to larger reduced temperature.

Associated with the steep slope of the specific heat difference below T_c is the zero crossing of the specific heat difference. We would expect that the zero crossing might shift to higher temperatures due to the relation for the change in entropy, ΔS,

$$\Delta S = \int_0^{T_c} \frac{\Delta C}{T} dT = 0 \tag{3.57}$$

If the jump becomes large, the zero crossing may shift to higher reduced temperature to satisfy this constraint. We have calculated the specific heat difference below T_c and show our results in figure 3.6. We chose to fix g=0.7, and we plot curves for various values of $\frac{T_c}{\omega_{ln}}$. The figure clearly exhibits the steepening of the slope below T_c as $\frac{T_c}{\omega_{ln}}$ is increased. We also observe a shift to larger reduced temperature of the zero crossing. The maximum value found in the figure is $t = 0.72$ for $\frac{T_c}{\omega_E} = 0.25$. This is larger than the values which are obtained with $g = 1$, which are typically ~ 0.65[45].

3.7 ENERGY GAP

We have also considered the ratio of twice the zero temperature gap edge to the critical temperature, $\frac{2\Delta(0)}{k_B T_c}$. In order to do this, we must extend our calculation to zero temperature. This is accomplished by making the substitution

$$\pi T \sum_{n=-\infty}^{\infty} F(\omega_n) \rightarrow \int_{-\infty}^{\infty} F(\omega) d\omega \tag{3.58}$$

Numerically, one can never actually calculate at zero temperature. In our numerical calculation, we cut off the sums at some large, finite value, which is determined by increasing the cutoff until the results no longer change

to the desired level of accuracy. This then sets the cutoff frequency, ω_c, which is used to calculate the limits on the sums, N_c, through

$$N_c = \frac{\omega_c}{2\pi T} + \frac{1}{2} \tag{3.59}$$

As $T \to 0$, $N_c \to \infty$, and hence we can only calculate at finite T. We are able to extract the zero temperature results by reducing the temperature until the result is no longer changing. We have performed numerical calculations of the gap ratio as well as strong coupling correction calculations. We show the numerical results in figure 3.7a. All of the curves start at the BCS value of 3.53 for $\frac{T_c}{\omega_E}$=0. For $g = 1$, the curve increases rather smoothly, and reaches a value of ≈ 5.7 for $\frac{T_c}{\omega_E} = 0.25$. We note that the curve gives no indication that it may be starting to turn over. This is in contrast to the results for both the jump and slope of the specific heat. Both of these quantities displayed a maximum and then began to decrease as $\frac{T_c}{\omega_E}$ increased. The gap ratio does not exhibit this behaviour. In fact, it can be shown[46] that the gap ratio continues to increase as $\frac{T_c}{\omega_E}$ increases, and saturates at some finite value as $\frac{T_c}{\omega_E} \to \infty$. This feature allows one to uniquely determine $\frac{T_c}{\omega_E}$ given a value for $\frac{2\Delta(0)}{k_B T_c}$. This cannot be done with specific heat data.

We have also derived a strong coupling formula for the gap ratio for this model. The form of the equation is

$$\frac{2\Delta(0)}{k_B T_c} = 3.54[1 + a(\frac{T_c}{\omega_{ln}})^2 \ln(\frac{\omega_{ln}}{bT_c})] \tag{3.60}$$

The coefficients a_1 and b_1 are functions of g and are given in Appendix A. They are of the form

$$\begin{aligned} a &= \alpha + \frac{\beta}{g} \\ b &= e^{\frac{\gamma + \frac{\delta}{g}}{\alpha}} \end{aligned} \tag{3.61}$$

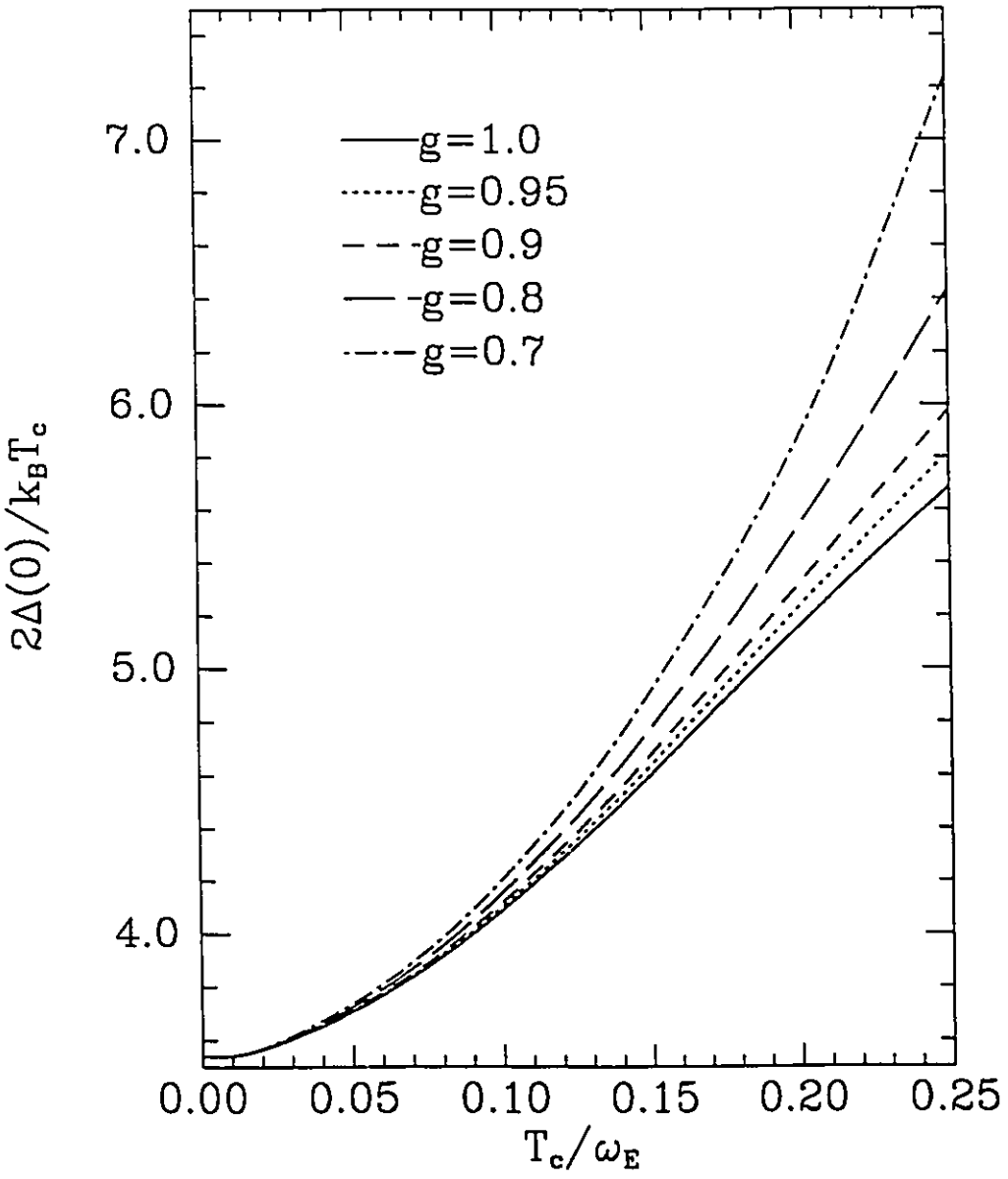

Figure 3.7a-Numerical results for the energy gap ratio, $\frac{2\Delta(0)}{k_B T_c}$, versus $\frac{T_c}{\omega_E}$. The g<1 results are enhanced above the $g = 1$ results for fixed $\frac{T_c}{\omega_E}$. However, the g<1 results never exceed the maximum value of ≈13 found in the $g = 1$ case when $\frac{T_c}{\omega_{ln}} \rightarrow \infty$.

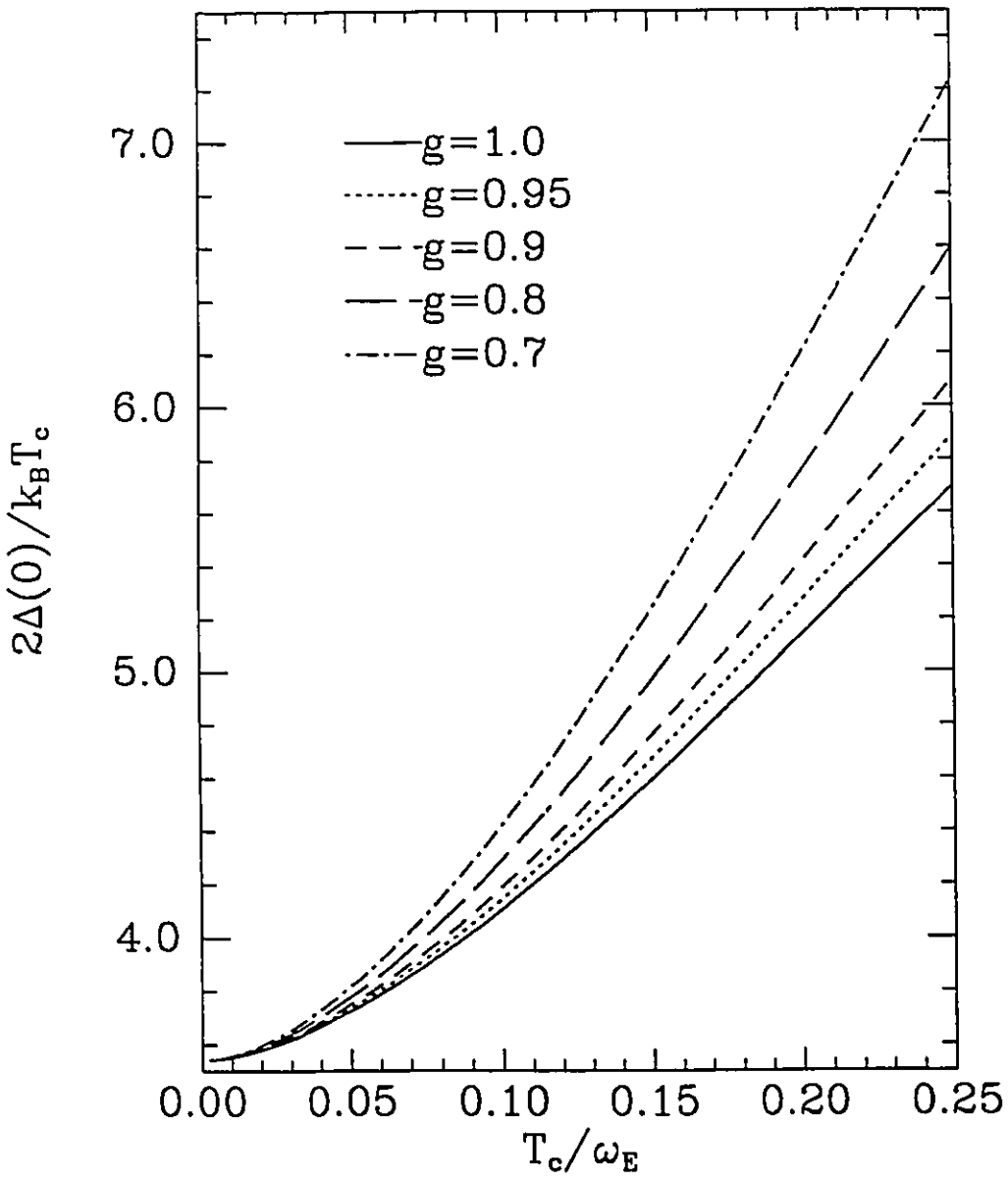

Figure 3.7b-Analytic results for $\frac{2\Delta(0)}{k_B T_c}$ versus $\frac{T_c}{\omega_E}$. We again find, as in the case of the specific heat results, that the trends are reproduced well for small $\frac{T_c}{\omega_E}$, but the agreement becomes poor as $\frac{T_c}{\omega_E}$ increases.

If we set g = 1, these expressions reduce to the results which have been obtained previously by other authors[32]. α, β, γ, and δ are functions of $\bar{a}(T)$, $\bar{b}$, $\bar{c}(T)$ which take on definite values for a given spectral density. As for the specific heat results, our analytic form is not able to capture the quantitative trends of the numerical data well.

As g decreases from 1, we observe an enhancement of the gap ratio above the $g = 1$ values. Our analytic results are displayed in figure 3.7b. We note that they capture this behaviour qualitatively, but the quantitative agreement is not good.

For the gap ratio, we do not see the spectacular enhancement when g≠1 that was observed in our results for the specific heat. This is related to the pair breaking at low frequencies. As g is decreased, we are unable to go to arbitrarily large $\frac{T_c}{\omega_E}$, as discussed previously (see equation 3.53). For g=0.7, the largest value of $\frac{T_c}{\omega_E}$ for which we could obtain convergence was 0.26. At this point, we found $\frac{2\Delta(0)}{k_B T_c} = 7.61$. This is still less than the maximum value of ≈13[53] that is found in the $g = 1$ case, although this maximum only occurs in the limit of λ going to infinity. Nevertheless, a measurement of the gap ratio does not provide us with an unambiguous indication that the system of concern is described by a g≠1 theory. However, if we find a $\frac{\Delta C}{\gamma T_c}$ that is larger than the maximum value for the $g = 1$ case, then it should be possible to ascertain a g and a $\frac{T_c}{\omega_E}$ using both the $\frac{\Delta C}{\gamma T_c}$ and the $\frac{2\Delta(0)}{k_B T_c}$ results.

3.8 ASYMPTOTIC LIMIT

It is also of some interest, albeit perhaps strictly mathematical, to consider the properties of this model in the limit $\lambda \to \infty$. We will only state

results here, and will leave the details of the derivations to a subsequent chapter.

For the critical temperature, we find

$$T_c = \frac{\omega_E}{2\pi}\sqrt{\frac{\lambda(2g-1)-1}{1+\lambda(1-g)}} \tag{3.62}$$

One can see that the dependence of T_c upon λ is markedly different in the two cases, $g = 1$, and g≠1. For $g = 1$, $T_c = \frac{\omega_E}{2\pi}\sqrt{\lambda-1}$, a result first obtained by Allen and Dynes[29]. For g≠1, $T_c = \frac{\omega_E}{2\pi}\sqrt{\frac{2g-1}{1-g}}$, independent of λ. This result is only valid for g>$\frac{1}{2}$. We would expect to find a constraint such as this, as we are taking the limit of $\frac{T_c}{\omega_E} >> 1$. Again, the relation of equation 3.53 is having its effect. The linearity of T_c with ω_E has been checked numerically in this limit, and is shown in figure 3.8. We also note that as g decreases, so does T_c, as was also found in the BCS limit. The analytic result also displays this behaviour.

We have also considered the specific heat jump and its slope in this limit. For $\frac{\Delta C}{\gamma T_c}$ we find

$$\frac{\Delta C}{\gamma T_c} = \frac{3}{2}\frac{b-a\lambda}{g(1+\lambda)}U^2\Big[1-\frac{1}{2}\frac{\lambda(3gU-28g+24+3U)+24}{\lambda g}(1-t)\Big] \tag{3.63}$$

where a=g-1, b=g+1, and $U = \frac{4[\lambda(2g-1)-1)(1-a\lambda)]}{\lambda(b-a\lambda)}$. In figure 3.9 we show the specific heat jump and slope as a function of g. Both curves tend to zero at g=0.5 and $g = 1$, and display a maximum for g≈0.8. The maximum value for the jump is $\frac{\Delta C}{\gamma T_c}$=2.16 for g=0.81, while for the slope, $\frac{\Delta C'}{\gamma T_c}$=19.8 at g=0.82. The ratio $T_c\frac{\Delta C'}{\Delta C}$= 9.2 is of the order of the maximum found numerically, but it should be stressed that this is probably not significant. All of the asymptotic results are not expected to give qualitatively correct results. They do however give the correct dependencies upon λ and ω_E. The T_c result for example, is a lower bound upon T_c. This will be discussed in more detail in chapter 5.

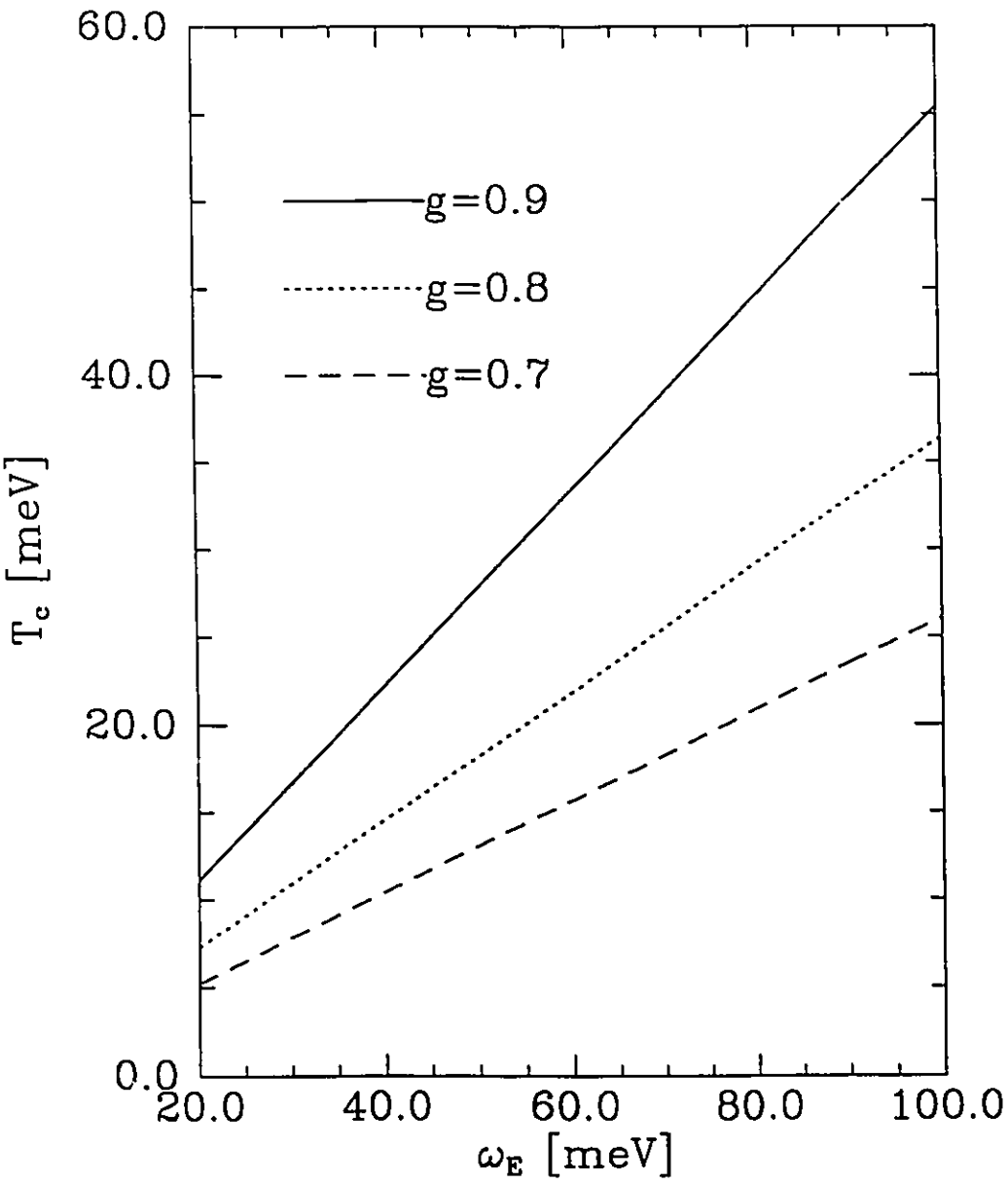

Figure 3.8-Critical temperature versus ω_E in the asymptotic limit $\lambda \to \infty$. T_c increases linearly with ω_E, as was found in the one gap calculation. As g decreases, so does T_c, again consistent with the one gap result.

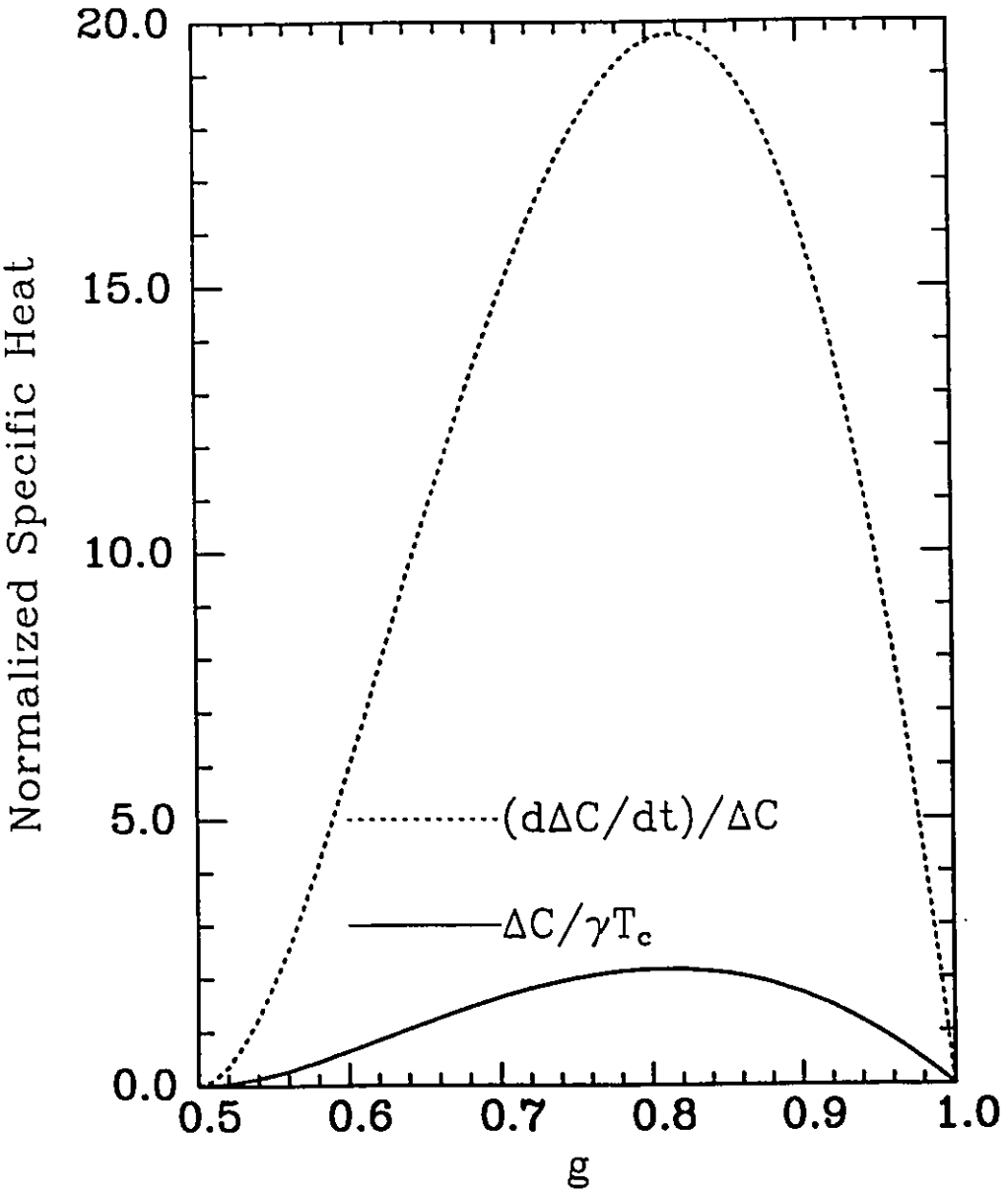

Figure 3.9-One gap model results for the specific heat jump, $\frac{\Delta C}{\gamma T_c}$, and the normalized slope, $T_c \frac{\Delta C'}{\Delta C}$ versus g, in the limit $\lambda \to \infty$. Both results tend to zero for $g = 1$. In addition, they go to zero at g=0.5, as our solution breaks down at this point.

We can also show that the gap ratio, $\frac{2\Delta(0)}{k_B T_c}$, is a constant times some function of g. Unfortunately, the form of the function is not readily determined. However, we note that the gap ratio saturates for large $\frac{T_c}{\omega_E}$ for both $g = 1$ and g$\neq$1.

3.9 MARGINAL FERMI LIQUID MODEL

Kuroda and Varma[21] have proposed a model for the high temperature superconductors which they refer to as a marginal Fermi liquid (MFL). The model is motivated by a phenomenological ansatz about the excitations which exist in these systems. By making this ansatz, they are able to explain many of the normal state properties of the high T_c materials.

In a non-interacting system of fermions at zero temperature, there is a discontinuity in the momentum distribution of the particles, referred to as the Fermi surface. All the states at that particular energy are occupied. As a result, there are no unoccupied states available for elastic scattering. The particles have well defined energies and infinite lifetimes. Such a state is a Fermi liquid.

In reality, the electrons interact with one another via the Coulomb interaction. The main effect of the Coulomb interaction is a plasma mode which occurs at high frequencies for a dense electron gas. However, there are also low-lying charge fluctuations which shift the energies of the non-interacting system. They lead to a finite lifetime, τ, for excitations away from the Fermi surface, but at the Fermi surface, the lifetime is still infinite. The shift in the energies, as well as the lifetime effects are given by the self energy, $\Sigma(\vec{k},\omega)$, such that

$$E_{\vec{k}} = \epsilon_{\vec{k}} + Re\Sigma(\vec{k}, E_{\vec{k}} + i\Gamma_{\vec{k}}) \qquad (3.64a)$$

$$\frac{1}{2\tau_{\vec{k}}} = -\Gamma_{\vec{k}} = -Im\Sigma(\vec{k}, E_{\vec{k}} + i\Gamma_{\vec{k}}) \tag{3.64b}$$

In terms of the self-energy, the one-particle Green's function is

$$G(\vec{k},\omega) = \frac{1}{\omega - \epsilon_k - \Sigma(\vec{k},\omega)} \tag{3.64c}$$

For the non-interacting case, there is no self-energy term. The Green's function is then entirely real. The pole of the Green's function occur at $\omega = \epsilon_k$. In real space and time, the Green's function is then an undamped traveling wave. Once the interactions lead to a finite self- energy, the poles of the Green's functions are shifted by the real part of the self-energy, and the imaginary part leads to damping. In this case, the Green's function can be written, near the Fermi surface, as

$$G(\vec{k},\omega) = \frac{z_k}{\omega - E_k + iIm\Sigma(\vec{k},\omega)} \tag{3.65}$$

where $z_k^{-1} = 1 - \frac{\partial Re\Sigma}{\partial\omega}|_{\omega=E_k}$. z_k is the spectral weight.

Earlier, we discussed the microscopic origin of spin fluctuations, and we introduced the susceptibility, $\chi(\vec{q},\omega)$, which described the response of the system to an external magnetic field. The response of a system to an external electric charge is given by the dielectric response function, $\epsilon(\vec{q},\omega)$, defined by

$$\langle\rho_{total}(\vec{q},\omega)\rangle = \rho_{external}(\vec{q},\omega) + \langle\rho_{induced}(\vec{q},\omega)\rangle = \frac{\rho_{external}(\vec{q},\omega)}{\epsilon(\vec{q},\omega)} \tag{3.66}$$

where $\rho(\vec{q},\omega)$ is the Fourier transform in both space and time of the charge density $\rho(\vec{x},t)$. This problem can be analyzed in a fashion similar to that for the charge fluctuations, and one finds

$$\epsilon^{-1}(\vec{q},\omega) = [1 - P_o^R(\vec{q},\omega)V(\vec{q})]^{-1} \tag{3.67}$$

$V(\vec{q}) = \frac{4\pi e^2}{q^2}$ is the Fourier transform of the Coulomb potential, and $P_o^R(\vec{q},\omega)$ is the retarded polarizability. It is given by

$$P_o^R(\vec{q},\omega) = \sum_{\vec{p}} \frac{f_{\vec{p}}^- - f_{\vec{p}+\vec{q}}^-}{\omega - (\tilde{\epsilon}_{\vec{p}} - \tilde{\epsilon}_{\vec{p}+\vec{q}}) - i\eta} \tag{3.68}$$

with $f_{\vec{p}}^- = \frac{1}{e^{\frac{\tilde{\epsilon}_{\vec{p}}}{k_B T}}+1}$ and $\tilde{\epsilon}_{\vec{p}} = \frac{p^2}{2m} - \mu$. This is the same expression that we obtained for $\Gamma^{-+}(\vec{q},\omega)$ in the context of spin fluctuations. These charge fluctuations lead to a self-energy which has a real part $Re\Sigma(\vec{k},\omega) \sim \omega$, and the imaginary part $Im\Sigma(\vec{k},\omega) \sim -\omega^2$ Hence, the lifetime τ still goes to infinity at the Fermi surface, $\omega = \tilde{E}_{\vec{k}} = 0$. The spectral weight is reduced somewhat from the non-interacting value, but is non-zero.

The model of reference 21 is based on the hypothesis that there are charge and spin density fluctuations which are described by a polarizability

$$ImP(\vec{q},\omega) = \begin{cases} -N(0)\frac{\omega}{T}, & \text{for } |\omega| < T; \\ -N(0)sgn\omega, & \text{for } |\omega| > T. \end{cases} \tag{3.69}$$

with $N(0)$ the single particle density of states. This polarizability leads to a one-particle self-energy of the form

$$\Sigma(\vec{k},\omega) \sim g^2 N^2(0)(\omega ln\frac{x}{\omega_c} - i\frac{\pi}{2}x). \tag{3.70}$$

$x = max(|\omega|, T)$, ω_c is a cut-off, and g is a coupling constant. The quasi-particle lifetime is still infinite at the Fermi surface. However, the spectral weight

$$z_k \sim \frac{1}{ln|\frac{\omega_c}{E_k}|} \tag{3.71}$$

now vanishes at the Fermi surface. Varma refers to this as a marginal Fermi liquid.

With the polarizability of equation 3.68, Varma reports agreement with various normal state properties of the high T_c materials. For example,

one obtains the d.c resistivity from the imaginary part of the self energy at zero frequency, $\rho \sim Im\Sigma(\omega = 0) \sim T$, in agreement with experiment.

In addition, Kuroda and Varma have considered the properties of a s-wave spin singlet superconductor, where they have used for the kernels in the Eliashberg equations

$$F^{\pm}(i\omega_n) = \lambda^{\pm} \int_{-\infty}^{\infty} \frac{dx}{\pi} \frac{ImP(x)}{i\omega_n - x} \tag{3.72}$$

with

$$\lambda^{\pm} = \lambda_\rho \pm \lambda_\sigma \tag{3.73}$$

where λ_ρ and λ_σ are the coupling constants to the charge and spin fluctuations respectively. For their calculations, they model $ImP(\omega)$ by

$$ImP(\omega) = \begin{cases} -N(0)tanh\frac{\omega}{2T}, & |\omega| < \omega_c; \\ 0, & |\omega| > \omega_c. \end{cases} \tag{3.74}$$

Kuroda and Varma[21] report results for T_c, $\frac{\Delta C}{\gamma T_c}$, and $\frac{2\Delta(0)}{k_B T_c}$. They have used the following parameters; $\lambda^+ \approx 3.0$, $\lambda^- \approx 1.4$, $\omega_c \approx 3000$ K, and obtain $T_c \approx 110$ K, $\frac{2\Delta(0)}{k_B T_c} \approx 8$, and predict that $\frac{\Delta C}{\gamma T_c}$ will be less than the BCS value of 1.43. Using these parameters, we obtain $T_c \approx 35$ K and $\frac{\Delta C}{\gamma T_c} \approx 2$. E.J. Nicol[48] has calculated the gap ratio for these same parameters, and found $\frac{2\Delta(0)}{k_B T_c} \approx 7$.

We have also performed calculations of various properties as a function of $\frac{T_c}{\omega_c}$ and g. The results are shown in figure 3.10, where we plot $\frac{\Delta C}{\gamma T_c}$, and $T_c \frac{\Delta C'}{\Delta C}$ versus $\frac{T_c}{\omega_c}$ for 3 values of g=$\frac{\lambda^-}{\lambda^+}$. We would expect that the results would be larger than the BCS results, due to the fact that there are two competing interactions. However, we do not expect that we will obtain results as large as was found using the delta function spectral densities. This is based on the shape of the functional derivatives. The positive divergence of the specific heat

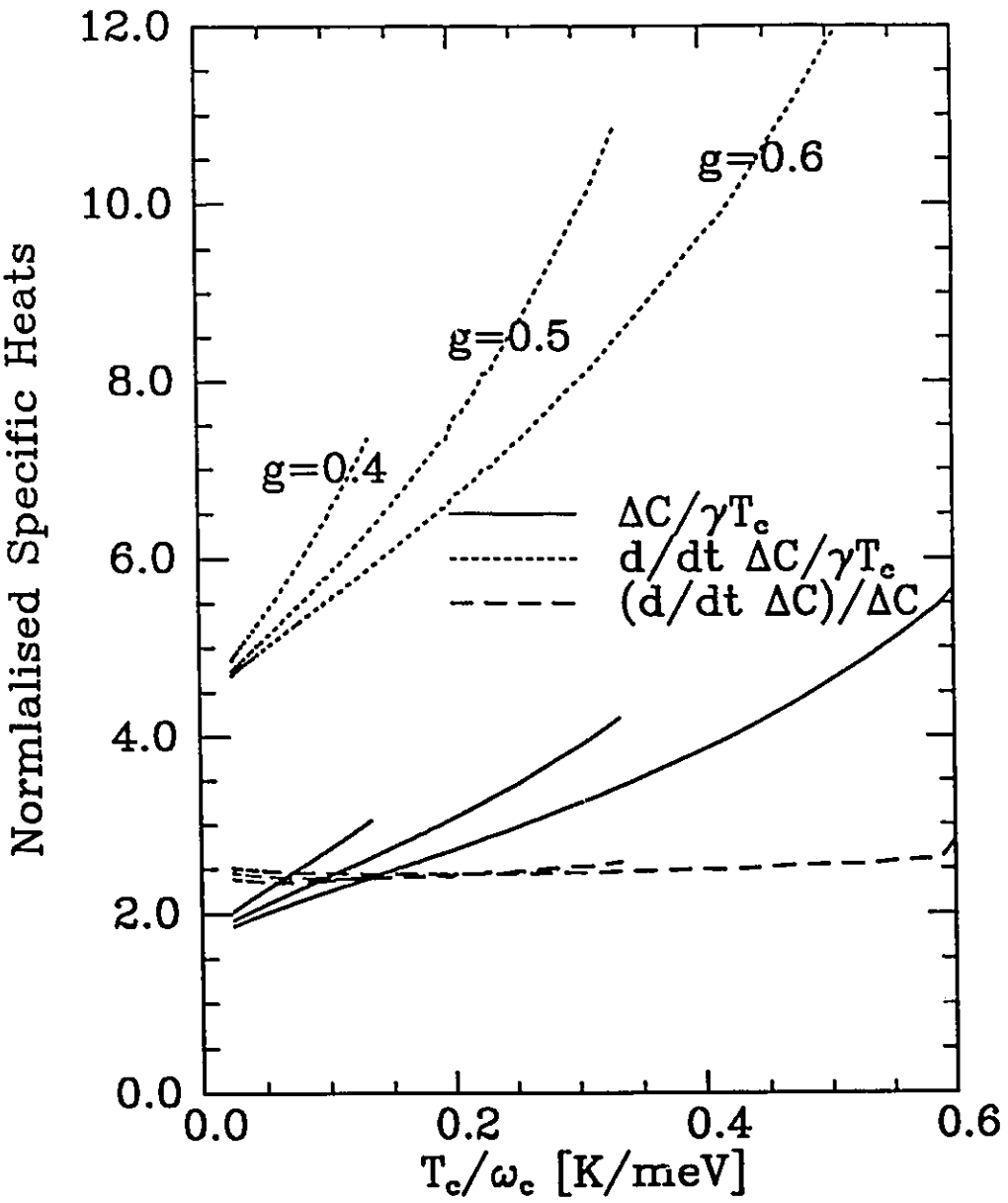

Figure 3.10-Numerical results for the specific heat jump and the normalized slope for the marginal Fermi liquid model. We find that the results are enhanced above the BCS values, but fall below the values obtained using Einstein spectral functions.

jump functional derivative implies that the specific heat jump is maximized by placing all of the spectral weight at low frequencies. The spectrum of 3.64 has spectral weight distributed throughout its entire frequency range, and as such, results for $\frac{\Delta C}{\gamma T_c}$ should be less than those found with Einstein spectral densities. For g=0.5, $\frac{T_c}{\omega_{ln}} \approx 0.1$, the Einstein spectral function yields $\frac{\Delta C}{\gamma T_c} \approx 3.4$, while the MFL model gives $\frac{\Delta C}{\gamma T_c} \approx 2.4$. We also note that there is not a great enhancement of the normalized jump, in contrast to the results found with Einstein spectral functions.

Chapter 4

Numerical Results

4.1 INTRODUCTION

In this chapter, we consider the case where both the frequency dependence and strengths of the attractive and repulsive interactions are different. This would correspond to a situation in which there are two distinctive interactions. The equations we wish to consider are the Eliashberg equations including spin fluctuations:

$$\Delta(i\omega_n)Z_s(i\omega_n) = \pi T \sum_{m=-\infty}^{\infty} \lambda^{-}(m-n)\frac{\Delta(i\omega_m)}{\sqrt{\Delta^2(i\omega_m)+\omega_m^2}}, \tag{4.1}$$

$$\omega_n Z_s(i\omega_n) = \omega_n + \pi T \sum_{m=-\infty}^{\infty} \lambda^{+}(m-n)\frac{\omega_m}{\sqrt{\Delta^2(i\omega_m)+\omega_m^2}}. \tag{4.2}$$

The kernels are given by

$$\lambda^{\pm}(m-n) = 2\int_0^{\infty} \frac{\omega\,[E(\omega)\pm P(\omega)]}{\omega^2+(\omega_m-\omega_n)^2}d\omega\,. \tag{4.3}$$

In this chapter we will treat the $E(\omega)$ and $P(\omega)$ as separate functions. This makes analytical work rather difficult, but it is possible to obtain some

analytic results. For our numerical work, we use Einstein spectral densities of the form

$$E(\omega) = \frac{\omega_E \lambda^E}{2} \delta(\omega - \omega_E)$$
$$P(\omega) = \frac{\omega_P \lambda^P}{2} \delta(\omega - \omega_P) \tag{4.4}$$

with λ^E and λ^P the mass enhancement parameters for $E(\omega)$ and $P(\omega)$ respectively.

If we solve in the BCS limit, using the square well model of 3.24, we get from 4.2

$$Z = 1 + \lambda^+ . \tag{4.5}$$

Putting this result into 4.1, and using the square well model, we find, for $T = T_c$

$$1 = \pi T \frac{\lambda^E}{1+\lambda^+} \sum_{m=-N_E}^{N_E} \frac{1}{|\omega_m|} - \pi T \frac{\lambda^P}{1+\lambda^+} \sum_{m=-N_P}^{N_P} \frac{1}{|\omega_m|} , \tag{4.6}$$

where

$$\lambda^E = 2 \int_0^\infty \frac{E(\omega)}{\omega} d\omega ,$$
$$\lambda^P = 2 \int_0^\infty \frac{P(\omega)}{\omega} d\omega , \tag{4.6a}$$
$$N_{E,P} = \frac{\omega_{E,P}}{2\pi T_c} + \frac{1}{2} ,$$
$$\lambda^\pm = \lambda^E \pm \lambda^P .$$

We perform the sums as in 3.12 to obtain

$$1 + \lambda^+ = \lambda^E ln \frac{1.13\omega_E}{k_B T_c} - \lambda^P ln \frac{1.13\omega_P}{k_B T_c}$$
$$T_c \simeq e^{\frac{1+\lambda^+ - \lambda^E ln(1.13\omega_E) + \lambda^P ln(1.13\omega_P)}{\lambda^-}} . \tag{4.7}$$

One can also calculate thermodynamics in this limit, and obtain the usual BCS results, independent of any material parameters.

If one attempts to calculate strong coupling corrections to the BCS limit in this model, the results are highly unsatisfactory. The final expressions

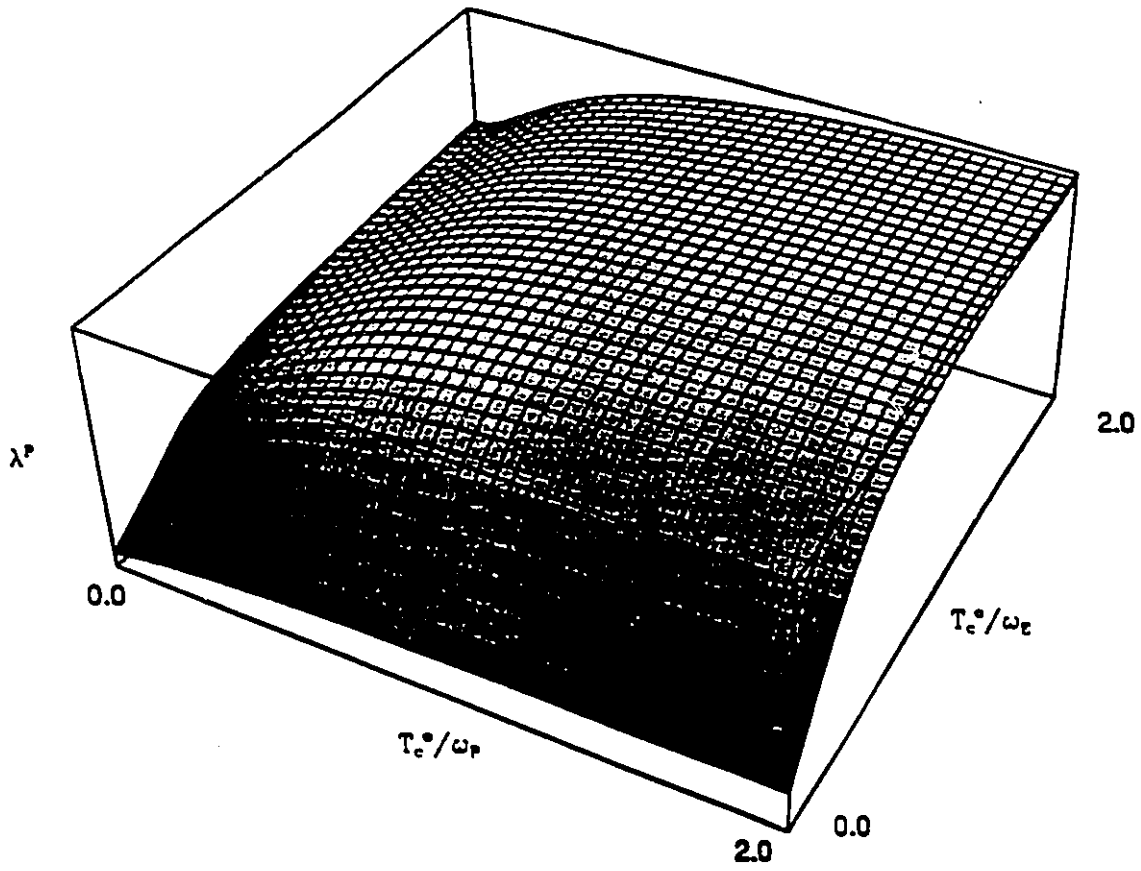

Figure 4.1-Electron-spin fluctuation mass enhancement factor, λ^P, versus $\frac{T_c^*}{\omega_E}$ and $\frac{T_c^*}{\omega_P}$, for $\frac{T_c}{T_c^*} = 0.5$. The surface has a height of ≈ 0.05 at (0,0), and a maximum value of ≈ 1.7 at (2,2).

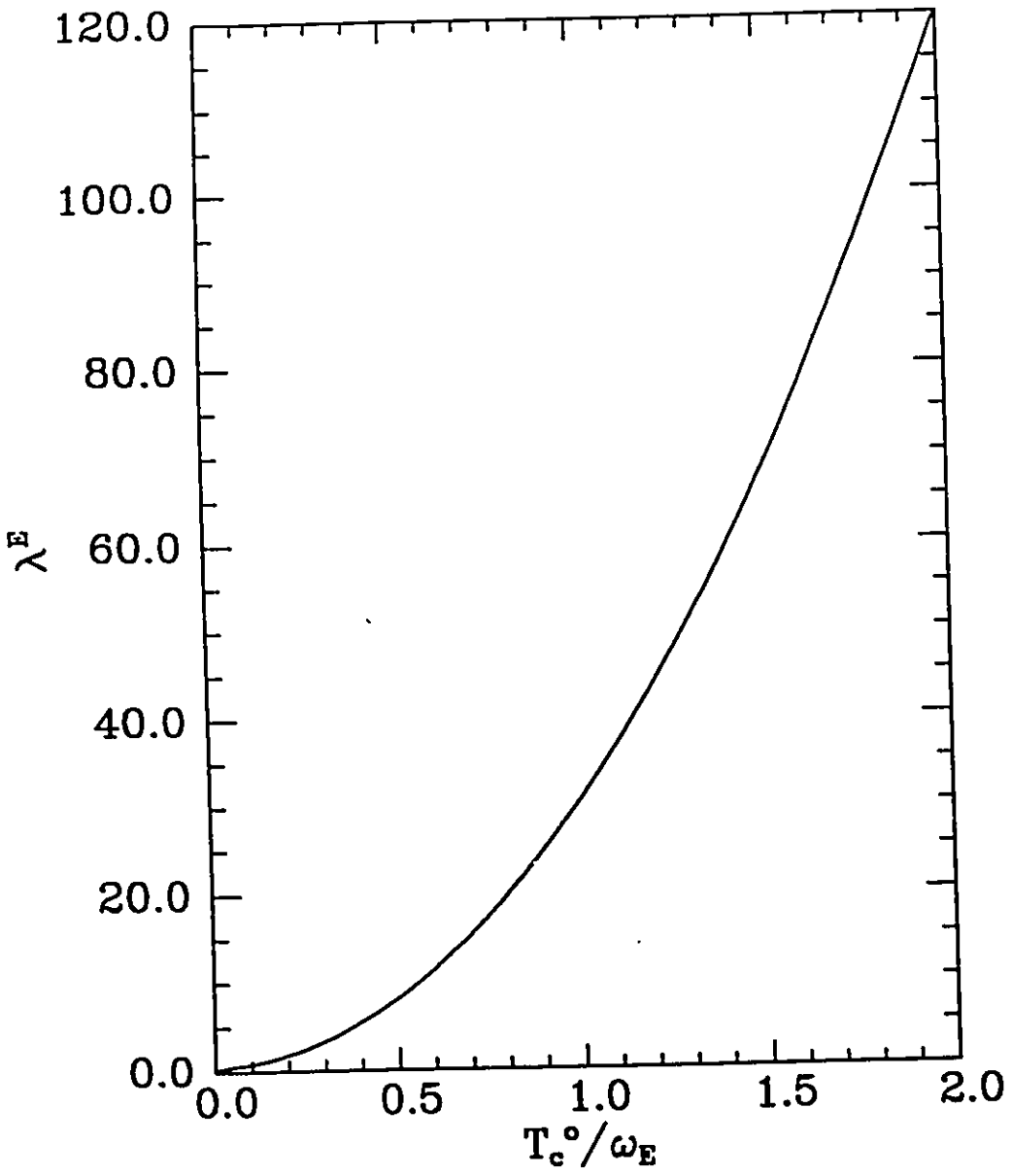

Figure 4.2-Electron-boson mass enhancement factor, λ^E, versus $\frac{T_c^\circ}{\omega_E}$. λ^E is determined by choosing an ω_E and then calculating λ^E to give $T_c^\circ = 200$ K. For $\frac{T_c^\circ}{\omega_E} \geq 0.5$, λ^E appears to be unphysically large.

which one obtains are very complicated, with a profusion of parameters. This seems to violate the spirit of such calculations, and we will not present the results.

It is possible to solve the equations in the extreme strong coupling limit for the pairing mechanism. We treat the spin fluctuations in the BCS limit, and we find

$$T_c = \frac{\omega_E}{2\pi} \frac{\lambda^E}{1 + 2\lambda^P} . \tag{4.8}$$

This result is the same as the result obtained by Allen and Dynes[29] with λ^P playing the role of μ^*. μ^* is a static pair breaking term, and we lose the dynamic pair breaking effects that we saw in chapter 3. It is difficult to take the general limit of both λ^E and λ^P going to infinity, as we would need to include some constraint which would ensure that $\frac{\lambda^P}{\lambda^E} \lesssim 1$, or else we would no longer expect to have a finite critical temperature.

When we treat the spin fluctuations in the BCS approximation, all of the results for the purely attractive case are relevant, with μ^* playing the role of λ^P.

We have solved equations (4.1) and (4.2) numerically and used the results to calculate the specific heat given by equation (2.17). In our calculations, we choose a critical temperature (T_c°) for a pure system which we hold fixed. We then choose a value of ω_E and calculate λ^E to give us our chosen T_c°. We then add spin fluctuations at some frequency ω_P, and calculate a λ^P which will suppress the critical temperature to 100 K. Two values of T_c°, 150 K and 200K were used. For both values of T_c°, the results were qualitatively the same. We will only show results for T_c°=200 K. In our calculations, we have varied the frequencies of both the pairing and spin fluctuation spectra.

We use the parameters $\frac{T_c^\circ}{\omega_E}$ and $\frac{T_c^\circ}{\omega_P}$ to discuss the results. Our numerical studies have spanned the range of 0 to 2 for both $\frac{T_c^\circ}{\omega_E}$ and $\frac{T_c^\circ}{\omega_P}$. We point out that conventional phonon materials lie in the range $0 \leq \frac{T_c}{\omega_{ln}} \leq 0.25$.

In figure 4.1 we display λ^P, the electron-spin fluctuation mass enhancement factor versus $\frac{T_c^\circ}{\omega_E}$ and $\frac{T_c^\circ}{\omega_P}$. We note that λ^P rises rapidly for small values of both parameters and then levels off. For $T_c^\circ = 200$ K, the maximum value of λ^P is 1.7 for $\frac{T_c^\circ}{\omega_E} = \frac{T_c^\circ}{\omega_P} = 2.0$. In figure 4.2 we show λ^E versus $\frac{T_c^\circ}{\omega_E}$. We note that for $\frac{T_c^\circ}{\omega_E} = 2.0$, $\lambda^E \approx 120$, which seems rather unphysical. If we restrict ourselves to a $\lambda^E \leq 5.0$, we find that we only need $\lambda^P \leq 1.0$ to suppress T_c from 200 K to 100 K. For very weak coupling in both the pairing and spin fluctuations, a T_c suppression of 50% is achieved with $\lambda^P \approx 0.05$. Thus even weakly coupled spin fluctuations can have a dramatic effect upon the critical temperature of a superconductor. Such weakly coupled excitations would be difficult to detect experimentally in the superconducting properties.

4.2 SPECIFIC HEAT JUMP

Figure 4.3 displays the normalized specific heat jump $\frac{\Delta C}{\gamma T_c}$. For $\frac{T_c^\circ}{\omega_E}$ and $\frac{T_c^\circ}{\omega_P}$ equal to zero, we obtain the usual BCS value of 1.43. As $\frac{T_c^\circ}{\omega_E}$ increases, $\frac{\Delta C}{\gamma T_c}$ increases, reaches a maximum of $\approx$ 4.1 for $\frac{T_c^\circ}{\omega_E} = 0.4$ and then decreases below the BCS value. As $\frac{T_c^\circ}{\omega_P}$ increases, the specific heat jump is enhanced. For $\frac{T_c^\circ}{\omega_E} = 0.4$ and $\frac{T_c^\circ}{\omega_P} = 2.0$ we find that $\frac{\Delta C}{\gamma T_c} = 9.6$, which is much larger than the maximum value obtained without spin fluctuations[26]. It is interesting to note that in the case of paramagnetic impurities the specific heat jump is always suppressed below it's pure value[49]. Figure 4.4 shows the slope of the specific heat difference at T_c normalized by γ, $\frac{1}{\gamma}\frac{d\Delta C}{dT}$($\gamma$ is the Sommerfeld value). For $\frac{T_c^\circ}{\omega_E} = \frac{T_c^\circ}{\omega_P} = 0$, we obtain the BCS result of 3.77. As $\frac{T_c^\circ}{\omega_E}$ increases,

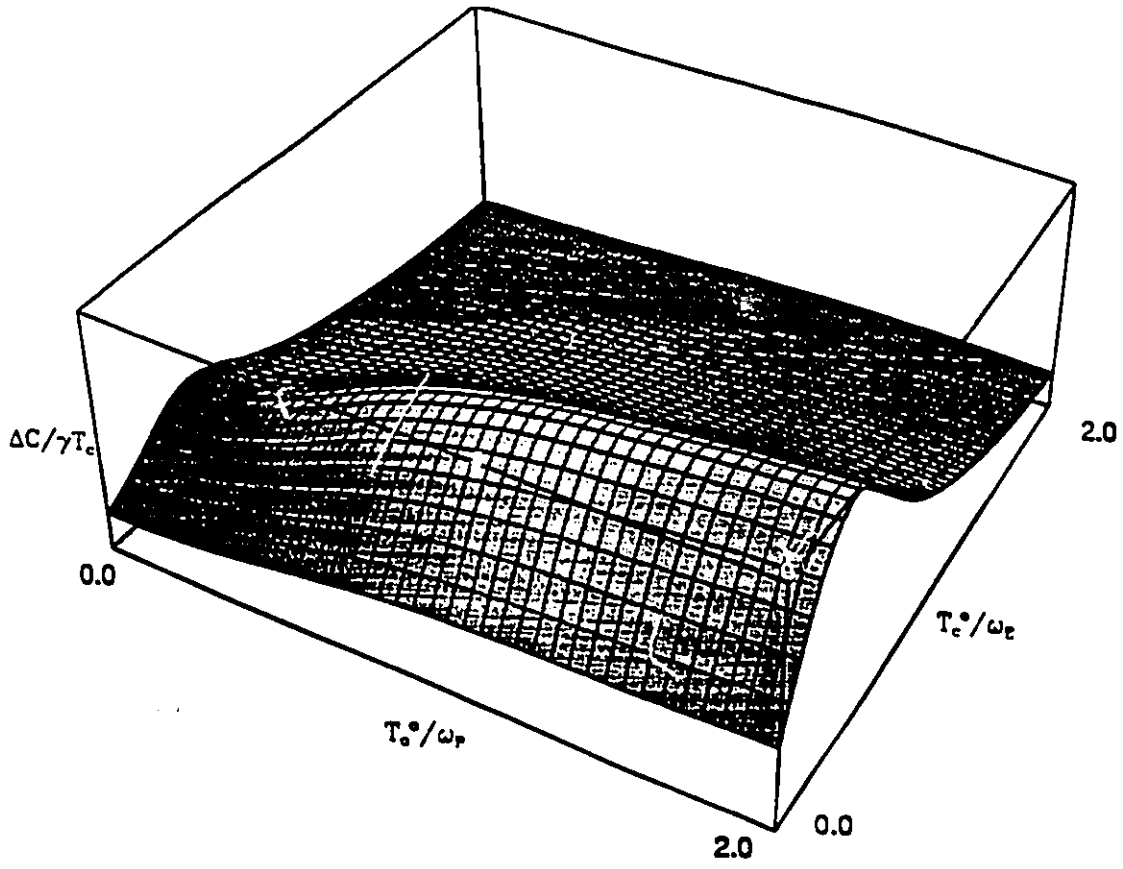

Figure 4.3-Normalized specific heat jump, $\frac{\Delta C}{\gamma T_c}$, versus $\frac{T_c^*}{\omega_E}$ and $\frac{T_c^*}{\omega_P}$,for $\frac{T_c}{T_c^*} = 0.5$. At (0,0) the height is 1.43, the B.C.S. value. The maximum of 11.4 occurs at $\frac{T_c^*}{\omega_E} = 0.4$ and $\frac{T_c^*}{\omega_P} = 2.0$. This is much larger that the maximum value that can be obtained in a purely attractive system.

the normalized slope increases, reaches a maximum and then decreases. For $\frac{T_c^\circ}{\omega_P} = 0$, a maximum value of $\approx$ 21 is attained for $\frac{T_c^\circ}{\omega_E} = 0.4$. The maximum value obtained was 67.3 for $\frac{T_c^\circ}{\omega_E} = 0.4$ and $\frac{T_c^\circ}{\omega_P} = 2.0$. The slope of the specific heat behaves qualitatively like the specific heat jump. This is not particularly surprising, as one would expect them to be correlated to one another in order to satisfy the entropy sum rule.

When we compare these results to those obtained for systems where no dynamic pair breaking mechanism is included (μ^*, a static, repulsive coulomb psuedopotential is included) we find that the results are qualitatively similar, but there are large quantitative differences. In the case of both the jump and the slope, other authors[45] find a maximum in these values at $\frac{T_c}{\omega_E} = 0.2$. Note that the position of these maximum agrees with the values obtained here when we recall that $\frac{T_c}{T_c^\circ} = 0.5$. However, the maxima obtained for the jump, with $\mu^* = 0.0$, is $\approx$ 3.4. Even in the weak-coupling limit for the spin fluctuations, we obtain a maximum of 4.1. Similarly, the maximum value for the slope in the purely attractive case is $\approx$ 14.5 whereas we get a value, again in the weak coupling SF regime, of $\approx$ 21. Once again, as for the critical temperature, we see that even very weakly coupling spin fluctuations can have a dramatic effect upon the properties of a superconductor.

4.3 SLOPE OF THE SPECIFIC HEAT JUMP

In order to measure the normalized jump or slope of the specific heat, it is necessary to know the value of the Sommerfeld constant γ. Due to the large critical temperatures and low temperature critical fields, γ is not a well known quantity for the high-T_c superconductors. A quantity which contains

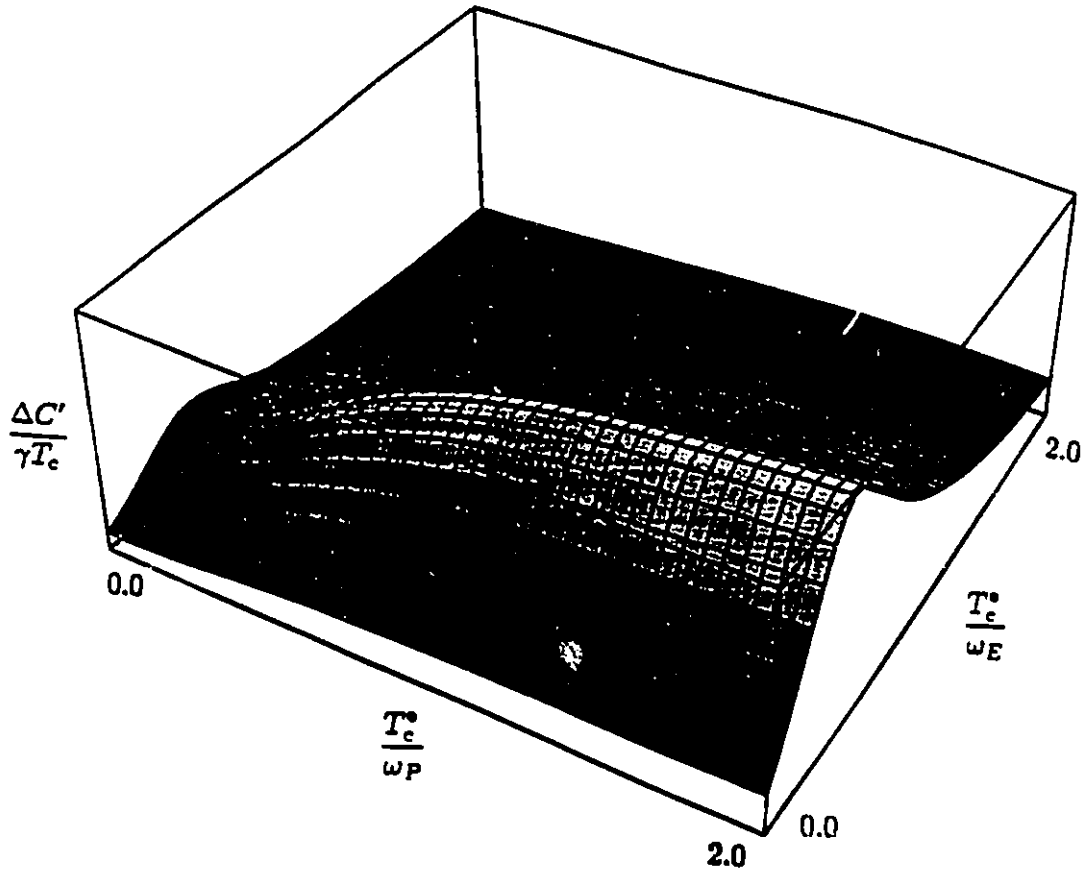

Figure 4.4-$\frac{1}{\gamma}\frac{d\Delta C}{dT}$ versus $\frac{T_c^*}{\omega_E}$ and $\frac{T_c^*}{\omega_P}$, with $\frac{T_c}{T_c^*} = 0.5$. At (0,0), we obtain the B.C.S. value of 3.77. The maximum value of 23 occurs at $\frac{T_c^*}{\omega_E} = 0.4$ and $\frac{T_c^*}{\omega_P} = 2.0$, the same place where the maximum of the specific heat jump occurs.

information about both the jump and the slope in the specific heat is the ratio of the slope to the jump. In particular, we have calculated $\frac{T_c}{\Delta c}\frac{d}{dT}\Delta C$. This quantity is independent of γ. In addition, if we restrict ourselves to values at T_c, one would hope that experimental results for this quantity would be reasonably insensitive to the details of the subtraction of the lattice contribution to the specific heat. Results of our calculations are shown in figure 4.5. Along the $\frac{T_c^\circ}{\omega_P} = 0.0$ line we see a sharp rise to a maximum of ≈ 5.2 for $\frac{T_c^\circ}{\omega_E} = 0.4$ and then a gradual fall as $\frac{T_c^\circ}{\omega_E}$ increases further. In this case, the value does not fall below the BCS value of 2.64 which we obtain for $\frac{T_c^\circ}{\omega_E} = \frac{T_c^\circ}{\omega_P} = 0.0$. As we move away from $\frac{T_c^\circ}{\omega_P} = 0.0$, we see a further increase. For both $\frac{T_c^\circ}{\omega_E}$ and $\frac{T_c^\circ}{\omega_P} \gtrsim 0.5$, a plateau is reached at ≈ 7.25. As we move further out, a slow increase to 7.6 is observed at $\frac{T_c^\circ}{\omega_E} = \frac{T_c^\circ}{\omega_P} = 2.0$. Comparing these results to values obtained for pure systems, we find that they are larger. Akis and Carbotte[45] report values in the range of 2.64 (BCS) to 5.0. For $\mu^* = 0.0$, they give a maximum value of 4.6.

We are able to compare these results with experiment. Akis and Carbotte[45] have analyzed specific heat data of Junod *et al.* [50] for $YBa_2Cu_3O_7$, and find a value for $\frac{T_c}{\Delta c}\frac{d}{dT}\Delta C$ in the range of 8 to 14, depending upon the temperature interval that they use to calculate the slope. We note that there is evidence that the fluctuation regime in these materials is large[51], which would tend to sharpen the specific heat anomaly. As a consequence, perhaps the lower bound of their estimate is the more relevant. Our results would seem to fit with the lower bound. However, we are only able to achieve these values in the strong coupling regime for the pairing mechanism.

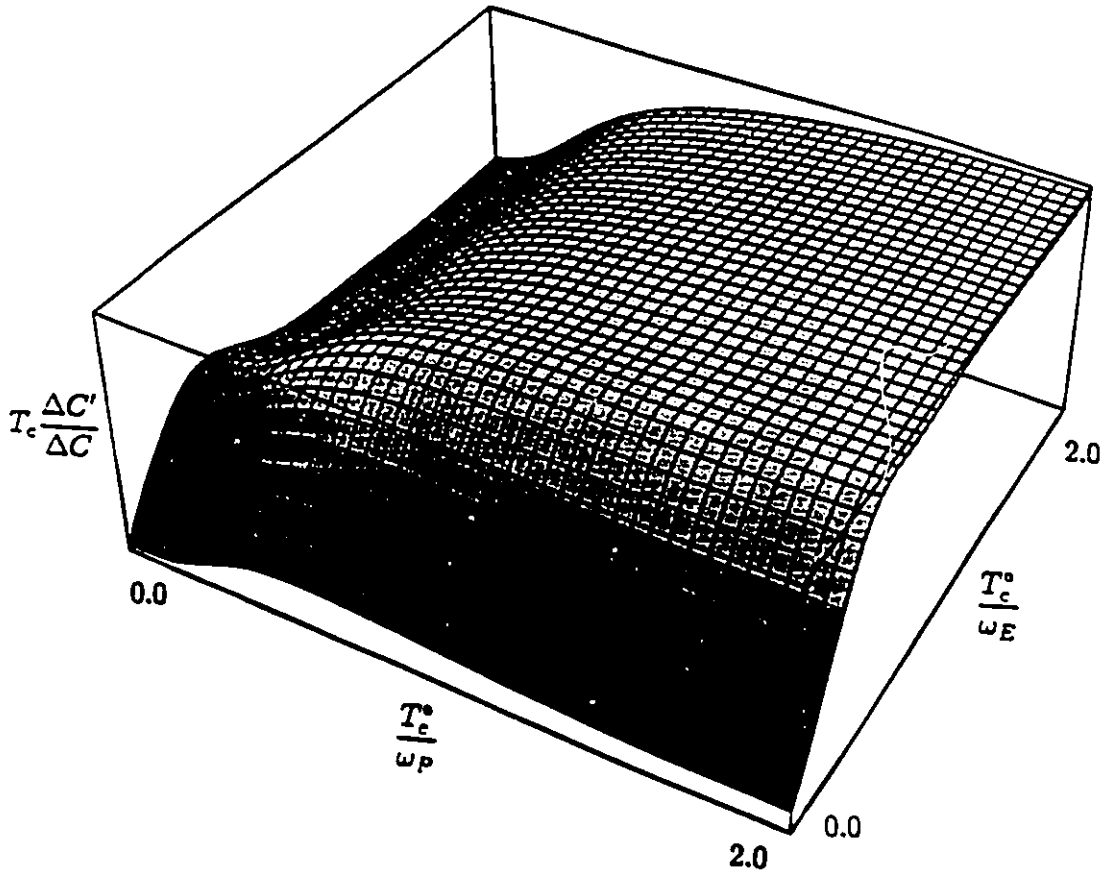

Figure 4.5-Ratio of the temperature derivative of the specific heat to the specific heat at T_c versus $\frac{T_c^\circ}{\omega_E}$ and $\frac{T_c^\circ}{\omega_P}$. $\frac{T_c}{T_c^\circ} = 0.5$. This ratio is independent of γ, the coefficient of the linear term in the normal state specific heat. We obtain the B.C.S. result 0f 2.64 at (0,0), and a maximum of 7.6 at (2,2). At (0.5,0.5), we obtain 7.25.

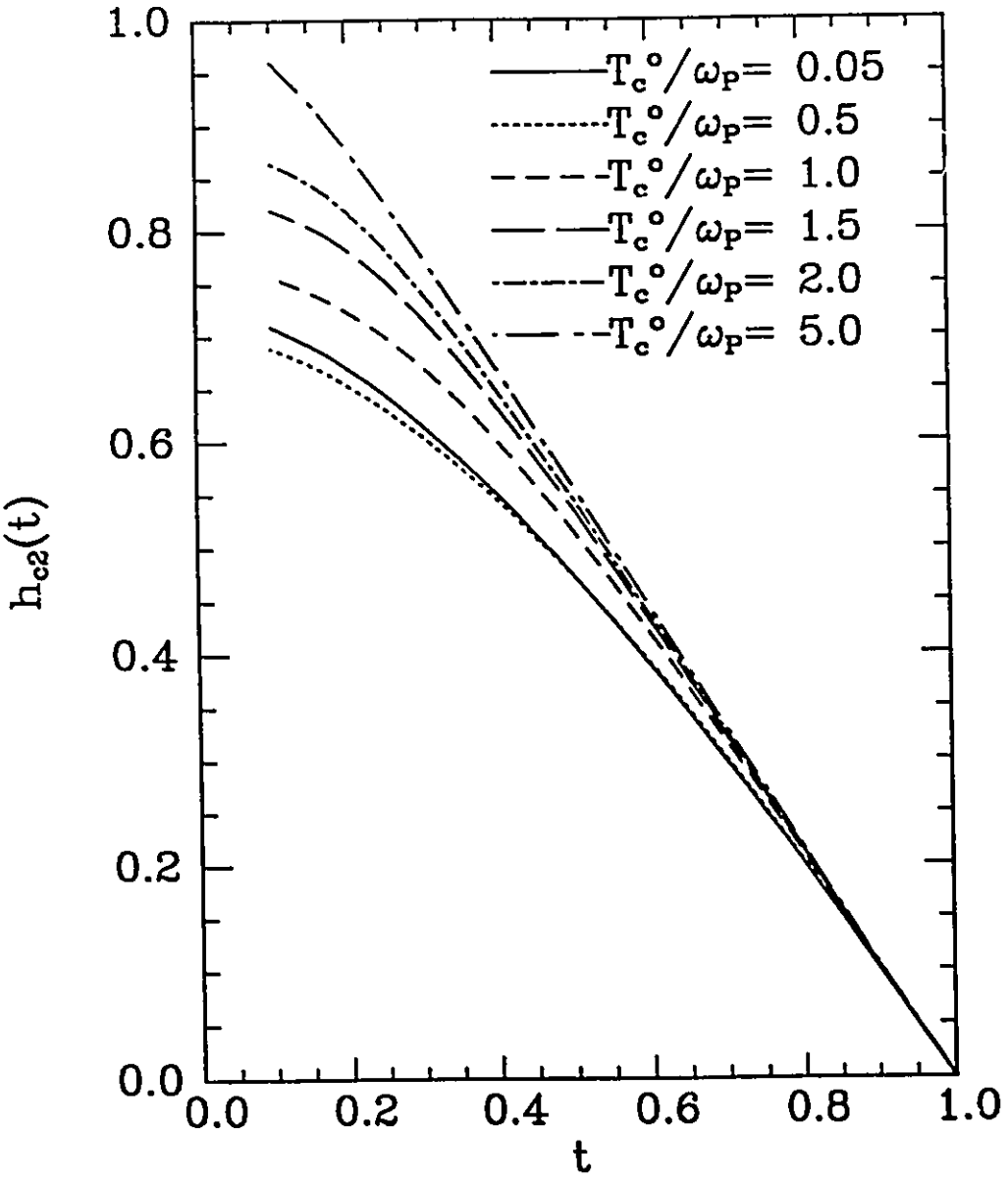

Figure 4.6-Reduced upper critical field versus reduced temperature for $\frac{T_c}{T_c°}$ = 0.66. For all curves, $\frac{T_c°}{\omega_E}$ = 0.05. The trend for increasing $\frac{T_c°}{\omega_P}$ is shown clearly in figure 4.7.

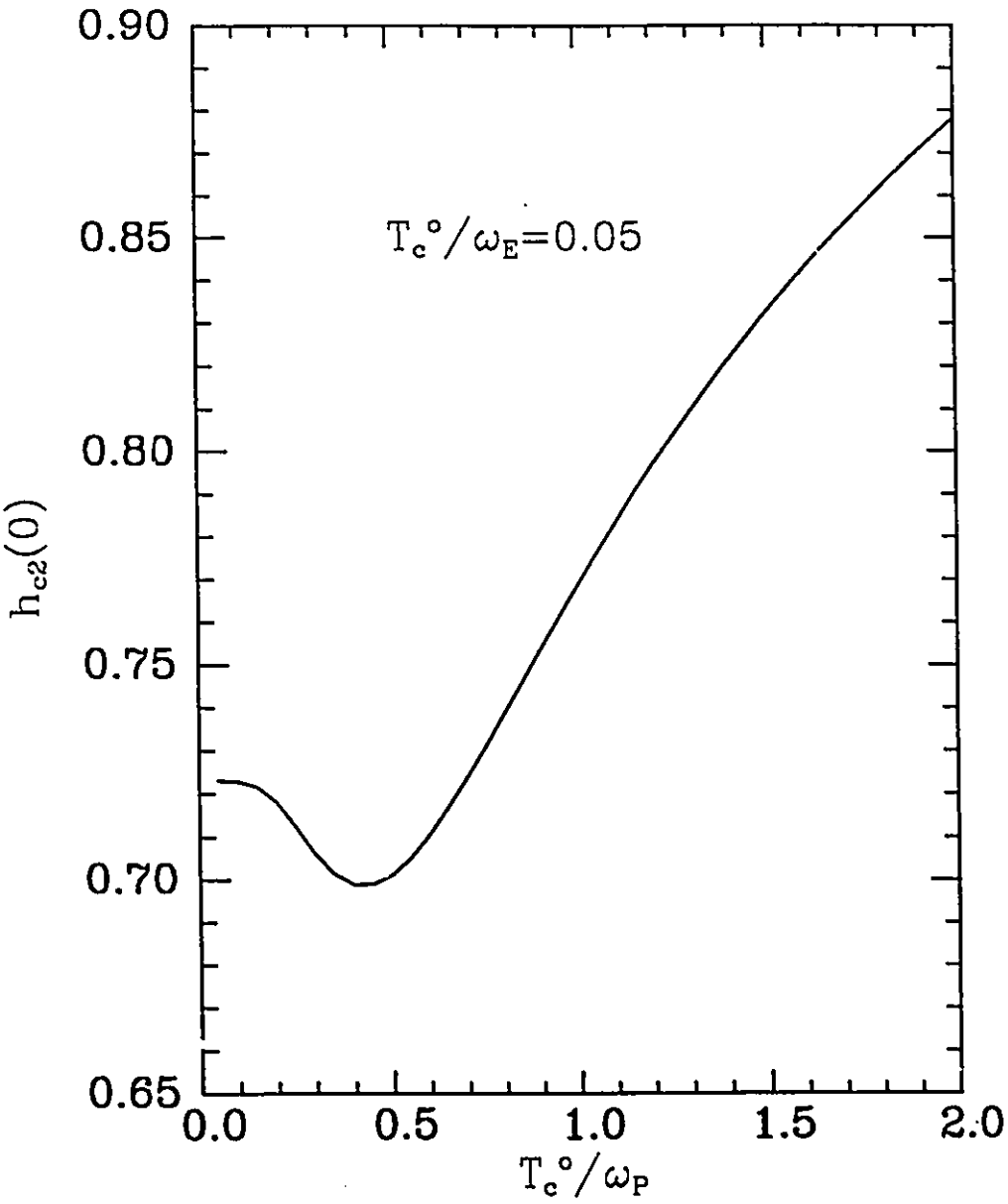

Figure 4.7-The zero temperature reduced critical field versus $\frac{T_c^\circ}{\omega_P}$ for $\frac{T_c}{T_c^\circ} = 0.5$. This type of behaviour is qualitatively similar to that of a purely attractive system as a function of $\frac{T_c^\circ}{\omega_E}$. For $\frac{T_c^\circ}{\omega_P} = 0$, we agree with the B.C.S. result of 0.73.

4.4 CRITICAL FIELD

We now consider our results for the reduced upper critical field which were obtained by solving equations (2.7) and (2.8). Figure 4.6 shows the reduced upper critical field versus reduced temperature t. For all curves $\frac{T_c^\circ}{\omega_E} =$ 0.05 and T_c°=200 K. The curve for $\frac{T_c^\circ}{\omega_P} = 0.05$ seems to be tending smoothly to the BCS value of 0.73 at zero temperature. The spin fluctuations have no observable effect upon the reduced upper critical field in the weak coupling regime. This is in marked contrast to both the critical temperature and the specific heat. In figure 4.7 we show $h_{c2}(0)$ versus $\frac{T_c^\circ}{\omega_P}$. We observe that it starts off slightly below 0.73, dips and then rises, reaching a value of ≈ 0.88 for $\frac{T_c^\circ}{\omega_P} = 2.0$. This type of behaviour is similar to the behaviour seen by Schossmann *et al.* [52] as a function of $\frac{T_c^\circ}{\omega_E}$. They obtain a maximum value near 1.5 for $\frac{T_c^\circ}{\omega_E} = 1.5$. Our maximum value is smaller than this, although our curve is still increasing.

4.5 ENERGY GAP

Figure 4.8 shows the ratio of $\frac{2\Delta(0)}{k_B T_c}$ versus $\frac{T_c^\circ}{\omega_P}$. This quantity was also computed for $\frac{T_c^\circ}{\omega_E} = 0.05$. The curve starts off slightly above the BCS value of 3.53, exhibits a small dip, and then rises. The values obtained for these parameters are all well below the maximum possible value of approximately 13 that can be obtained in the extreme strong coupling regime with no pair breaking mechanism[53]. For comparison with conventional phonon superconductors, we remind the reader that Pb has an energy gap ratio of 4.5.

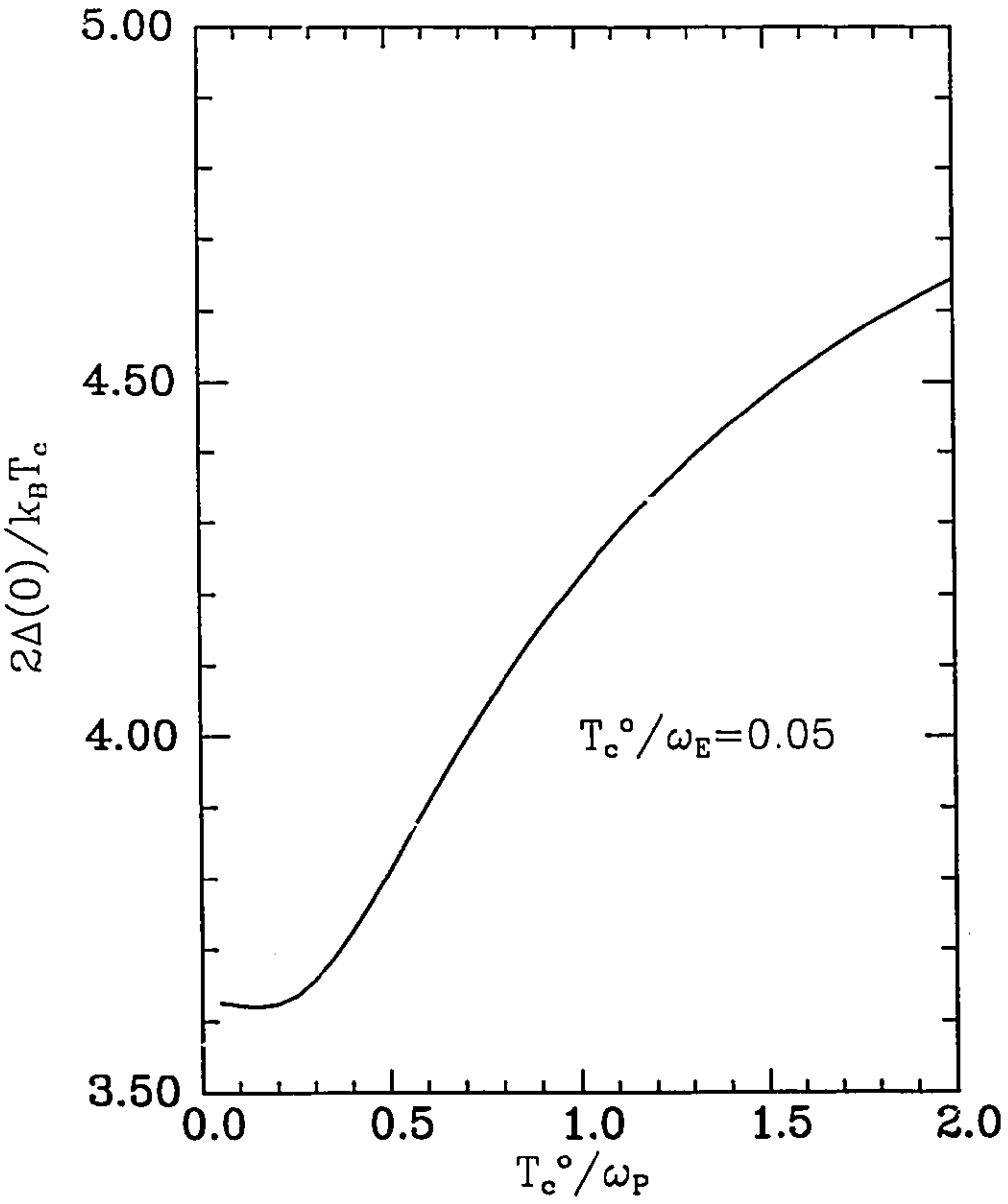

Figure 4.8-The zero temperature gap ratio versus $\frac{T_c^\circ}{\omega_P}$ for $\frac{T_c}{T_c^\circ} = 0.5$. $\frac{T_c}{\omega_{ph}} = 0.05$. The values obtained are all well below the maximum values that can be obtained in a purely attractive system.

4.6 ISOTOPE EFFECT

We now focus our attention upon the isotope effect that we would expect in such systems if we assume that the pairing interaction is due only to phonons. As we have already stated, we do not believe that phonons alone are responsible for the superconductivity in the high-T_c superconductors. Indeed, our results for the isotope effect will demand that if the scenario that we have discussed is to be applicable, the pairing mechanism cannot be phonons alone, and some other pairing mechanism must be invoked.

We have performed numerical as well as analytic calculations of the isotope effect, β, which is given by

$$\beta \equiv \frac{d\,log(T_c)}{d\,log(M)}, \tag{4.9}$$

where M is the ionic mass. In all of the results below, we have assumed that all of the attractive interaction is due to phonons;

$$E(\omega) = \alpha^2 F(\omega) = A\delta(\omega_{ph} - \omega) \tag{4.10}$$

Numerical results are shown in figure 4.9. This curve was calculated for $\frac{T_c}{\omega_{ph}} = 0.05$, and $T_c^\circ = 200$ K. We see that β is everywhere larger than $\frac{1}{2}$, the BCS result. The peak occurs at $\frac{T_c^\circ}{\omega_P} = 0.28$. We can gain more insight into this result by considering the Rainer-Culetto formula for the isotope effect[54]

$$\beta_{total} = \int_0^\infty d\omega R(\omega)\alpha^2 F(\omega)\,. \tag{4.11}$$

$R(\omega)$ is defined as

$$R(\omega) = \frac{1}{2T_c}[\frac{\delta T_c}{\delta\alpha^2 F(\omega)} + \omega\frac{d}{d\omega}\frac{\delta T_c}{\delta\alpha^2 F(\omega)}]\,. \tag{4.12}$$

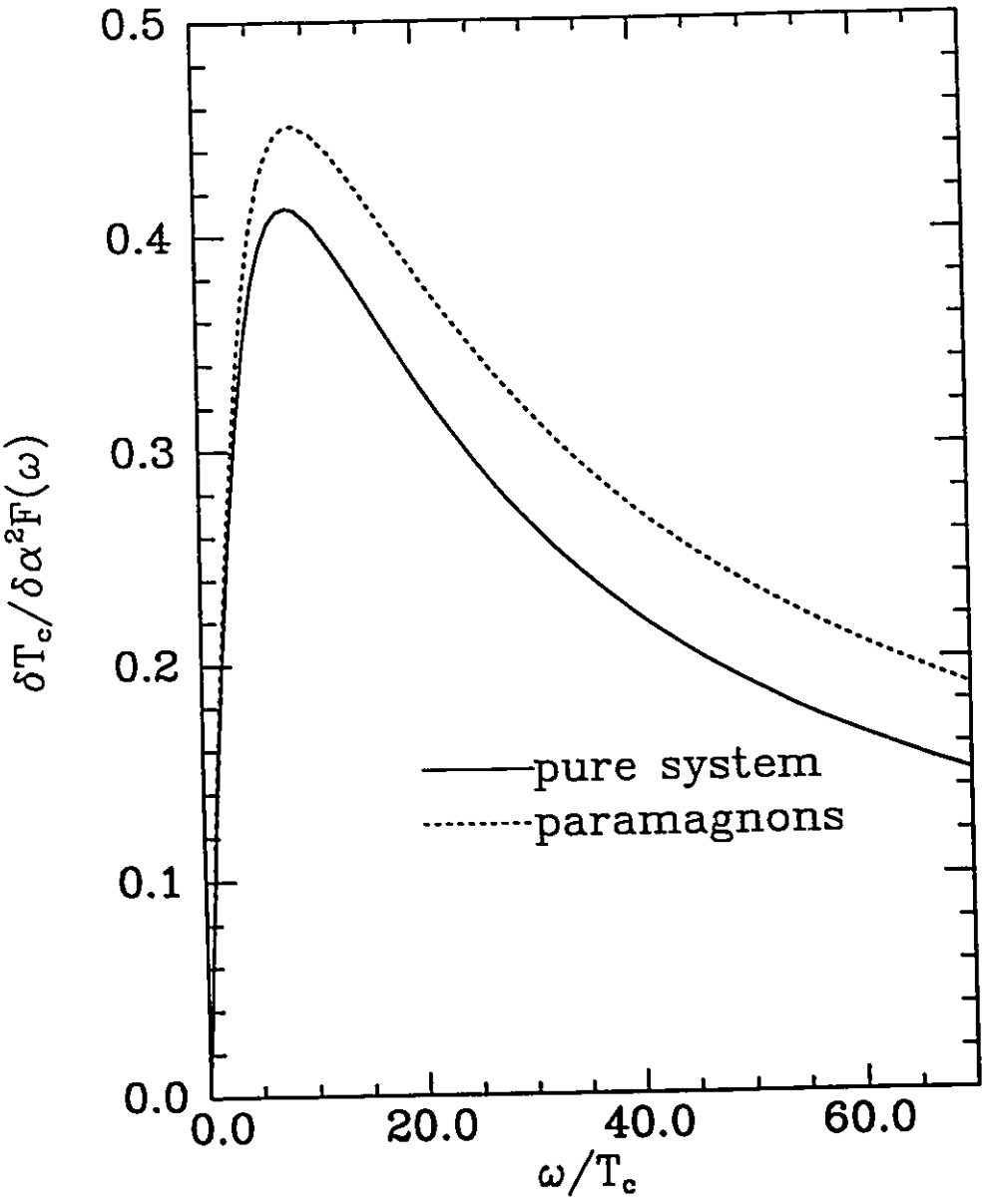

Figure 4.10-Functional derivative of the critical temperature with respect to the electron-boson spectral density versus $\frac{\omega}{T_c}$. For both curves $\frac{T_c}{\omega_{ph}} = 0.05$, and for the system with spin fluctuations, $\frac{T_c^s}{\omega_P} = 0.05$ and $\frac{T_c}{T_c^s} = 0.5$. The derivative for the purely attractive system is smaller and shifted to slightly lower $\frac{\omega}{T_c}$ than the derivative for the system with the spin fluctuations.

For Einstein spectral densities β is simply equal to $AR(\omega_{ph})$. We need to know the functional derivative of the critical temperature with respect to the electron-phonon spectral density in order to see why the isotope effect is larger than $\frac{1}{2}$. In figure 4.10 we show the functional derivative $\frac{\delta T_c}{\delta \alpha^2 F(\omega)}$ for two cases; a 200 K superconductor with no spin-fluctuations, and the same system with its critical temperature suppressed to 100 K by spin fluctuations. In both cases $\frac{T_c}{\omega_{ph}} = 0.05$, and for the second case $\frac{T_c^o}{\omega_P} = 0.05$. Both curves are everywhere positive definite, and the curve with spin fluctuations is everywhere larger than the curve for the pure system.

The curve for the system with the spin fluctuations does not diverge negatively at low frequencies as was seen in chapter 3. This is because we are treating the pairing and the depairing mechanisms distinctly in this calculation. In chapter 3, when we calculated the functional derivative of the critical temperature, we added spectral weight to both mechanisms. In this calculation, we have only enhanced the pairing mechanism. Marsiglio has calculated the functional derivative of T_c with respect to the spin fluctuation spectral density in the BCS limit. It is everywhere negative, and diverges negatively at zero frequency. The result of chapter 3 is the sum of these two terms in the special case of the two spectral functions being the same.

There are various factors contributing to the change in β when we add the spin fluctuations to the system. There is a suppression of T_c which tends to cause β to increase. In addition to this effect, there is a change in the functional derivative. One must remember that the functional derivative is plotted versus $\frac{\omega}{T_c}$, and hence the relevant data is at $\frac{\omega}{T_c}$=20.0 for T_c=200 K, and $\frac{\omega}{T_c}$=40.0 for T_c=100 K. One can see that both the functional derivative and its derivative with respect to frequency are smaller for the system with

spin fluctuations. However, both of them have been reduced by less than $\frac{1}{2}$, which in combination with the factor of two coming from the T_c suppression leads to an enhanced isotope effect.

Let us now look at the isotope effect for the two limiting cases that we considered at the start of the chapter, the BCS limit and the extreme strong coupling limit. In the BCS limit, T_c is given by equation 4.6, and hence

$$\beta = \frac{1}{2}\frac{\lambda^E}{\lambda^E - \lambda^P} \tag{4.13}$$

In the limit of $\lambda^P - 0$, we recover the BCS result of $\frac{1}{2}$. As λ^P becomes finite, β become greater than $\frac{1}{2}$, as our numerical results indicate. In the extreme strong coupling limit, T_c is given by equation 4.7 which yields

$$\beta = \frac{1}{2} \tag{4.14}$$

Our numerical results indicate that β is approaching this limit as $\frac{T_c}{\omega_{ln}}$ becomes large.

Chapter 5

Asymptotic Limits

In this chapter, we will consider Eliashberg theory in the limit in which the critical temperature, T_c, is much larger than the characteristic frequency of the spectral density function, ω_{ln}. This is the opposite of the BCS limit, which assumes that $\frac{T_c}{\omega_{ln}} << 1$. We should point out that for conventional phonon superconductors, $0 \leq \frac{T_c}{\omega_{ln}} \leq 0.3$. We will be considering the regime of $\frac{T_c}{\omega_{ln}} \rightarrow \infty$.

It is questionable whether this regime is physically relevant, as in this limit, $\lambda \rightarrow \infty$. As mentioned previously, if the pairing is mediated by phonons, it is widely believed that the lattice will become unstable for too strong an electron-phonon interaction[17]. However, it is still interesting to examine this regime if one wishes to know the range of values for superconducting properties that is predicted by the Eliashberg equations.

We will restrict ourselves to the model of Chapter 3, and consider both the g=1 and g$\neq$1 cases. We could consider the model of Chapter 4, but

the results are quite complicated due to the different frequency dependences of the competing interactions. As such, it seems to defeat the purpose of gaining some understanding of this limit of the equations.

We will begin by considering the equations at T_c. They are

$$\Delta(i\omega_n)Z_s(i\omega_n) = g\pi T \sum_{m=-\infty}^{\infty} \lambda(m-n)\frac{\Delta(i\omega_m)}{|\omega_m|} \tag{5.1a}$$

$$\omega_n Z_s(i\omega_n) = \omega_n + \pi T \sum_{m=-\infty}^{\infty} \lambda(m-n)sign(\omega_m) \tag{5.1b}$$

Equations 5.1a and 5.1b can be transformed into a Hermitian eigenvalue problem by introducing a parameter $\rho(T)$[24], defined by

$$\tilde{\Delta}(i\omega_n) = \frac{\tilde{\Delta}(i\omega_n)}{|\tilde{\omega}(i\omega_n)| + \pi T\rho(T)} \tag{5.2}$$

T_c is given by $\rho(T_c) = 0$.

We can then write 5.1a and 5.1b as

$$\begin{aligned} &\sum_{m=1}^{\infty}[K_{m,n} - \rho\delta_{m,n}]\tilde{\Delta}(i\omega_n) = 0, \quad n \geq 1 \\ &K_{m,n} = g[\lambda(m-n) + \lambda(m+n-1)] - \delta_{m,n}[2m - 1 + \lambda(0) + \sum_{m'=1}^{m-1}\lambda(m')] \end{aligned} \tag{5.3}$$

We solve this problem by setting the determinant of K=0. For simplicity, we will use an Einstein spectral function.

$$E(\omega) = \frac{\lambda\omega_E}{2}\delta(\omega - \omega_E) \tag{5.4}$$

Let us first consider the case g=1. For this case, we note that $\lambda(0)$ does not contribute to the solution. In the limit of $\omega_E << T_c$, we are able to make the approximation

$$\lambda(m-n) = \frac{\lambda\omega_E^2}{\omega_E^2 + 4\pi^2T_c^2(m-n)^2} \approx \frac{\lambda\omega_E^2}{4\pi^2T_c^2(m-n)^2} \tag{5.5}$$

If we define

$$\bar{T}_c \equiv \frac{T_c}{\sqrt{\bar{A}}\omega_E} \tag{5.6}$$

we can then write $K_{m,n}$ in terms of $\bar{T}_c$ alone, and there are no other material parameters present. $\bar{T}_c$ is then a universal number. We have neglected μ^*, the Coulomb psuedopotential.

Allen and Dynes[29] consider a lower bound on T_c by taking only the m=n=1 term in the determinant. This leads to

$$K_{1,1} = \lambda(1) - 1 = 0\,, T_c = \frac{\omega_E}{2\pi}\sqrt{\lambda} \tag{5.7}$$

Had we not made the approximation of equation 5.5, we would replace $\sqrt{\lambda}$ with $\sqrt{\lambda - 1}$. This result shows that there is no limit upon T_c imposed by the Eliashberg equations themselves, and that one must look elsewhere to find such a limit.

For g≠1, we obtain for T_c, again considering only the m=n=1 term of the determinant

$$T_c = \frac{\omega_E}{2\pi}\sqrt{\frac{\lambda(2g-1)-1}{1+\lambda(1-g)}} \approx \frac{\omega_E}{2\pi}\sqrt{\frac{2g-1}{1-g}} \tag{5.8}$$

in the limit of large λ. We are not able to make the approximation of 5.5 in this case, as $K_{m,n}$ depends on $\lambda(0)$. This result is qualitatively different than the g = 1 case. We first note that it is independent of $\lambda(0)$. In addition, it also breaks down for g≤ $\frac{1}{2}$, as T_c would then become complex.

It is possible to improve upon this estimate of T_c by including the m,n=2 terms. The result for g = 1 is

$$T_c = 0.180\sqrt{\lambda}\omega_E \tag{5.9}$$

One can solve the Eliashberg equations numerically using the approximation of equation 5.5 and one finds[53]

$$T_c = 0.182\sqrt{\lambda}\omega_E \tag{5.10}$$

Hence, our 2×2 result is very close to the exact result. More importantly, the dependence upon λ and ω_E is the same. We will only work within the m=n=1 approximation henceforth, as it is sufficient to give us the λ and ω_E dependence.

We have also calculated the specific heat jump in the asymptotic limit. In order to perform this calculation, we must use the nonlinear equations, 3.22a and 3.22b, and include terms to first order in $(\frac{\Delta_1}{\omega_1})^2$. Upon expanding and combining 3.1 and 3.2, we obtain

$$(g-1)\lambda(0) + g\lambda(1) - 1 - \frac{1}{2}(g-1)\lambda(0)(\frac{\Delta_1}{\omega_1})^2 - \frac{1}{2}(g+1)\lambda(1)(\frac{\Delta_1}{\omega_1})^2 = 0 \tag{5.11}$$

We then expand in T about T_c and use the result of equation 5.8 for T_c to obtain

$$(\frac{\Delta_1}{\omega_1})^2 = 4\frac{[\lambda(2g-1)-1][1+(1-g)\lambda]}{(1+g)\lambda+(1-g)\lambda^2}(1-t) \tag{5.12}$$

We have retained the λ dependence, as if we wish to recover the g=1 results, we must set g=1 before taking the limit $\lambda \to \infty$.

We also expand the free energy, given by 2.16, to obtain

$$\frac{\Delta F}{N(0)} = -\frac{(\pi T)^2}{2}(1+\lambda(1))(\frac{\Delta_1}{\omega_1})^4 \tag{5.13}$$

Expanding in T about T_c, and using 5.8 and 5.12, we find

$$\frac{\Delta C}{\gamma T_c} = \frac{24}{(1+\lambda)g}\frac{[\lambda(2g-1)-1]^2[1+(1-g)\lambda]^2}{\lambda^2[1+g+(1-g)\lambda]} \tag{5.13}$$

If we let $\lambda \to \infty$ with g$\neq$1, we obtain

$$\frac{\Delta C}{\gamma T_c} = 24\frac{(2g-1)(1-g)}{g} \tag{5.14}$$

If we set g=1, and then take the limit of $\lambda \to \infty$, we obtain

$$\frac{\Delta C}{\gamma T_c} = \frac{12}{1+\lambda} \tag{5.15}$$

The two results show distinctly different behavior, as was discussed in Chapter 3.

All of the results that we have considered so far have been restricted to temperatures at or near T_c. It is rather straight forward to obtain explicit expressions near T_c, as the equations are linear, or at most quadratic. For quantities away from T_c, it is not so simple to obtain explicit expressions, but it is possible to infer the λ and ω_E dependence of the quantity of interest.

We can combine equations 3.1 and 3.2 and write them in the form

$$\Delta(i\omega_n) = \pi T \sum_{m=-\infty}^{\infty} \frac{\lambda\omega_E^2}{\omega_E^2 + 4\pi^2T^2(m-n)^2}\left[g\Delta(i\omega_m) - \frac{\omega_m}{\omega_n}\Delta(i\omega_n)\right]\frac{1}{\sqrt{\Delta^2(i\omega_m)+\omega_m^2}} \tag{5.16}$$

where we have used an Einstein spectral density. If we introduce the notation $\bar{Q} \equiv \frac{Q}{\omega_E}$, and rewrite equation 5.16 in terms of these quantities, we obtain

$$\bar{\Delta}(i\omega_n)\frac{\omega_E}{A} = \pi t\bar{T}_c \sum_{m=-\infty}^{\infty} \frac{1}{1+4\pi^2t^2\bar{T}_c^2(m-n)^2}\left[g\bar{\Delta}(i\omega_m) - \frac{\bar{\omega}_m}{\bar{\omega}_n}\bar{\Delta}(i\omega_n)\right]\frac{1}{\sqrt{\bar{\Delta}_m^2+\bar{\omega}_m^2}} \tag{5.17}$$

Taking the limit of $\omega_E \to 0$, the left-hand side of 5.17 drops out, and we are left with an equation with no material parameters. This implies that $\bar{T}_c = f(g)$, and $\bar{\Delta}(i\omega_n) = j(t,g)$. With these results, we are able to determine

the dependence of the free energy upon λ and ω_E. Writing equation 2.14 in terms of $\bar{\Delta}(i\omega_n)$ and $\bar{T}_c$ gives

$$\frac{\Delta F}{N(0)} = 2\pi t\bar{T}_c\omega_E \sum_{n=-\infty}^{\infty} \bar{\omega}_n\omega_E[\frac{\bar{\omega}_n}{\sqrt{\bar{\Delta}_n^2+\bar{\omega}_n^2}} - sign(\bar{\omega}_n)] + \pi^2 t^2\bar{T}_c^2\omega_E^2 \sum_{n=-\infty}^{\infty}\sum_{m=-\infty}^{\infty} [\frac{\bar{\omega}_n\bar{\omega}_m + g\bar{\Delta}_n\bar{\Delta}_m}{\sqrt{\bar{\Delta}_n^2+\bar{\omega}_n^2}\sqrt{\bar{\Delta}_m^2+\bar{\omega}_m^2}} - sign(\omega_n\omega_m)] \times \frac{\lambda(0)}{1+4\pi^2t^2T_c^2(m-n)^2} \tag{5.18}$$

This has the form $\frac{\Delta F}{N(0)} = a(t)\omega_E^2 + b(t,g)A\omega_E$, which in the limit of $\omega_E \to 0$ is proportional to $b(t,g)A\omega_E$. This relation holds only for g≠1. From $\frac{\Delta F}{N(0)}$, one obtains the thermodynamic critical field, $H_c(T)$, through

$$\frac{H_c^2(T)}{8\pi} = \Delta F \tag{5.19}$$

and hence the thermodynamic critical field is proportional to $\sqrt{A\omega_E}$. We have verified this dependence numerically. We have also computed the critical field as a function of temperature for various values of g. The results are shown in figure 5.1. Rather than plot $H_c(T)$, we have plotted the reduced thermodynamic critical field, given by

$$h_c(t) \equiv \frac{H_c(T)}{T_c|dH_c(T)/dT|_{t=T_c}} \tag{5.20}$$

The temperature dependence is completely different for g≠1 than for g=1. For g=1[56], the curve has a rather large linear region for t near 1, and curves upwards as t decreases. For g≠1, there is no linear region, and the curvature is of the opposite sign to the g=1 case.

Appendices 2 and 3 are publications[83,90] of work that was done in collaboration with F. Marsiglio and J.P. Carbotte. They deal with the asymptotic limit in purely attractive systems, and as such were not included in the main body of the thesis. They are submitted as part of the thesis.

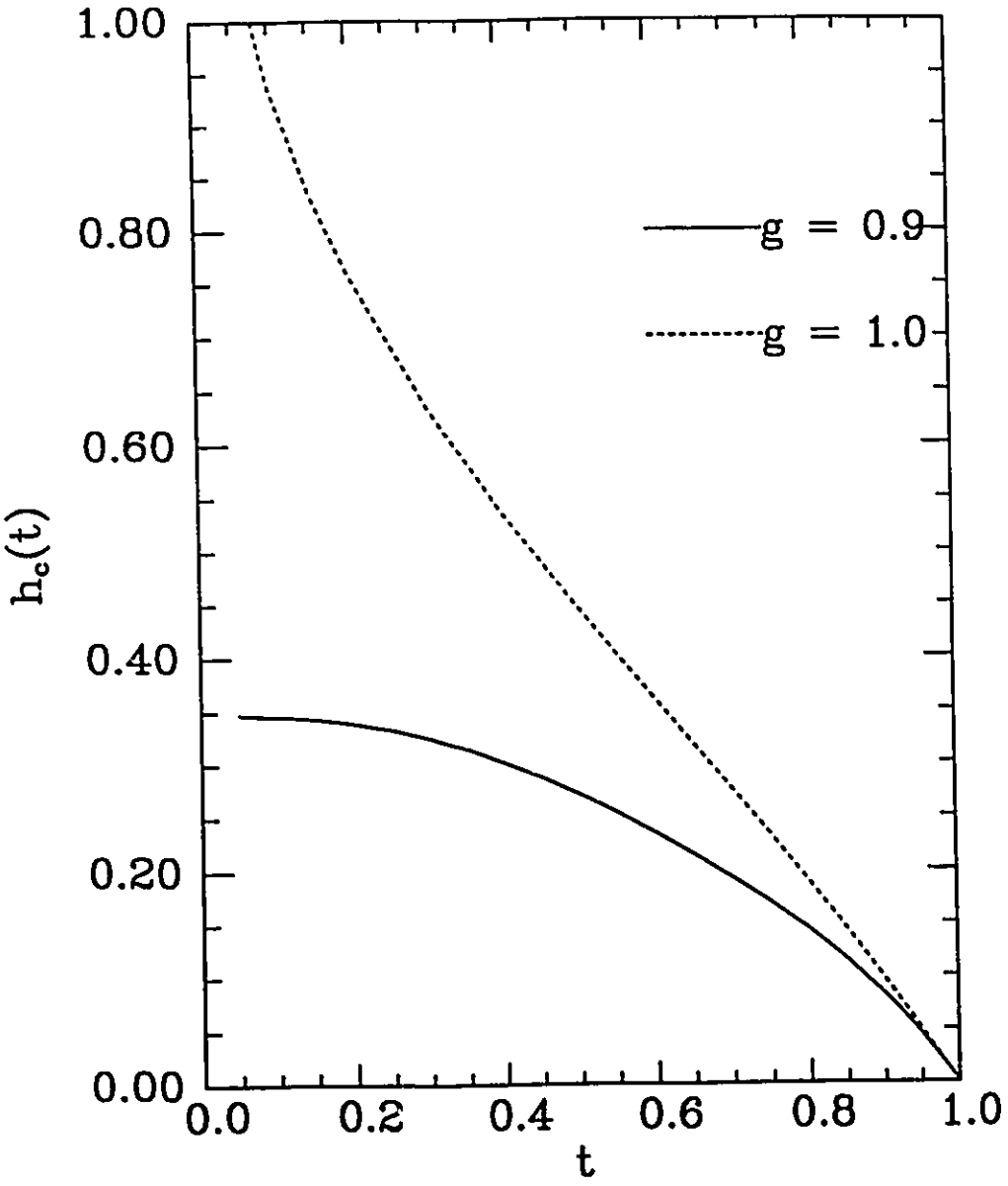

Figure 5.1-Reduced thermodynamic critical field versus reduced temperature for g=1 and g=0.9. The temperature dependence is completely different in the two cases.

Chapter 6

Conclusion

Our theoretical results can be rather neatly summarized. In a model of superconductivity in which there are two competing dynamical interactions, there are distinct signatures in the specific heat data. In particular, we would expect that the jump in the specific heat would be enhanced over the value that one would observe in a material where there is no competing mechanism, and the ratio of the critical temperature to the characteristic energy of the excitations is comparable. We would also expect that the slope of the specific heat just below T_c would be steeper than in the attractive case. Associated with this steep slope would be a move to a larger reduced temperature of the zero crossing of the specific heat difference. We would also predict that the energy gap ratio would be larger in a model with competing mechanisms than in a purely attractive model.

The asymptotic behavior of this model was also seen to be distinctly different from the usual behavior. In addition, we obtained results for the isotope effect which are greater than $\frac{1}{2}$, the BCS value.

Unfortunately, the experimental results for the specific heat and the energy gap ratio are not completely certain, as both the experiments and their interpretation are difficult.

Measurement of the electronic component of the specific heat is complicated by various factors. The quantity of interest is the difference between the specific heats of the normal and superconducting states. In materials with reasonably low critical temperatures and critical magnetic fields, such data are readily attainable. At low temperatures, the lattice contribution to the total specific heat is small, and can be accurately subtracted. The normal state specific heat can be obtained by applying a magnetic field of sufficient strength to cause the sample to be normal. In the oxide superconductors, there are difficulties associated with these measurements. Because the critical temperatures of these materials are relatively high, the lattice contribution to the total specific heat is quite large compared to the electronic contribution. In Figure 6.1 we show some experimental results for specific heat measurements on YBCO[57]. The two insets show details of the curve at T_c and low T. Notice that the anomaly at T_c is only about 2 - 3 % of the total specific heat. As such, it is imperative that the non-electronic contributions to the specific heat be known to a high degree of accuracy and precision in order to be able to obtain useful information about the electronic specific heat.

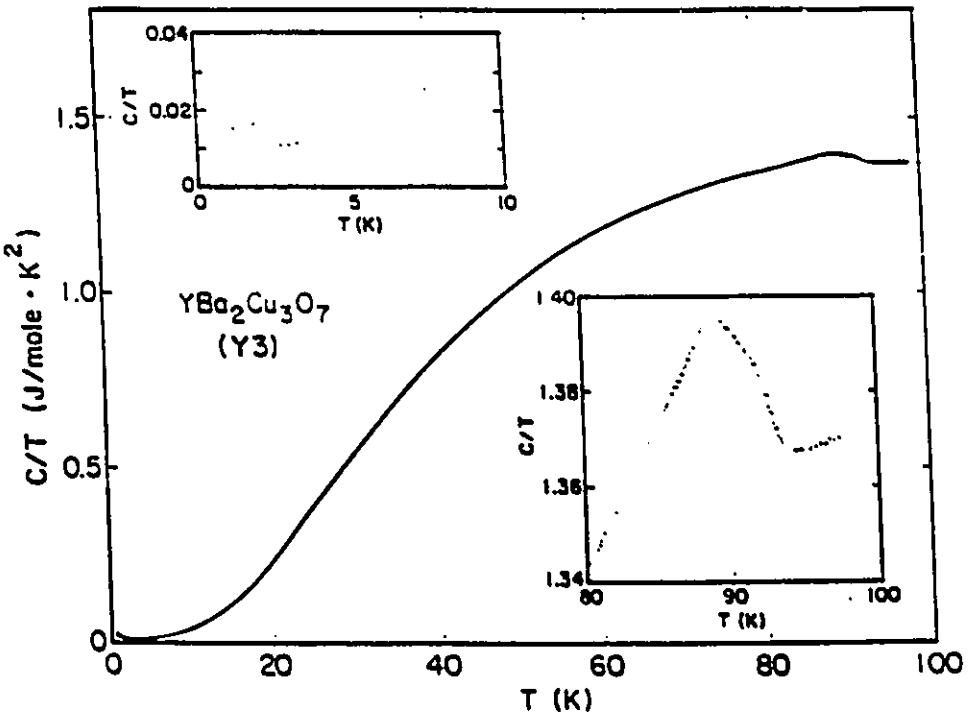

Figure 6.1-Experimental results for the specific heat of $YBa_2Cu_3O_7$. Note how small the anomaly at T_c is compared to the total signal. Also, there is an upturn at low temperature, rather than the usual exponential decay, as shown in figure 1.3.

An additional complication is that it is only possible to get normal state data close to T_c, as the critical fields are quite large and difficult to obtain in the laboratory.

At low temperatures, there is an upturn in the specific heat rather than the expected exponential decay. It is felt that this upturn is related to ordering of magnetic impurities[58]. However, there is still a linear term at low temperature. Various suggestions have been put forward to explain this term. Part of the sample could remain normal, it could be gapless superconductivity or perhaps due to impurity phases[58]. However, there is as yet no concensus on the origin of the linear term.

Because of these difficulties, the analysis of the experimental data is usually done by assuming that the BCS relation, $\frac{\Delta C}{\gamma T_c}$=1.43 holds [59]. However, Beckman *et al.* point out that the γ extracted by this analysis is not in good agreement with values extracted from high temperature magnetization [60] experiments or band structure calculations[61], which are in reasonable agreement with one another.

Some groups have analysed their data without making the assumption that $\frac{\Delta C}{\gamma T_c}$=1.43. Loram and Mirza[62] have used differential calorimetry on YBCO samples and report $\frac{\Delta C}{\gamma T_c}$=4.1 and $\frac{2\Delta(0)}{k_B T_c}$=6$\pm$.5 Recently, Phillips *et al.* [63] have reported $\frac{\Delta C}{\gamma T_c}$=4.8 and $\frac{2\Delta(0)}{k_B T_c}$=7.

The normalized slope of the specific heat is a quantity that is independent of γ. In addition, if the slope is determined in a fairly narrow temperature range near T_c, one might hope that the results would be reasonable insensitive to the details of the subtraction of the lattice specific heat. Akis and Carbotte[45] have analysed specific heat data for YBCO[46] and find $T_c\frac{\Delta C'}{\Delta C}$ in the range of 8 - 14, depending upon the temperature interval used

in the analysis. Unfortunately, this is the only determination of this quantity that we are aware of.

We should also mention that it has been suggested that there are fluctuation effects in the specific heat near T_c, due to the short coherence length in the high T_c oxides[64]. These effects would tend to make the slope steeper than the mean field slope.

We now consider the zero crossing of the specific heat difference. Phillips *et al.* [65] have determined ΔC by subtracting measurements performed in high magnetic fields from low field measurements. Their data exhibit a zero crossing at $t = \frac{T}{T_c} \approx 0.8$ in LaCaCuO with T_c= 37 K. Junod *et al.* [46] find a zero crossing at t=0.8 in a YCBO sample. Such large values of t for the zero crossing of the specific heat support the hypothesis that the specific heat jump and the slope of the specific heat difference are large in the oxide superconductors. This is motivated by the entropy constraint on the specific heat difference

$$\Delta S = \int_0^{T_c} \frac{\Delta C}{T} dT = 0 \tag{6.1}$$

If the zero crossing of ΔC occurs at high t, then ΔC must get large in order to compensate for this. The $\frac{1}{T}$ accentuates this effect. Therefore, it would seem that there is strong evidence for the specific heat jump to be large in the high T_c materials. In particular it appears that $\frac{\Delta C}{\gamma T_c}$ is larger than the maximum value of $\approx$3.73 which Blezius and Carbotte [26] find for a superconductor with only attractive dynamical interactions.

The experimental results for the energy gap are also difficult to interpret. The main techniques used to measure the energy gap are infrared spectroscopy and tunnelling spectroscopy. In addition, Raman spectroscopy

and high resolution photo-emission experiments have been employed on the high T_c materials.

In both the tunnelling and the far infrared measurements, there is fairly good agreement upon the general features of the data. However, the interpretation of the data and an extraction of a value for $\frac{2\Delta(0)}{k_B T_c}$ has proved to be difficult. There does seem to be a consensus emerging from the various techniques however[66,67]. It seems that there is a reduction in the electronic density of states at the Fermi surface in the superconducting state. Whether the reduction is complete or not (is there a well developed energy gap) is not entirely clear. The energy scale of the reduction seems to scale with the critical temperature, and if it is interpreted as an energy gap, it leads to a value of $\frac{2\Delta(0)}{k_B T_c} \approx 8$. The temperature dependence of this gap-like feature is very non-BCS like. There are groups who would dispute the assignment of this feature to the energy gap, particularly in the infrared results[68]. However, their estimates would place the gap at an even larger value. It would seem to be fairly safe to conclude then, that $\frac{2\Delta(0)}{k_B T_c}$ is certainly much larger than 3.54, the BCS value, and is around 8. This estimate agrees well with photo-emmission and Raman work as well.

This large value of the energy gap, in conjunction with the specific heat results are consistent with the model that we have discussed in this thesis. It would seem that the experimental results cannot be accounted for in Eliashberg theory without competing interactions. This conclusion has to be reconciled with the isotope effect results.

Isotope effect experiments have been done for the high T_c oxide materials, and again there is a certain amount of variability in the results. The

most commonly reported results are for the oxygen isotope effect, β_{Ox}, but there are results for the other species in the various compounds.

For YBCO, the oxygen isotope effect seems to be small, but measurable. A typical value is $\beta_{Ox} \approx 0.02$[6], but there are results giving $\beta_{Ox} \approx 0.1$[69]. In LaSrCuO, the oxygen isotope effect is considerably larger, although there is a fair degree of variability in the reported values. Typical values are in the range of 0.1 to 0.2[70] for β_{Ox}. However, there have been reported values of as high as $\beta_{Ox} \approx 0.8$[71] in this material. A recent study[72] of β_{Ox} in $La_{2-x}Sr_xCuO_4$ as a function of x has yielded some interesting results. They find $\beta_{Ox} \approx 0.4$ for x≈0.07, rising to 0.6 for x≈0.11, and then falling to 0.1 and remaining fairly constant for any further increases of x. For this material, T_c is also a function of x, as shown in figure 3.1, the phase diagram for $La_{2-x}Sr_xCuO_4$. The peak in β_{Ox} found by Crawford *et al.* occurs for a fairly low critical temperature. Measurements of the isotope effect for elements other than oxygen all seem to give no measurable effect, at least in YBCO[6].

Values of β greater than $\frac{1}{2}$ are difficult to account for in a model where there are only attractive interactions. In such a model, one can get enhanced isotope effects if there is structure in $N(\epsilon)$ [73], the electronic density of states, near the Fermi surface which varies rapidly on the scale of ω_D, the typical energy for the exchange boson. One can also get $\beta > \frac{1}{2}$ in a model with paramagnetic impurities, however in that case, $\frac{\Delta C}{\gamma T_c}$ is suppressed below the BCS value of 1.43.

The conclusion that one can draw from the isotope effect measurements would seem to be that there is an isotope effect, but it is small. In order for the competing interaction model to be consistent with this conclusion, we would require that the attractive interaction have two components

to it, one due to phonons, and one due to some other mechanism which is not affected by the isotopic substitution. There is a long history of alternate pairing mechanisms such as excitons[74,75] and plasmons[76]. Whether such excitations exist in the oxide superconductors, and whether they couple to the conduction electrons is not well known. Combined exciton-phonon models have been studied theoretically[77], and a value of $\frac{\lambda_{exciton}}{\lambda_{phonon}}$ deduced that produces the observed isotope shifts. If there is in addition a repulsive interaction as we have considered, then such estimates would have to be revised.

Appendix 1

Strong Coupling Corrections

In this appendix, we will outline the calculation of the strong coupling correction to the specific heat jump, $\frac{\Delta C}{\gamma T_c}$. We will treat the model of Chapter 3,

$$Z(i\omega_n)\Delta(i\omega_n) = g\pi T \sum_{m=-\infty}^{\infty} \lambda(m-n)\frac{\Delta(i\omega_m)}{\sqrt{\Delta^2(i\omega_m)+\omega_m^2}} \qquad (A1.1)$$

$$Z(i\omega_n) = 1 + \frac{\pi T}{\omega_n} \sum_{m=-\infty}^{\infty} \lambda(m-n)\frac{\omega_m}{\sqrt{\Delta^2(i\omega_m)+\omega_m^2}} \qquad (A1.2)$$

We expand for $T \sim T_c$ to obtain

$$Z(i\omega_n)\Delta(i\omega_n) = g\pi T \sum_{m=-\infty}^{\infty} \lambda(m-n)\frac{\Delta(i\omega_m)}{|\omega_m|}[1 - \frac{1}{2}(\frac{\Delta(i\omega_m)}{\omega_m})^2...] \qquad (A1.3)$$

$$Z(i\omega_n) = 1 + \frac{\pi T}{\omega_n} \sum_{m=-\infty}^{\infty} \lambda(m-n)sign(\omega_m)[1 - \frac{1}{2}(\frac{\Delta(i\omega_m)}{\omega_m})^2...] \qquad (A1.4)$$

In A1.4, this leads us to consider terms like

$$\sum_{m=-\infty}^{\infty} \frac{1}{\omega_m^{2i}} \frac{1}{\nu^2 + (\omega_n - \omega_m)^2} \qquad (A1.5)$$

We are interested in corrections to the BCS results, which are obtained by neglecting the m and n dependence in $\frac{1}{\nu^2+(\omega_n-\omega_m)^2}$. We therefore expand as follows

$$\begin{aligned}
&\sum_{m=-\infty}^{\infty} \frac{1}{\omega_m^{2i}} \frac{1}{\nu^2 + (\omega_n - \omega_m)^2} \\
&= \sum_{m=1}^{\infty} \frac{1}{\omega_m^{2i}} [\frac{1}{\nu^2 + (\omega_n - \omega_m)^2} - \frac{1}{\nu^2 + (\omega_n + \omega_m)^2}] \\
&= \sum_{m=1}^{\infty} \frac{1}{\omega_m^{2i}} \frac{4\omega_n\omega_m}{(\nu^2 + \omega_n^2 + \omega_m^2)^2 - 4\omega_n^2\omega_m^2} \\
&\cong \sum_{m=1}^{\infty} \frac{4\omega_n}{\omega_m^{2i-1}} \frac{1}{(\nu^2 + \omega_n^2 + \omega_m^2)^2} [1 + \frac{4\omega_m^2\omega_n^2}{(\nu^2 + \omega_n^2 + \omega_m^2)^2} - ...]
\end{aligned}$$

We recall that the Matsubara frequencies are proportional to the temperature, and hence we are expanding in powers of $(\frac{T}{\nu})$. We can see that the second term is of order $(\frac{T}{\nu})^6$, and we will drop this term. Hence we need to evaluate sums like

$$U_i = \omega_n 4\pi T \sum_{m=1}^{\infty} \frac{1}{\omega_m^{2i-1}} \frac{1}{(\nu^2 + \omega_n^2 + \omega_m^2)^2} \qquad (A1.6)$$

They give

$$U_1 = \frac{2\omega_n}{(\omega_n^2 + \nu^2)^2} \ln \frac{1.13\sqrt{\nu^2 + \omega_n^2}}{k_B T} - \frac{\omega_n}{(\nu^2 + \omega_n^2)^2} \qquad (A1.6a)$$

and

$$U_2 = \omega_n \frac{7}{2} \frac{\zeta(3)}{(\pi T)^2} \frac{1}{(\nu^2 + \omega_n^2)^2} \qquad (A1.6b)$$

with $\zeta(3)$ the Riemann zeta-function. If we define

$$Z_N(i\omega_n) \equiv 1 + \frac{\pi T}{\omega_n} \sum_{m=-\infty}^{\infty} \lambda(m-n) sign(\omega_m) \qquad (A1.7)$$

and substitute the results of A1.6 into A1.4, we obtain

$$Z_S(i\omega_n) - Z_N(i\omega_n) = -\Delta^2(T) \int_0^{\infty} \frac{2\nu\alpha^2 F(\nu) d\nu}{(\nu^2 + \omega_n^2)^2} [2\ln \frac{1.13\sqrt{\nu^2 + \omega_n^2}}{k_B T} - 1] \qquad (A1.8)$$

A1.3, expanded in a fashion similar to A1.4, gives

$$Z_S(i\omega_n)\Delta(T) = g\Delta(T)\int_0^\infty 2\nu\alpha^2F(\nu)d\nu[2\pi T\sum_{m=1}^{\infty}\frac{1}{\omega_m}\frac{1}{\nu^2+\omega_n^2+\omega_m^2} + 2\pi T\sum_{m=1}^{\infty}\frac{4\omega_n^2\omega_m}{(\nu^2+\omega_n^2+\omega_m^2)^3} - \frac{1}{2}\Delta^2(T)2\pi T\sum_{m=1}^{\infty}\frac{1}{\omega_m^3}\frac{1}{\nu^2+\omega_n^2+\omega_m^2}] \quad (A1.9)$$

Evaluating the sums yields

$$2\pi T\sum_{m=1}^{\infty}\frac{1}{\omega_m}\frac{1}{\nu^2+\omega_n^2+\omega_m^2} = \frac{1}{\nu^2+\omega_n^2}\ln\frac{1.13\sqrt{\nu^2+\omega_n^2}}{k_BT} - \frac{(\pi T)^2}{6(\nu^2+\omega_n^2)} \quad (A1.10a)$$

$$2\pi T\sum_{m=1}^{\infty}\frac{4\omega_n^2\omega_n}{(\nu^2+\omega_n^2+\omega_m^2)^3} = \frac{\omega_n^2}{(\nu^2+\omega_n^2)^2} \quad (A1.10b)$$

$$2\pi T\sum_{m=1}^{\infty}\frac{1}{\omega_m^3}\frac{1}{\nu^2+\omega_n^2+\omega_m^2} = \frac{7}{4}\frac{\zeta(3)}{(\pi T)^2}\frac{1}{\nu^2+\omega_n^2} - \frac{1}{(\nu^2+\omega_n^2)^2}\ln\frac{1.13\sqrt{\nu^2+\omega_n^2}}{k_BT} \quad (A1.10c)$$

and hence

$$Z_S(i\omega_n)\Delta(T) = g\Delta(T)\int_0^\infty 2\alpha^2F(\nu)d\nu[\frac{1}{\nu^2+\omega_n^2}\ln\frac{1.13\sqrt{\nu^2+\omega_n^2}}{k_BT} - \frac{(\pi T)^2}{6(\nu^2+\omega_n^2)} + \frac{\omega_n^2}{(\nu^2+\omega_n^2)^2} - \frac{1}{2}\Delta^2(T)[\frac{7}{4}\frac{\zeta(3)}{(\pi T)^2}\frac{1}{\nu^2+\omega_n^2} - \frac{1}{(\nu^2+\omega_n^2)^2}\ln\frac{1.13\sqrt{\nu^2+\omega_n^2}}{k_BT}]] \quad (A1.11)$$

We evaluate for n=1, and use $Z_N(1) = 1+\lambda$, to get

$$1 = F(T) + \Delta^2(T)G(T) \quad (A1.12)$$

where

$$F(T) \equiv g\frac{\lambda}{1+\lambda}\ln\frac{1.13\omega_{ln}}{k_BT} - g\frac{(\pi T)^2}{1+\lambda}[a(T) - \frac{4}{3}b] \quad (A1.12a)$$

and

$$G(T) \equiv \frac{-g\lambda}{1+\lambda}\frac{g7}{8}\frac{\zeta(3)}{(\pi T)^2} + \frac{g}{2}\frac{a(T)}{1+\lambda} + \frac{a}{1+\lambda} - \frac{b}{2(1+\lambda)} \quad (A1.12b)$$

In this expresssion,

$$a(T) = \int_0^\infty \frac{2\nu\alpha^2 F(\nu)d\nu}{\nu^4} \ln\frac{1.13\nu}{k_B T}$$

and

$$b = \int_0^\infty \frac{2\nu\alpha^2 F(\nu)d\nu}{\nu^4}$$

We have neglected the n dependence in the square root factors for simplicity.

In order to calculate the specific heat jump we need an expression for the free energy difference. We expand equation 2.16 in similar fashion to find

$$\frac{\Delta F}{N(0)} = \frac{1}{2}\frac{(1+\lambda)^2}{\lambda}\Delta^4(T)K(T) \qquad (A1.13)$$

where

$$K(T) = \frac{-g\lambda}{1+\lambda}\frac{7}{8}\frac{\zeta(3)}{(\pi T)^2} + \frac{g\lambda}{(1+\lambda)^2}\frac{1}{T}[c(T) - a(T) + \frac{b}{4}]$$

with

$$c(T) = \int_0^\infty \frac{2\nu\alpha^2 F(\nu)d\nu}{\nu^4} \ln^2\frac{1.13\nu}{k_B T}$$

Solving A1.12 for $\Delta(T)$ in powers of $(T - T_c)$, and putting the solution into A1.13, we obtain for the normalised specific heat jump

$$\frac{\Delta C}{\gamma T_c} = 1.43[1 + a_1(\frac{T_c}{\omega_{ln}})^2 \ln\frac{\omega_{ln}}{b_1 T_c}] \qquad (A1.14)$$

with

$$a_1 = \pi^2\Big[(4 + \frac{8}{7\zeta(3)}(1 + \frac{2}{g}))\alpha_1 - \frac{1}{g}\frac{8}{7\zeta(3)}\alpha_3\Big]$$

and

$$b_1 = \frac{1}{1.13} exp\Big\{\frac{(\frac{16}{3} + \frac{1}{g}\frac{8}{7\zeta(3)}\alpha_2 - \frac{8}{7\zeta(3)}\alpha_3 \ln\beta_3 - \frac{8}{7\zeta(3)}\alpha_1}{(4 + \frac{8}{7\zeta(3)}(1 + \frac{2}{g}))\alpha_1 - \frac{1}{g}\frac{8}{7\zeta(3)}\alpha_3}\Big\}$$

The coefficient α_1 is obtained from $a(T)$ through

$$\begin{aligned} a(T) &= \int_0^\infty \frac{2\nu\alpha^2 F(\nu)d\nu}{\nu^4}\ln\frac{1.13\nu}{k_BT} \\ &= \frac{\alpha_1}{\omega_{ln}^2}\int_0^\infty \frac{2\nu\alpha^2 F(\nu)d\nu}{\nu^2}\ln\frac{1.13\nu}{k_BT} \\ &= \frac{\alpha_1\lambda}{\omega_{ln}^2}\ln\frac{1.13\omega_{ln}}{k_BT} \end{aligned}$$

The first step follows from the mean value theorem, and the second follows from the definition of ω_{ln}. The other coefficients are derived in similar fashion from b (α_2) and $c(T)$ (α_3 and β_3). For Einstein spectral densities, all of the coefficients are equal to one.

We have also derived expressions for other quantities. They are all obtained in a fashion similar to that sketched above. As such, we will just present the results, and omit the derivations.

For the normalised slope of the specific heat we obtain

$$\frac{d}{dt}\frac{\Delta C}{\gamma T_c} = 3.77[1 + a_2(\frac{T_c}{\omega_{ln}})^2\ln\frac{\omega_{ln}}{b_2T_c}] \qquad (A1.15)$$

with

$$a_2 = \frac{3}{4-2A}\pi^2[(\frac{28}{3} + \frac{160}{21\zeta(3)}(\frac{1}{g}+\frac{1}{2}) - 4A - \frac{32}{7}\frac{A}{\zeta(3)}(\frac{1}{g}+\frac{1}{2})]\alpha_1 + (A-\frac{5}{3})\frac{16}{7\zeta(3)}\alpha_3$$

and

$$b_2 = \frac{1}{1.13}exp\left\{\frac{(\frac{-112}{9} + (\frac{1}{2}-\frac{7}{3g})\frac{8}{7\zeta(3)} + \frac{16A}{3} + \frac{16A}{g7\zeta(3)})\alpha_2 - (A-\frac{5}{3})\frac{16}{7\zeta(3)}\alpha_3\ln\beta_3}{[\frac{28}{3} + \frac{160}{21\zeta(3)}(\frac{1}{g}+\frac{1}{2}) - 4A - \frac{32}{7}\frac{A}{\zeta(3)}(\frac{1}{g}+\frac{1}{2})]\alpha_1 + (A-\frac{5}{3})\frac{16}{7\zeta(3)}\alpha_3}\right\}$$

with $A = \frac{93}{98}\frac{\zeta(5)}{\zeta^2(3)}$.

The expression for the gap ratio is

$$\frac{2\Delta(0)}{k_BT_c} = 3.54[1 + a_3(\frac{T_c}{\omega_{ln}})^2\ln\frac{\omega_{ln}}{b_3T_c}] \qquad (A1.16)$$

with

$$a_3 = \frac{3.54^2}{4}(\frac{1}{g} + \frac{1}{2})\alpha_1 + \pi^2\alpha_1$$

and

$$b_3 = \frac{1}{1.13}exp\left\{\frac{\frac{3.54^3}{4}(\frac{1}{g} + \frac{1}{4})\alpha_2 + \frac{4}{3}\pi^2\alpha_2}{\frac{3.54^2}{4}(\frac{1}{g} + \frac{1}{2})\alpha_1 + \pi^2\alpha_1}\right\}$$

We have also obtained an expression for $\frac{\gamma T_c^2}{H_c^2(0)}$

$$\frac{\gamma T_c^2}{H_c^2(0)} = 0.168[1 + a_4(\frac{T_c}{\omega_{ln}})^2 \ln\frac{\omega_{ln}}{b_4 T_c}] \qquad (A1.17)$$

where

$$a_4 = (\frac{3.54^2}{2}(\frac{1}{2} + \frac{1}{g}) + 2\pi^2)\alpha_1 - (\frac{3.54}{2})^2\frac{1}{g}\alpha_3$$

and

$$b_4 = \frac{1}{1.13}exp\left\{\frac{(\frac{3.54^2}{8}(1+g) + \frac{8}{3}\pi^2)\alpha_2 - (\frac{3.54}{2})^2\frac{1}{g}\alpha_1 - (\frac{2.54}{2})^2\frac{1}{g}\alpha_3\ln\beta_3}{(\frac{3.54^2}{2}(\frac{1}{2} + \frac{1}{g}) + 2\pi^2)\alpha_1 - (\frac{3.54}{2})^2\frac{1}{g}\alpha_3}\right\}$$

We have also calculated the specific heat jump for the model of chapter 4. The result is rather complicated, and seems to defeat the intent of deriving a simple expression for the quantity of interest. We give the result as

$$\frac{\Delta C}{\gamma T_c} = 1.43\Big[1 + a_1\Big(\frac{T_c}{\omega_{ln}^{ph}}\Big)^2 \ln\frac{\omega_{ln}^{ph}}{b_1 T_c} + a_2\Big(\frac{T_c}{\omega_{ln}^{P}}\Big)^2 \ln\frac{\omega_{ln}^{P}}{b_2 T_c}$$
$$+ U^{-1}\Big[a_3\Big(\frac{T_c}{\omega_{ln}^{ph}}\Big)^2 \ln^2\frac{\omega_{ln}^{ph}}{b_3 T_c} + a_4\Big(\frac{T_c}{\omega_{ln}^{P}}\Big)^2 \ln^2\frac{\omega_{ln}^{P}}{b_4 T_c}$$
$$+ a_5\Big(\frac{T_c}{\omega_{ln}^{ph}}\Big)^2 \ln\frac{\omega_{ln}^{ph}}{b_5 T_c} + a_6\Big(\frac{T_c}{\omega_{ln}^{P}}\Big)^2 \ln\frac{\omega_{ln}^{P}}{b_5 T_c}\Big]\Big]$$

In these expressions, the superscripts ph and P refer to the pairing and the pair breaking mechanisms respectively, and

$$U^{-1} = \frac{\lambda^- \frac{8}{7\zeta(3)}}{\lambda^{ph}\ln\frac{1.13\omega_{ln}^{ph}}{k_B T} - \lambda^P \ln\frac{1.13\omega_{ln}^{P}}{k_B T}}$$

$\lambda^- = \lambda^{ph} - \lambda^P$.

$$a_1 = \pi^2 \frac{\lambda^{ph}}{\lambda^-} \frac{24}{7\zeta(3)} + 4)\alpha_1$$

$$a_2 = \pi^2 \frac{\lambda^P}{\lambda^-} \frac{8}{7\zeta(3)} - 4)\rho_1$$

$$b_1 = \frac{1}{1.13} exp\left\{ \frac{(\frac{8}{7\zeta(3)} + \frac{16}{3})\alpha_2}{(\frac{24}{7\zeta(3)} + 4)\alpha_1} \right\}$$

$$b_2 = \frac{1}{1.13} exp\left\{ \frac{(\frac{8}{7\zeta(3)} - \frac{16}{3})\rho_2}{(\frac{8}{7\zeta(3)} - 4)\rho_1} \right\}$$

$$a_3 = \pi^2 \frac{\lambda^{ph}}{\lambda^-} \alpha_3$$

$$a_4 = \pi^2 \frac{\lambda^P}{\lambda^-} \rho_3$$

$$b_3 = \frac{1}{1.13} = b_4$$

$$a_5 = \pi^2 \frac{\lambda^{ph}}{\lambda^-} (-\alpha_3 \ln\beta_3 - \alpha_1)$$

$$a_6 = \pi^2 \frac{\lambda^P}{\lambda^-} (-\rho_3 \ln\sigma_3 - \rho_1)$$

$$b_5 = \frac{1}{1.13} exp\left\{ \frac{\alpha_2}{4(\alpha_3 \ln\beta_3 + \alpha_1)} \right\}$$

$$b_6 = \frac{1}{1.13} exp\left\{ \frac{\rho_2}{4(\rho_3 \ln\sigma_3 + \rho_1)} \right\}$$

ρ_1, ρ_2, ρ_3, and σ_3 are defined in analogy with α_1, α_2, α_3, and β_3, except that they refer to the pair breaking spectral density.

Appendix 2

Asymptotic Limit for the Thermodynamics of a Boson Exchange Superconductor

We establish formulas for the free energy difference (ΔF) between superconducting and normal state of an Eliashberg superconductor valid in the asymptotic limit $\lambda \to \infty$ where λ is the mass renormalization. It is shown that (ΔF) goes like $\frac{1}{\lambda}$ times a universal function of the reduced temperature $t = \frac{T}{T_c}$. The universal function is calculated numerically for finite t>0.

Stimulated by the discovery of superconductivity in the oxides[78] with values of the critical temperature T_c now as high as 160K, Marsiglio, Akis, and Carbotte[79] considered the thermodynamics and other properties of an Eliashberg superconductor for values of T_c comparable in size or greater than the characteristic boson energy ω_{ln}. The parameter ω_{ln} was first introduced by Allen and Dynes[29] and is well defined in terms of the electron-boson spectral density $\alpha^2 F(\omega)$ which enters the kernels of the Eliashberg equations. In their work, Marsiglio *et al.* [79] carry out calculations somewhat beyond $\frac{T_c}{\omega_{ln}}$=1. This corresponds to large, as compared with conventional cases, but still quite

finite values of λ. Here we wish to consider the limit of $\lambda \rightarrow \infty$. While this regime is not likely to ever be reached in real materials, it gives particularly simple results which can help in understanding the large but finite λ region.

The work starts from the Eliashberg equations in the Matsubara representation[80,81] for the gap $\Delta(i\omega_n)$ and renormalization $Z(i\omega_n)$ at the Matsubara frequencies $i\omega_n$=$i\pi$T(2n-1) n=0,±1, ±2... with T the temperature. They are

$$\Delta(i\omega_n)Z_s(i\omega_n) = \pi T \sum_{m=-\infty}^{\infty} \lambda(m-n)\frac{\Delta(i\omega_m)}{\sqrt{\Delta^2(i\omega_m)+\omega_m^2}} \qquad (A2.1)$$

and

$$\omega_n Z_s(i\omega_n) = \omega_n + \pi T \sum_{m=-\infty}^{\infty} \lambda(m-n)\frac{\omega_m}{\sqrt{\Delta^2(i\omega_m)+\omega_m^2}} \qquad (A2.2)$$

where, for convenience, we have ignored the Coulomb pseudopotential μ^* and where $\lambda(m-n)$ contains the information on the spectral density $\alpha^2F(\omega)$ for boson exchange. While the form of equations (A2.1) and (A2.2) is based on Migdal's theorem and is valid only for the electron-phonon interaction, they can still be used as a first approximation for other more exotic exchange bosons so that our asymptotic limit will be approximately valid in such cases as well. In terms of $\alpha^2F(\omega)$ we have

$$\lambda(m-n) = 2\int_0^{\infty} \frac{\omega\,\alpha^2F(\omega)}{\omega^2+(\omega_m-\omega_n)^2}d\omega \qquad (A2.3)$$

If we use for $\alpha^2F(\omega)$ a delta function centered at the Einstein energy ω_E and of weight A, we obtain

$$\lambda(m-n) = \frac{2\omega_E A}{\omega_E^2+(\omega_n-\omega_m)^2} \qquad (A2.3)$$

If we assume A to be fixed and increase λ by decreasing ω_E (λ=$\frac{2A}{\omega_E}$), the $\lambda \rightarrow \infty$ limit corresponds to $\omega_E \rightarrow$0. In this case, the ω_E^2 term in the denominator

of equation (A2.4) can be neglected provided it is assumed that $\omega_E << 2\pi T$, a condition we will return to later. Substitution of (A2.4) into (A2.1) and (A2.2) and insertion of (A2.2) into (A2.1) leads to a simple equation for $\Delta(i\omega_n)$ which can be rewritten in the form

$$\bar{\Delta}(i\bar{\omega}_n) = \pi t \bar{T}_c \sum_{m \neq n} \frac{2}{(\bar{\omega}_n - \bar{\omega}_m)^2} [\frac{\bar{\Delta}(i\bar{\omega}_m) - \frac{\bar{\omega}_m}{\bar{\omega}_n}\bar{\Delta}(i\bar{\omega}_n)}{\sqrt{\bar{\omega}_m^2 + \bar{\Delta}^2(i\bar{\omega}_m)}}] \qquad (A2.5)$$

where any $\bar{Q}=\frac{Q}{\sqrt{A\omega_E}}$ and the reduced temperature $t = \frac{T}{T_c}$. On examination of equation (A2.5), we see that all reference to material parameters has dropped out so that, $\bar{\Delta}(i\bar{\omega}_n)$ is simply a universal function ($f_n(t)$) of the reduced temperature t, ie. $\bar{\Delta}(i\bar{\omega}_n)=f_n(t)$. In particular, iteration of the linearized version of (A2.5) yields the critical temperature $\bar{T}_c=0.2584$ which is a universal number first given by Allen and Dynes. Thus, in the asymptotic limit the critical temperature is

$$T_c = 0.2584\sqrt{A\omega_E} = 0.183\omega_E^2\sqrt{\lambda} \qquad (A2.6)$$

To calculate the thermodynamics in the asymptotic limit, we need to know the free energy difference between superconducting and normal state $\Delta F(t)$ which is given in terms of the $\Delta(i\omega_n)$'s and Z's by the Bardeen-Stephen[34] formula

$$\frac{\Delta F}{N(0)} = -2\pi T \sum_{n=1}^{\infty} \omega_n [Z^S(i\omega_n) - \frac{Z^N(i\omega_n)}{\sqrt{1+\frac{\Delta^2(i\omega_n)}{\omega_n^2}}}][\sqrt{1+\frac{\Delta^2(i\omega_n)}{\omega_n^2}} - 1] \qquad (A2.7)$$

where N(0) is the single spin electronic density of states at the Fermi energy. From equation (A2.5), it is clear that the square root factor in (A2.7) is independent of λ as it depends only on $\bar{\Delta}(i\bar{\omega}_n)$. Further, the superconducting state renormalization factor can be written as

$$Z^S(i\omega_n) = 1 + \frac{\pi\bar{T}}{\sqrt{\bar{\omega}_n^2 + \bar{\Delta}^2(i\bar{\omega}_n)}}\lambda + \frac{\pi\bar{T}}{\bar{\omega}_n}\sum_{m \neq n} \frac{2}{(\bar{\omega}_n - \bar{\omega}_m)^2} \frac{\bar{\omega}_m}{\sqrt{\bar{\omega}_n^2 + \bar{\Delta}^2(i\bar{\omega}_n)}} \qquad (A2.8)$$

and its normal state value Z^N is obtained from (A2.8) by setting $\bar{\Delta}(i\bar{\omega}_n)$ equal to zero in the last two terms on the right hand side. We note that for both Z^N and Z^S, the second term depends on λ and hence, on material parameters, but the last term does not since $\bar{\Delta}(i\bar{\omega}_n)$ is universal. On inserting (A2.8) into (A2.7), it is clear that the λ dependence in Z^S and Z^N cancel so that the expression in the square bracket is material independent leaving us with a free energy that scales like T_c^2 because of the presence of an overall factor of T and so[82]

$$\frac{\Delta F}{N(0)} = \frac{A^2}{\lambda} g(t) \qquad (A2.9)$$

where g(t) is a universal function of reduced temperature. This function, which is independent of material parameters, can be calculated from the universal equation (A2.5) for $\bar{\Delta}(i\bar{\omega}_n)$ and from the free energy difference (A2.7) noting that λ, which still appears explicitly in both Z^N and Z^S, cancels in the combination needed in formula (A2.7).

The thermodynamic critical magnetic field H_c (T) follows from $\Delta F(T)$ as does the specific heat difference $\Delta C(T)$. Thermodynamics yields

$$H_c(T) = \sqrt{8\pi\Delta F}\,, \text{ and } \Delta C(T) = T\frac{d^2F}{dT^2} \qquad (A2.10)$$

Direct calculation of g(t) as a function of reduced temperature yields H_C(t) and $\Delta C(t)$. The results of our numerical calculations are given in Fig. A2.1.

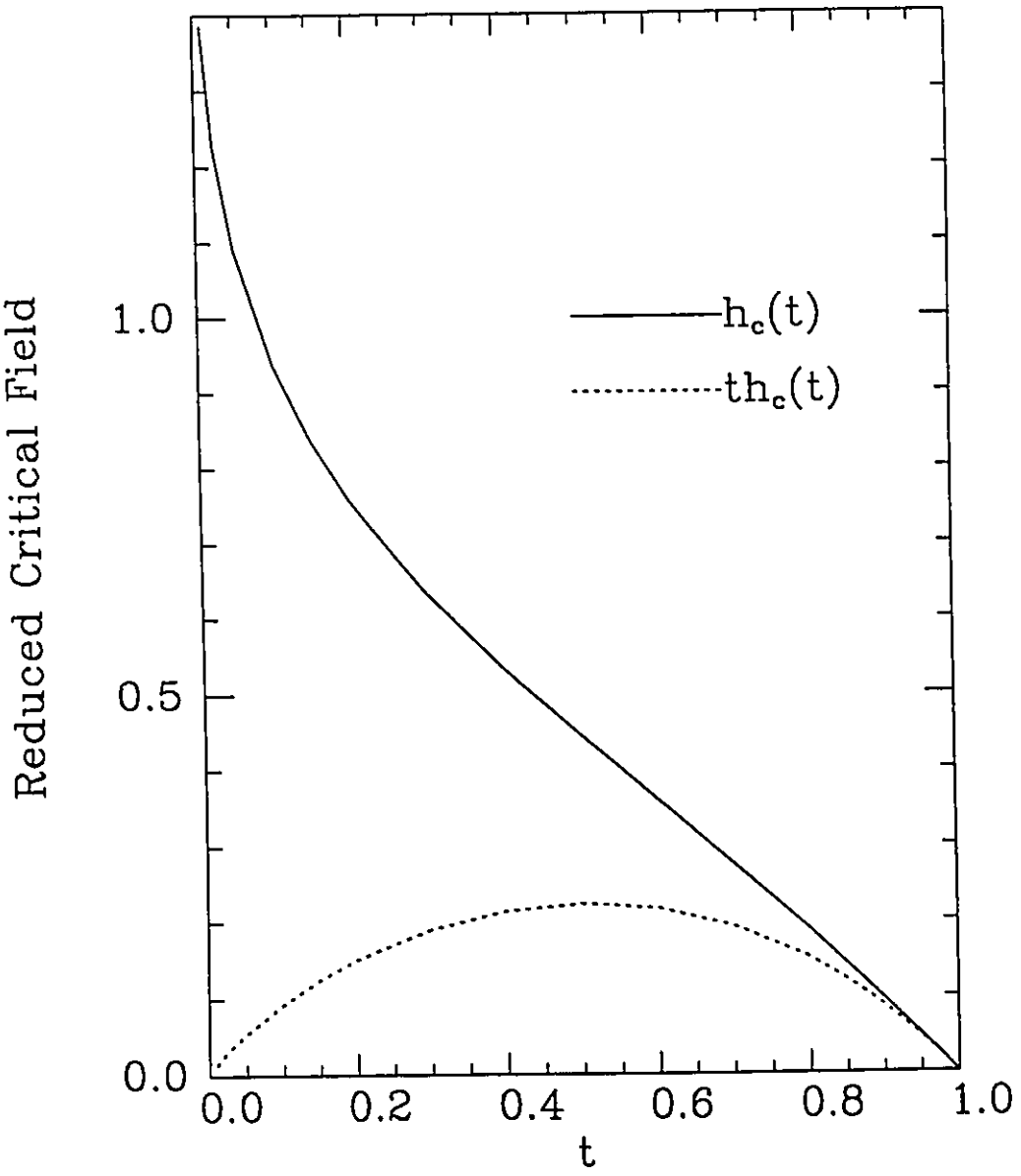

Figure A2.1- Plot of the reduced critical thermodynamic magnetic field (solid curve) as a function of reduced temperature t in the limit $\lambda \rightarrow \infty$. The curve has pronounced positive curvature with the zero temperature value unclear. The dotted curve is t times the reduced field $h_c(t)$ and shows a finite limit at $t \rightarrow 0$.

Instead of g(t) itself, we have chosen to plot $h_c(t)$ (the reduced thermodynamic critical magnetic field) defined by

$$h_c(t) = \frac{H_c(t)}{|\frac{dH_c(t)}{dt}|_{t=1}} = \frac{\sqrt{g(t)}}{|\frac{d\sqrt{g(t)}}{dt}|_{t=1}} \qquad (A2.11)$$

which is simply $\sqrt{g(t)}$ normalized to its slope at t=1 i.e. T=T_c. From the solid curve of Fig. A2.1, it is clear that in the asymptotic limit the reduced critical field looks very different from its value in BCS theory. For example, within BCS, the $h_c(t)$ curve has negative curvature at all temperatures and at t=0 $h_c(0)$=0.576. In contrast, in the asymptotic limit $h_c(t)$ exhibits a large region of near linear dependence below t=1 and then shows the opposite curvature bending upward as t decreases. It is still rising rapidly at t=0.008. This is the lowest reduced temperature we could handle in our numerical work due to computer time limitations. Consequently, we do not have information on its zero temperature behaviour. To understand that this is not a serious limitation, we return to the condition $\omega_E << 2\pi T$ introduced from the very beginning into our formalism. It can easily be changed, with the help of equation (A2.6) for T_c valid in the asymptotic limit, into an inequality

$$\sqrt{\lambda}t >> 1 \qquad (A2.12)$$

which is central to our work. Recalling that

$$H_c(t) = \sqrt{8\pi}\frac{A}{\sqrt{\lambda}}\sqrt{g(t)} = \sqrt{8\pi}\frac{A}{\sqrt{\lambda}}|\frac{d\sqrt{g(t)}}{dt}|_{t=1}h_c(t) \qquad (A2.13)$$

we rewrite it in the form

$$H_c(t) \propto \frac{1}{\sqrt{\lambda}}h_c(t) \equiv \frac{1}{\sqrt{\lambda}t}(th_c(t)) \qquad (A2.14)$$

We see that condition (A2.12) requires $\frac{1}{\sqrt{\lambda t}} << 1$. Also, we note that t $h_c(t)$ shown in Fig. A2.1 (dotted curve) is well behaved even for t=0. Thus, expression (A2.14) is also well behaved in the range $\frac{1}{\sqrt{\lambda t}} << 1$. What we need to remember is that λ must go to ∞ before t goes to zero for the condition $\frac{1}{\sqrt{\lambda t}} << 1$ to be satisfied. From formula (A2.14), we get $H_c(t)=0$ for $\lambda \rightarrow \infty$ and so also $\Delta F(t)=0$. There is no transition to the superconducting state in this case.

Our results for $h_c(t)$ or t $h_c(t)$ cover the entire temperature dependence of the free energy difference and so the specific heat should follow as well (formula (A2.10)). Evaluation of the jump in $\Delta C(T)$ at T_c and its slope give respectively

$$\frac{\Delta C(T_c)}{\gamma(0)T_c} = \frac{19.9}{\lambda} \qquad (A2.15)$$

and

$$\frac{d}{dt}\frac{\Delta C(T_c)}{\gamma(0)T_c} = \frac{39.2}{\lambda} \qquad (A2.16)$$

These values of jump and slope cannot be compared directly with the universal BCS values of 1.43 and 3.77 respectively. BCS is the weak coupling case which is the opposite limit to that considered here. It is clear, however, that for large λ's, both quantities fall below BCS. This behaviour, which can be taken to be a signature of the asymptotic limit, is very different from the conventional strong coupling case for which the corrections to BCS tend to increase these coefficients over the BCS value. More specifically Marsiglio and Carbotte[32] find

$$\frac{\Delta C(T_c)}{\gamma(0)T_c} = 1.43[1 + 53(\frac{T_c}{\omega_{ln}})^2 \ln(\frac{\omega_{ln}}{3T_c})] \qquad (A2.17)$$

and

$$\frac{d}{dt}\frac{\Delta C(T_c)}{\gamma(0)T_c} = 3.77[1 + 117(\frac{T_c}{\omega_{ln}})^2 \ln(\frac{\omega_{ln}}{2.9T_c})] \qquad (A2.18)$$

where $\frac{T_c}{\omega_{ln}}$ is the characteristic strong coupling parameter and ω_{ln} is the average boson energy of Allen and Dynes which is given by

$$\omega_{ln} = exp\Big[-\frac{2}{\lambda}\int_o^\infty \frac{\alpha^2 F(\omega)\ln(\omega)}{\omega}\, d\omega\Big] \qquad (A2.19)$$

Equations (A2.17) and (A2.18) apply only for $\frac{T_c}{\omega_{ln}} \leq 0.25$.

While both the normalized jump and slope go to zero as $\lambda \rightarrow \infty$ their ratio remains constant. It is equal to 1.96 which is to be compared with a BCS value of 2.64. For conventional superconductors, it is found to be somewhat greater.

In conclusion, we have solved for the free energy difference between normal and superconducting state at any finite reduced temperature t in the asymptotic limit $\lambda \rightarrow \infty$. The free energy is found to scale like $\frac{1}{\lambda}$ times a universal function of t which is independent of any material parameter. The formula obtained holds only for $\sqrt{\lambda}t >> 1$ so that very large values of λ are needed if the low temperature region is to be investigated. Our calculations are based on equations that are independent of λ and therefore, universal. The normalized jump and slope at T_c of the specific heat were computed and found to go like $\frac{1}{\lambda}$ for large λ with coefficients universal numbers. While the asymptotic limit is not likely to be reached in real systems, it nevertheless, gives information on how a very strong coupling superconductor is likely to behave.

Appendix 3

Asymptotic Limit for H_{c2} in Eliashberg Theory

We have calculated the reduced upper critical magnetic field $h_{c2}(t)$ as a function of reduced temperature (t) in the limit when the electron-boson mass renormalization parameter λ of Eliashberg theory goes towards ∞. Our results are valid for any reduced temperature t satisfying the inequality $\sqrt{\lambda}t >> 1$. At low temperature, the results in the finite impurity limit are smooth and can be extrapolated to get $h_{c2}(0) \simeq 0.57$ independent of impurity content.

I - Introduction

Bulaevskii *et al.* [82] have given results for the second upper critical magnetic field $H_{c2}(T)$ in the limit of Eliashberg theory when the mass enhancement parameter λ is assumed to tend towards infinity. While they consider both dirty and clean limits, they give results only at zero temperature and near T_c and use large but quite finite-λ numerical calculations to fit some

of the proportionality constants. In a recent paper Marsiglio *et al.* [83] have developed a technique to calculate the free energy of an Eliashberg superconductor using a numerical method which is valid for any reduced temperature t>0 provided λ is taken large enough for the inequality $\sqrt{\lambda}t >> 1$ to hold.

In this paper, we extend our previous work[83] to consider the second upper critical magnetic field $H_{c2}(T)$. This work complements and extends the paper of Bulaevskii *et al.* [82] as well as corrects it in one instance. In section II, we introduce the strong coupling equations for $H_{c2}(T)$ derived by Schossmann and Schachinger[36] and consider the dirty limit which, while not directly applicable to a physical situation, serves as a basis for section III where we consider a general finite impurity concentration. Conclusions are to be found in section IV.

II - General Formulation and Dirty Limit

The general equations for $H_{c2}(T)$ valid for any isotropic Eliashberg superconductor defined by an electron-boson spectral density $\alpha^2 F(\omega)$ and Coulomb pseudopotential μ^* were first derived by Schossmann and Schachinger[36] and are valid for any impurity concentration described by $t_+ \equiv \frac{1}{2\pi\tau}$ with τ the impurity scattering time. They are[36,84]

$$\tilde{\Delta}(i\omega_n) = \pi T \sum_{m=-\infty}^{\infty} [\lambda(m-n) - \mu^*] \frac{\tilde{\Delta}(i\omega_m)}{\mathcal{X}^{-1}(\tilde{\omega}(i\omega_m)) - \pi t_+} \qquad (A3.1)$$

and

$$\tilde{\omega}(i\omega_n) = \omega + \pi T \sum_{m=-\infty}^{\infty} \lambda(m-n) sign(\omega_m) + \pi t_+ sign(\omega_n) \qquad (A3.2)$$

In equation (A3.1), $\mathcal{X}(\tilde{\omega}(i\omega_n))$ is given by

$$\mathcal{X}(\tilde{\omega}(i\omega_m)) = \frac{2}{\sqrt{\alpha}} \int_0^{\infty} dq e^{-q^2} \tan^{-1} \frac{q\sqrt{\alpha}}{|\tilde{\omega}(i\omega_m)|} \qquad (A3.3)$$

with

$$\alpha = \frac{1}{2} e H_{c2}(T) v_F^2 \qquad (A3.4)$$

Finally, in equation (A3.1) and (A3.2), the parameter $\lambda(m-n)$ is given by

$$\lambda(m-n) = 2\int_0^\infty \frac{\omega\,\alpha^2 F(\omega)}{\omega^2 + (\omega_m - \omega_n)^2} d\omega \qquad (A3.5)$$

where $i\omega_n$ is the n'th Matsubara frequency $i\omega_n = i\pi T(2n-1)$, n=0, ±1, ±2, ... and T is the temperature.

We start with the dirty limit which, as we will see later, is somewhat artificial from a physical point of view. Nevertheless, it plays an important mathematical role since the finite impurity case can be related to it.

To start, rewrite equation (A3.2) in the form

$$\tilde{\omega}(i\omega_n) = \tilde{\omega}^\circ(i\omega_n) + \pi t_+ sign(\omega_n) \qquad (A3.6)$$

with

$$\tilde{\omega}^\circ(i\omega_n) \equiv \omega_n + \pi T \sum_{m=-\infty}^{\infty} \lambda(m-n) sign(\omega_n) \qquad (A3.7)$$

In the dirty limit

$$|\,\tilde{\omega}(i\omega_m)\,| = |\,\tilde{\omega}^\circ(i\omega_n)\,| + \pi t_+ >> 1 \qquad (A3.8)$$

and hence

$$tan^{-1}\frac{\sqrt{\alpha}q}{|\tilde{\omega}_n|} \cong \frac{\sqrt{\alpha}q}{|\tilde{\omega}_n|} - \frac{1}{3}\left[\frac{\sqrt{\alpha}q}{|\omega_n|}\right]^3 \qquad (A3.9)$$

which implies (equation (A3.3)) that

$$\chi^{-1}(\tilde{\omega}(i\omega_n)) \cong |\,\tilde{\omega}(i\omega_n)\,| \left[1 + \frac{1}{3}\frac{\alpha}{|\,\tilde{\omega}(i\omega_n)\,|^2}\right] \qquad (A3.10)$$

and so

$$\chi^{-1}(\tilde{\omega}(i\omega_n)) - \pi t_+ \cong |\,\tilde{\omega}^\circ(i\omega_n)\,| + \frac{1}{3}\frac{\alpha}{\pi t_+} \qquad (A3.11)$$

where $\mid \tilde{\omega}(i\omega_n) \mid$ in the denominator of the last term has been replaced by πt_+. Substitution of this last relationship into equation (A3.1) gives

$$\tilde{\Delta}(i\omega_n) = \pi T \sum_{m=-\infty}^{\infty} [\lambda(m-n) - \mu^*] \frac{\tilde{\Delta}(i\omega_n)}{\mid \tilde{\omega}^o(i\omega_m) \mid + \rho^{di}} \qquad (A3.12)$$

where we have defined

$$\rho^{di} \equiv \frac{1}{3} \frac{\alpha^{di}}{\pi t_+} = e H_{c2}^{di} D \qquad (A3.13)$$

with $D \equiv \frac{1}{3} v_F^2 \tau$ the diffusion constant.

It is convenient and conventional[33] to transform equation (A3.12) through the change

$$\tilde{\Delta}(i\omega_n) \equiv \frac{\tilde{\Delta}(i\omega_n)}{\mid \tilde{\omega}^o(i\omega_n) \mid + \rho^{di}} \qquad (A3.14)$$

which, when substituted into equation (12), gives

$$\tilde{\Delta}(i\omega_n)[|\omega_n| + \pi T \sum_{m=-\infty}^{\infty} \lambda(m-n) sign(\omega_n \omega_m) + \rho^{di}] = \pi T \sum_{m=-\infty}^{\infty} [\lambda(m-n) - \mu^*] \tilde{\Delta}(i\omega_m) \qquad (A3.15)$$

where use was made of equation (A3.7). A critical observation about equation (A3.15) is that the term n=m on the right hand side cancels against the similar term on the left hand side, so that both sums can be restricted to m≠n only. This means that the term

$$\lambda(0) \equiv \lambda = \int_0^{\infty} \frac{2\omega\alpha^2 F(\omega)}{\omega} d\omega$$

does not appear in equation (A3.15) and we require $\lambda(m-n)$ only for n≠m. For the spectral density, we will take a delta functio.. model of weight A centered at the Einstein frequency ω_E. In this case

$$\lambda(m-n) = \frac{2A\omega_E}{\omega_E^2 + (\omega_n - \omega_m)^2}, m \neq n \qquad (A3.16)$$

A great simplification arises if we assume $\omega_E << 2\pi T$. We will see later that this restricts our numerical work to the range $\sqrt{\lambda} t >> 1$ with t the reduced

temperature. In this approximation, we can neglect ω_E^2 in the denominator of (A3.16) since n≠m and get

$$\lambda(m-n) \cong \frac{2A\omega_E}{(2\pi T)^2(m-n)^2}, m \neq n \qquad (A3.17)$$

A simple transformation can now be used to change equation (A3.15) into an equation with dimensionless kernels in which no material parameters appear explicitly (for $\mu^*=0$). This equation, when solved numerically, will then yield a single universal curve for the reduced upper critical field

$$h_{c2}(t) = \frac{H_{c2}(T)}{T_c|(dH_{c2}/dT)|_{T_c}}$$

valid in the asymptotic limit ($\sqrt{\lambda}t >> 1$). If we introduce dimensionless temperature $\bar{T} = \frac{T}{\sqrt{A\omega_E}}$, equation (A3.17) reduces to

$$\lambda(m) = \frac{2}{(2\pi\bar{T})^2 m^2} \qquad (A3.18)$$

and equation (A3.15), with $\mu^*=0$ for convenience, can be rewritten as

$$\frac{\rho^{di}}{\pi T}\bar{\Delta}(i\omega_n) = \sum_{m=-\infty}^{\infty}\Big[\lambda(m-n)(1-\delta_{m,n}) + \lambda(m+n-1) - \delta_{m,n}[2m-1+2\sum_{m'=1}^{m-1}\lambda(m')]\Big]\bar{\Delta}(i\omega_m) \qquad (A3.19)$$

Noting (A3.18), we see that equation (A3.19) makes no reference to any material parameter and will yield an eigenvalue of the form

$$\frac{\rho^{di}}{\pi T} \equiv g(\bar{T}) = \frac{eH_{c2}^{di}(T)D}{\pi T} \qquad (A3.20)$$

where $g(\bar{T})$ is some well defined universal function of the dimensionless temperature $\bar{T}$. In particular, the critical temperature is obtained for $g(\bar{T}_c)=0$ which gives numerically

$$T_c = 0.183\omega_E\sqrt{\lambda} \qquad (A3.21)$$

a result first obtained by Allen and Dynes[29]. Solving (A3.19) for values of $\bar{T}$ below $\bar{T}_c$, we obtain

$$H_{c2}^{di}(T) = \frac{\pi T_c}{eD} k(t) \equiv \frac{0.183\pi}{eD} \omega_E \sqrt{\lambda} k(t) \qquad (A3.22)$$

where k(t) is a universal function of the reduced temperature related to $g(\bar{T})$. For t near 1 equation (A3.22) reduces to

$$H_{c2}^{di}(T) = \frac{2.24\pi T_c}{eD}(1-t) \qquad (A3.23)$$

which agrees well with the result of Bulaevskii *et al.* [82] . We are, however, able to produce results for any finite temperature t>0 provided the approximation $\omega_E << 2\pi T$ is satisfied. Referring to equation (A3.21), we can transform this condition to read $\sqrt{\lambda} t >> 1$. Instead of plotting H_{c2}, which depends on material parameters as (A3.22) and (A3.23) demonstrate, we have chosen to present our universal results for $h_{c2}^{di}(t)=0.447k(t)$. This is shown as the solid curve in Fig. A3.1. We note that this curve is really very different from the usual weak coupling curve for the reduced upper critical field which has downward curvature. In our case, $h_{c2}(t)$ is nearly linear over a large range of reduced temperature near t=1 and then shows a divergent behaviour as $t \to 0$. Note that our technique of solution does not permit us to reach the t=0 limit because of the condition $\sqrt{\lambda} t >> 1$ which must always be met. For T=0, Bulaevskii *et al.* [82] obtain, without proof, the result

$$H_{c2}^{di}0) = \frac{1.08 T_c}{eD} \sqrt{\lambda} = \frac{0.198 \omega_E \lambda}{eD} \qquad (A3.24)$$

and so find that $h_{c2}^{di}(0)=0.45\sqrt{\lambda}$. The λ dependence in (A3.24) is certainly consistent with our result that $h_{c2}(t) \to \infty$ as $t \to 0$ in the limit of infinite λ. Also the result $h_{c2}(0)=0.45\sqrt{\lambda}$ is confirmed in the previous numerical work

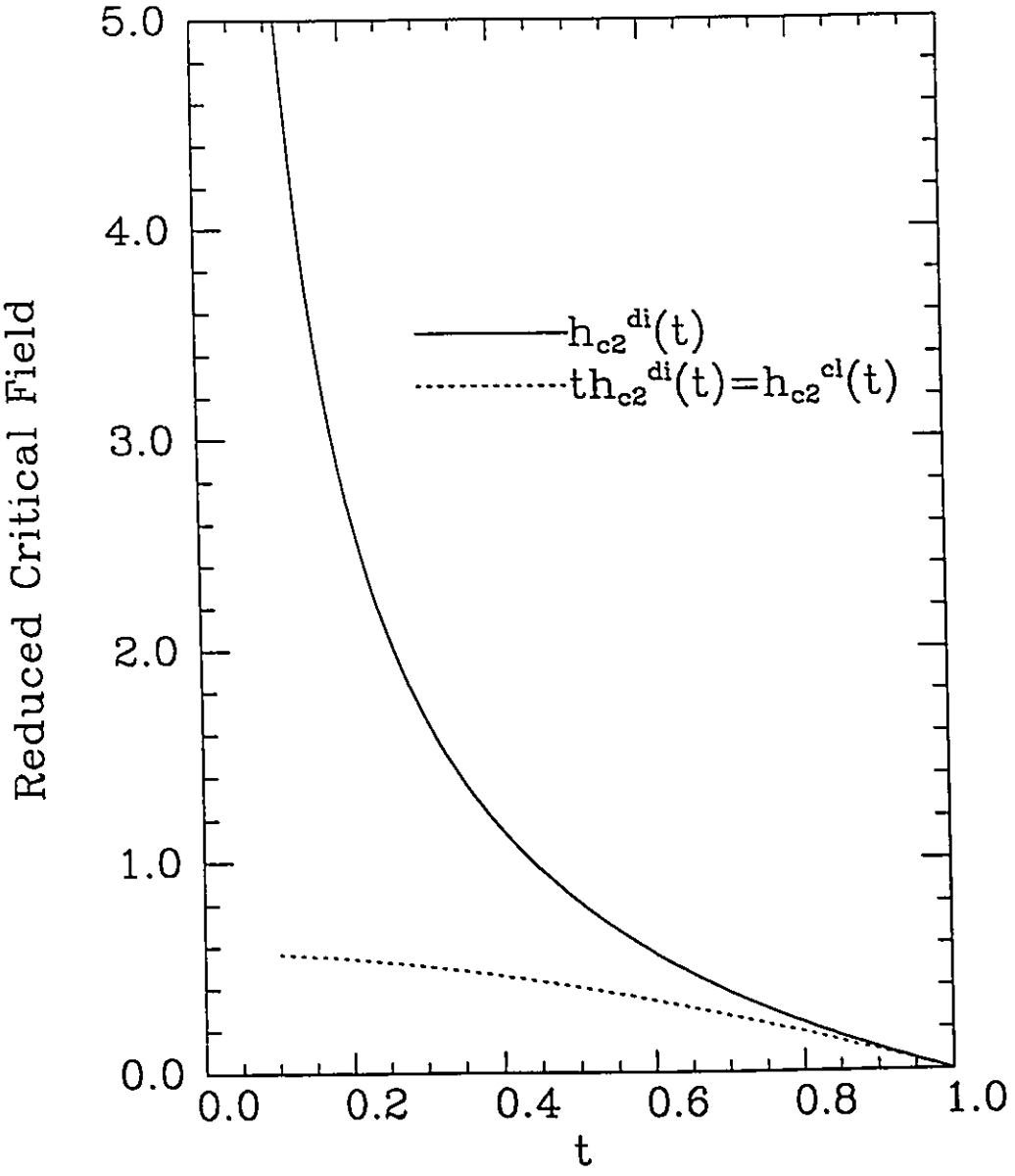

Figure A3.1- The asymptotic value ($\lambda \rightarrow \infty$) of the reduced upper critical field $h_{c2}^{di}(t)$ in the dirty limit (solid line) as a function of reduced temperature for t>0. The dotted curve applies to any finite impurity concentration and is related to $h_{c2}^{di}(t)$ by $h_{c2}^{cl}(t)=t\ h_{c2}^{di}(t)$.

of Schossmann *et al.* [52] . These authors have calculated $H_{c2}^{di}(0)$ numerically as a function of $\frac{T_c}{\omega_E}$ up to a value of about 1.4. Since $\frac{T_c}{\omega_E}$=0.183$\sqrt{\lambda}$, we note that their calculations end for $\sqrt{\lambda} \cong 7.7$ which extends beyond the numerical work of Bulaevskii *et al.* [82] . While it is certainly true that in this range of λ values $h_{c2}^{di}(0)$ appears to vary like $\sqrt{\lambda}$ with coefficient ~0.45 we may not yet be in the asymptotic limit. Certainly, we will see in the next section that for any finite impurity concentration we need to go to much higher values of λ in order to achieve the asymptotic limit. To end this section, we point out that an approximate analytic form for $H_{c2}(t)$ can be obtained from equation (A3.19) if we keep a single Matsubara gap, namely the m=1 term. This leads immediately to

$$\rho^{di} \simeq \pi T[\frac{2}{(2\pi T)^2} - 1] \qquad (A3.25)$$

from which follows

$$T_c \cong \frac{1}{2\pi}\omega_E\sqrt{\lambda}, \qquad (A3.26a)$$

$$H_{c2}^{di}(t) \cong \frac{2\pi T_c}{eD}(1-t) \quad \text{for } t \to 1 \qquad (A3.26b)$$

and

$$h_{c2}^{di}(t) \cong \frac{1}{2}[\frac{1}{t} - t] \quad \text{for } t > 0. \qquad (A3.26c)$$

This last result is compared with our exact numerical results in Fig. A3.2 We see that solid (exact) and dotted equation (A3.26c) curves are surprisingly close. They both diverge like $\frac{1}{t}$ as t→0 but with somewhat different coefficients.

III - Finite Impurity Case

The arguments we will use to reduce equation (A3.1) when πt_+ is finite are similar to those used in the previous section but somewhat different

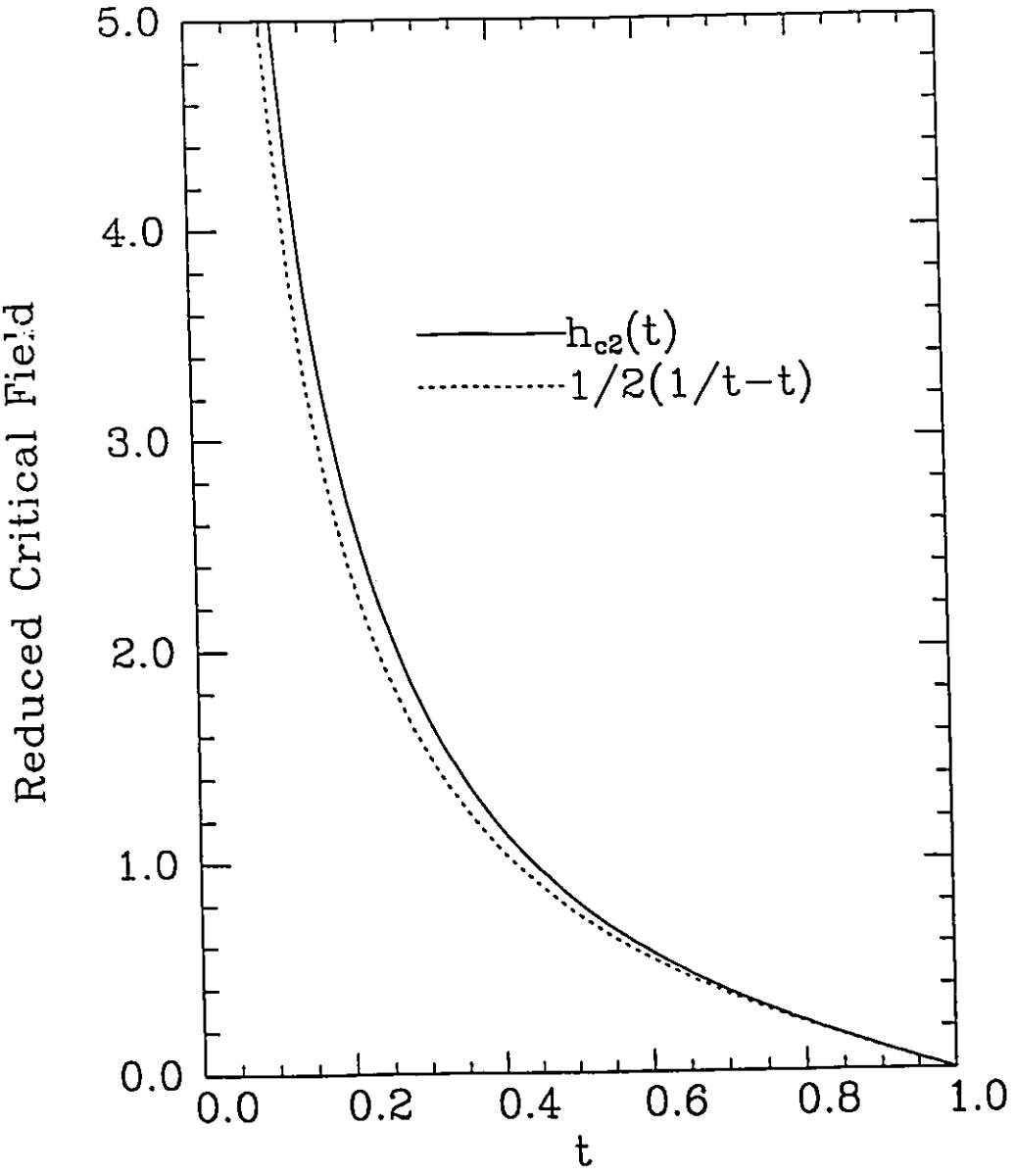

Figure A3.2-The reduced upper critical magnetic field $h_{c2}^{di}(t)$ versus reduced temperature t (solid curve) compared with the simple form $\frac{1}{2}(\frac{1}{t} - t)$ (dotted curve).

in details. We start by writing

$$| \tilde{\omega}(i\omega_n) | = \pi T\lambda + |\tilde{\omega}_1(i\omega_n)| \tag{A3.27}$$

with

$$\tilde{\omega}_1(i\omega_n) = \omega_n + \pi T \sum_{m\neq n} \lambda(m-n) sign(\omega_m) + \pi t_+ sign(\omega_n) \tag{A3.28}$$

For $\lambda \to \infty$ we have $\pi T\lambda >> |\tilde{\omega}_1(i\omega_n)|$ for any finite impurity concentration πt_+ and if we further hypothesize that $\pi T\lambda >> \sqrt{\alpha}$, as will be verified later, the same expansion of the inverse tangent as we used in the previous section can again be used with the result that

$$\begin{aligned} \chi^{-1}(|\tilde{\omega}(i\omega_n)|) - \pi t_+ &\cong \pi T\lambda + |\omega_n| + 2\pi T \sum_{m'=1}^{n-1} \lambda(m') + \frac{1}{3}\frac{\alpha}{\pi T\lambda} \\ &= | \tilde{\omega}^{\circ}(i\omega_n) | + \frac{1}{3}\frac{\alpha}{\pi T\lambda} \end{aligned} \tag{A3.29}$$

If we define $\rho^{cl} = \frac{1}{3}\frac{\alpha^{cl}}{\pi T\lambda}$ we recover equation (A3.12) with the eigenvalue ρ^{di} replaced by ρ^{cl} from which we immediately conclude that

$$\rho^{cl} = \rho^{di} \tag{A3.30}$$

Thus we have

$$H_{c2}^{cl}(T) = \frac{6\pi T\lambda}{ev_F^2} eD H_{c2}^{di}(T) \tag{A3.31}$$

On substituting (A3.22) into (A3.31), we find

$$H_{c2}^{cl}(T) = \frac{6\pi^2 T_c^2}{ev_F^2} \lambda k(i)t \tag{A3.32}$$

so that $H_{c2}^{cl}(T)$ in the $\lambda \to \infty$ limit is determined by the same universal function as $H_{c2}^{di}(T)$ except for a numerical coefficient and an extra factor of the reduced temperature t. It is the same whatever the impurity content as πt_+ has dropped out. In this sense, the dirty limit of the previous section

is unphysical and was not pursued further. The condition $\pi T\lambda >> \pi t_+$ is implied in our derivation and can be rewritten as $\sqrt{\lambda}\lambda t >> \frac{t_+}{\omega_E}$. If we think of taking λ to ∞ by having A fixed and $\omega_E \rightarrow 0$, we write $\sqrt{\lambda}t >> \frac{t_+}{A}$ which is always satisfied for any finite t_+ for sufficiently large λ. If instead ω_E is fixed and A$\rightarrow \infty$, we can again have $\lambda^{3/2}t >> \frac{t_+}{\omega_E}$ for any fixed value of t_+ .

Near t=1, i.e. around the critical temperature, we get

$$H_{c2}^{cl}(T) = \frac{13.4\pi^2 T_c^2 \lambda}{ev_F^2}(1-t) \qquad (A3.33)$$

which agrees well with the result of Bulaevskii *et al.* [82] provided we assume they have mistakenly left out a factor of π.

It follows from (A3.32) and (A3.33) that the clean limit reduced critical magnetic field

$$h_{c2}^{cl}(t) = t h_{c2}^{di}(t) \qquad (A3.34)$$

Numerical results for $h_{c2}^{cl}(t)$ based on the universal equation (A3.19) are shown as the dotted line in Fig. A3.1. We see that this curve appears to define a well behaved function of t for small t and so it can safely be extrapolated to t=0 to get $h_{c2}^{cl}(0)$=0.57. While we have worked only in the region $\sqrt{\lambda}t >> 1$ and hence t>0, we see that the zero temperature value of $H_{c2}^{cl}(0)$ can be obtained from our extrapolated $h_{c2}^{cl}(0)$ to get

$$H_{c2}^{cl}(0) = \frac{7.64\pi^2 T_c^2 \lambda}{ev_F^2} \qquad (A3.35)$$

This result is in serious disagreement with that found by Bulaevskii *et al.* [82] who get $h_{c2}^{cl}(0) \cong 1.5$ from their numerical work. The problem can easily be traced to the fact that, at $\sqrt{\lambda} \sim 5.5$, which is where these authors stop their calculations, we are, in reality, still far from the asymptotic limit. This is illustrated in Fig. A3.3 where we show h_{c2}(t=0.1)[8] as a function of $\frac{T_c}{\omega_E} = 0.183\sqrt{\lambda}$. We see

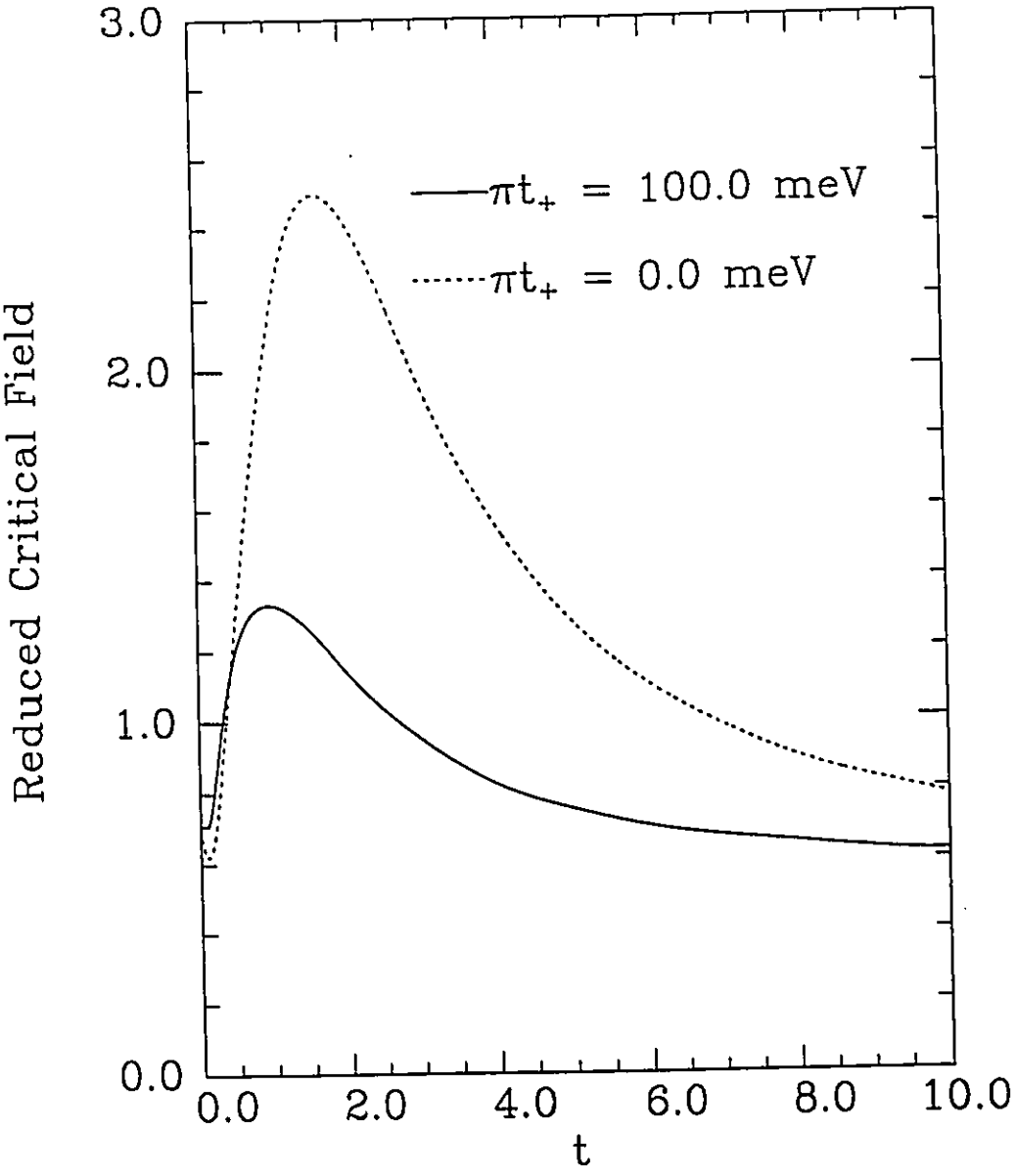

Figure A3.3-The reduced upper critical magnetic field at reduced temperature t=0.1 as a function of $\frac{T_c}{\omega_{ln}} = 0.183\sqrt{\lambda}$ for the clean limit t_+=0.0 (solid curve) and t_+=100.0 meV (dotted curve).

that for both the clean limit (solid curve) and for πt_+=100.0 meV (dotted curve) the curves do not reach their asymptotic limit until beyond $\frac{T_c}{\omega_E} \sim 10$ while Bulaevskii *et al.* [82] stop around 1, which is close to the maximum of the clean limit curve. This maximum value is almost a factor of three larger than the asymptotic value of 0.57. Also we note that, while for small λ, the clean and πt_+=100 meV curves can differ significantly, the two curves tend towards the same value as λ gets large. This is to be taken as a numerical illustration of the theorem we proved previously, namely that for $\lambda \to \infty$ the results do not depend on impurity concentration if finite.

To end, we consider our approximate analytic model solution obtained by using a single Matsubara gap approximation. We get from (A3.31) and (A3.25)

$$H_{c2}^{cl}(T) \cong \frac{6\pi^2 T_c^2 \lambda}{e v_F^2}(1-t^2) \qquad (A3.36a)$$

from which we find for t near 1

$$H_{c2}^{cl}(t) \cong \frac{12\pi^2 T_c^2 \lambda}{e v_F^2}(1-t) \qquad (A3.36b)$$

and for t=0

$$H_{c2}^{cl}(t) \cong \frac{6\pi^2 T_c^2 \lambda}{e v_F^2} \qquad (A3.36c)$$

which gives $h_{c2}^{cl}(0)$=0.5 instead of the exact result of 0.57. Also, our approximate $h_{c2}^{cl}(t)$ is

$$h_{c2}^{cl}(t) \cong \frac{1}{2}(1-t^2) \qquad (A3.37$$

Comparison of this last result with our exact numerical calculations are given in Fig. A3.4. We see a remarkable agreement between approximate and exact calculations except near t=0. Finally, we note that for any t, $H_{c2}^{cl}(t) \propto \lambda^2$ for fixed ω_E and hence $\sqrt{\alpha} \propto \lambda$. The condition $\pi T\lambda >> \sqrt{\alpha}$, which we assumed

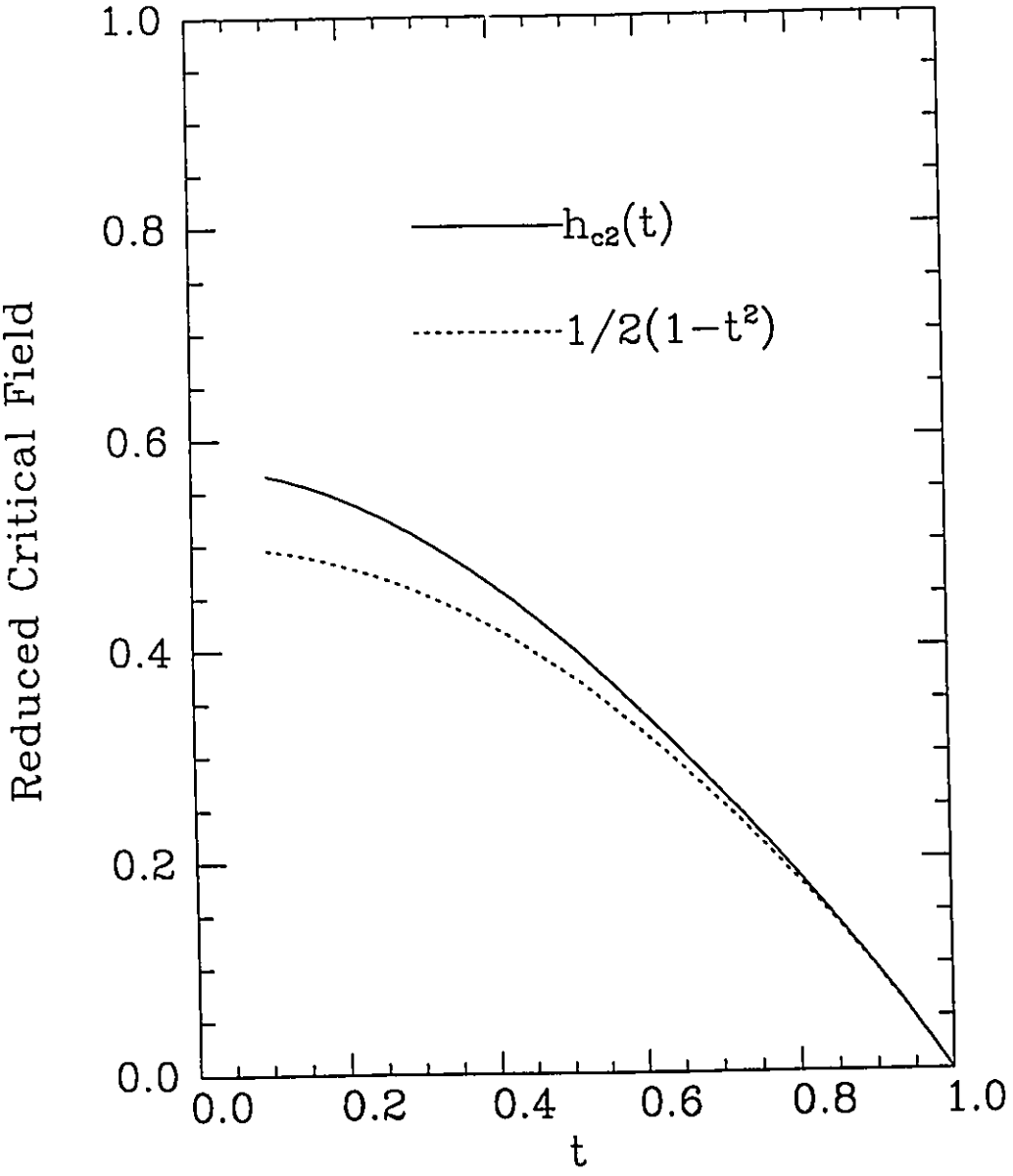

Figure A3.4-The asymptotic value ($\lambda \rightarrow \infty$) of the second upper critical magnetic field $h_{c2}^{cl}(t)$ in the clean limit (solid curve) as a function of reduced temperature (t) compared with the simple form $\frac{1}{2}(1-t^2)$.

to be satisfied at the beginning of our derivation, can be rewritten (dropping all numerical factors) as

$$\sqrt{\lambda}t >> 1$$

a condition which was assumed to hold in our derivation of the dirty limit critical magnetic field. No new restriction is implied.

IV - Conclusions

We have calculated the second upper critical magnetic field for any finite impurity concentration in the limit $\lambda \rightarrow \infty$. It is found that this asymptotic limit is independent of impurity content and that the reduced field $h_{c2}(t)$ is a universal and well behaved function of t. It behaves roughly like $0.5(1-t^2)$ for most of the temperature range. While our work is, strictly speaking, only valid for $t>0$, an extrapolation to zero temperature gives $h_{c2}^{cl}(0)=0.57$, in contradiction to a previous result which has appeared in the literature and is $\sim$1.5. We trace the discrepancy to the fact that the asymptotic limit is reached only for values of λ much larger than was previously expected.

Bibliography

1. H.K. Onnes, *Leiden Comm.* 1206 (1911), *Suppl.* 34 (1913).
2. M.K. Wu, J.R. Ashburn, C.J. Torng, P.H. Hor, R.L. Meng, L. Gao, Z.J. Huang, Y.Q. Wang, and C.W. Chu, *Phys. Rev. Lett.* **58**, 908 (1987).
3. D. Crandles, private communication.
4. D.C. Mattis and J. Bardeen, *Phys. Rev.* **111**, 412 (1958).
5. W. Meissner and R. Ochensfeld, *Naturwiss.* **21**, 787, (1933).
6. S. Hoen, W.N. Creager, L.C. Bourne, M.F. Crommie, T.W. Barbee III, M.L. Cohen, A. Zettl, L. Bernardez, and J. Kinney, *Phys. Rev. B* **39**, 2269 (1989).
7. C.J. Gorter and H. Casimir, *Physica* **1**, 306 (1934).
8. F. London and H. London, *Proc. Roy. Soc. (London)***A149**, 71, (1935).
9. A.B. Pippard, *Proc. Roy. Soc. (London)***A216**, 547, (1953).
10. V.L. Ginzburg and L.D. Landau, *Zh. Eksperim. i. Teor. Fiz.* **20**, 1064 (1950).
11. H. Fröhlich, *Phys. Rev.* **78**, 845 (1950).
12. E. Maxwell, *Phys. Rev.* **78**, 477 (1950).
13. L.N. Cooper, *Phys. Rev.* **104**, 1189 (1956).
14. J. Bardeen, L.N. Cooper, and J.R. Schrieffer, *Phys. Rev.* **108**, 1175 (1957).
15. G.M. Eliashberg, *Zh. Eksperim. i. Teor. Fiz.* **38**, 966 (1960); Soviet Physics JETP **11**, 696 (1960).
16. J.P. Carbotte, *Sci. Prog.*, Oxf.(1987)**71**, 327-350.

17. C.M. Varma, in *Superconductivity in d- and f-Band Metals*, edited by W. Buchel and W. Weber (Kernforschungszentrum, Karhsruhe, 1982) p. 603.

18. W.A. Little, in *Novel Superconductivity*, edited by S.A. Wolf and V.Z. Kresin (Plenum Press, New York, 1987) p. 341.

19. A.J. Millis, S. Sachdev, and C.M. Varma, *Phys. Rev. B* **37**, 4975 (1988).

20. P.W. Anderson, *Science* **235**, 1196 (1987).

21. Y. Kuroda and C.M. Varma, (preprint).

22. for example P.G. Tomlinson and J.P. Carbotte, *Can. J. Phys.* **51**, 922 (1973).

23. W.L. McMillan and J.M. Rowell, *Phys. Rev. Lett.* **14**, 108 (1965).

24. G. Bergmann and D. Rainer, *Z. Physik* **263**, 59 (1974).

25. B. Mitrović and J.P. Carbotte, *Solid State Comm.* **37**, 1009 (1981).

26. for example J. Blezius and J.P. Carbotte, *Phys. Rev. B* **36**, 3622 (1987).

27. P. Morel and P.W. Anderson, *Phys. Rev.* **125**, 1263 (1962).

28. W.L. McMillan, *Phys. Rev.* **167**, 331 (1968).

29. P.B. Allen and R.C. Dynes, *Phys. Rev. B* **12**, 905 (1975).

30. P.B. Allen and B. Mitrović, in *Solid State Physics*, edited by H. Ehrenreich, F. Seitz, and D. Turnbull (Academic, New York, 1982) Vol. 37, p.1 .

31. B. Mitrović, H.G. Zarate, and J.P. Carbotte, *Phys. Rev. B* **29**, 184 (1984).

32. F. Marsiglio and J.P. Carbotte, *Phys. Rev. B* **33**, 6141 (1986).

33. D. Rainer and G. Bergmann, *J. Low Temp. Phys.* **14**, 501 (1974).

34. J. Bardeen and M. Stephen, *Phys. Rev.* **136**, A1485 (1964).

35. G. Grimvall, *The Electron-Phonon Interaction in Metals*, Noth-Holland, New York, 1981.

36. M. Schossmann and E. Schachinger, *Phys. Rev. B* **33**, 6123 (1986).

37. R.J. Birgeneau and G. Shirane in *Physical Properties of High Temperature Superconductors I*, edited by Donald M. Ginsberg (World Scientific, Singapore, !989) p. 151.

38. A. Weidinger, Ch. Niedermayer, A. Golnik, R. Simon, E. Recknagel, J.I. Budnick, B. Chamberland, and C. Baines, *Phys. Rev. Lett.* **62**, 102 (1989).

39. J.H. Brewer *et al.* , *Physica C* **162-164**, 33 (1989).

40. G. Shirani *et al.* , *Phys. Rev. Lett.* **63**, 330 (1989).

41. J.M. Tranquada *et al.* , *Phys. Rev. Lett.* **64**, 800 (1990).

42. F. Marsiglio, E. Schachinger, and J.P. Carbotte, *J. Low Temp. Phys.* **65**, 305 (1986).

43. P.J. Williams and J.P. Carbotte, *Phys. Rev. B* **39**, 2180 (1989).

44. P.J. Williams, M.Sc. Thesis, McMaster University, 1987 (unpublished).

45. R. Akis and J.P. Carbotte, *Physica C* **157**, 395 (1989).

46. J.P. Carbotte, F. Marsiglio, and B. Mitrović, *Phys. Rev. B* **33**, 6135 (1986).

47. C.M. Varma, (preprint).

48. private communication.

49. for example K. Maki, in *Superconductivity*, edited by R.D. Parks (Dekker, New York, 1961) Vol. 1, Ch. 3.

50. A. Junod, A. Bezinge, D. Eckert, T. Graf, and J. Muller, *Physica C* **152**, 495 (1988).

51. M.B. Salamon, S.E. Inderhees, J.P. Rice, B.G. Pazol, D.M. Ginsberg, and N. Goldenfeld, *Phys. Rev. B* **38**, 885 (1988).

52. M. Schossman, J.P. Carbotte, and E. Schachinger, *J. Low Temp. Phys.* **70**, 537 (1988).

53. F. Marsiglio, Ph.D. Thesis, McMaster University, 1987 (unpublished).

54. D. Rainer and F.J. Culetto, *Phys. Rev. B* **19**, 2540 (1979).

55. F. Marsiglio, M.Sc. Thesis, McMaster University, 1984 (unpublished).

56. F. Marsiglio, P.J. Williams, and J.P. Carbotte, *Physica C* **162-164**, 1493 (1989).

57. R.A. Fisher, J.E. Gordon, N.E. Philips, and A.M. Stacy, *Physica C* **153-155**, 1092 (1988).

58. R.A. Fisher, J.E. Gordon, and N.E. Phillips, *Journal of Superconductivity* **1**, 231 (1988).

59. O. Beckman, L. Lundgren, P. Nordblach, L. Sandblum, P. Svenlindh, T. Lundstrom, and S. Rundquist, *Phys. Lett. A* **125**, 424 (1987).

60. A. Bezinge, J.L. Jorda, A. Junod, and J. MUller,

61. L.F. Matheiss and D.R. Hamann, *Solid State Comm.* **63**, 395 (1987).

62. J.W. Loram and K.A. Mizra, *Physica C* **153-155**, 1020 (1983).

63. N.E. Phillips, R.A. Fisher, J.E. Gordon, S. Kim, and A.M. Stacy, (preprint).

64. for example D.M. Ginsberg, S.C. Inderhees, M.B. Salamon, N. Goldenfeld, J.P. Rice, and B.G. Pazol, *Physica C* **153-155**, 1082 (1988).

65. N.E. Phillips, R.A. Fisher, S.E. Lacy, C. Marcenat, J.A. Olsen, W.K. Ham, and A.M. Stacy, in *Novel Superconductivity* edited by S.A. Wolf and V.Z. Kresin (Plenum Press, New York, 1987) p. 739.

66. J. Kirtley, *International Journal of Modern Physics B* 4, 201 (1990).

67. Z. Schlesinger, R.T. Collins, F. Holtzberg, C. Field, G. Koren, and A. Gupta, *Phys. Rev. B* **41**, 11257 (1990).

68. K. Kamarás, S.L. Herr, C.D. Porter, N. Taches, D.B. Tanner, S. Etemad, T. Venhatesan, E. Chase, A. Inam, X.D. Wu, M.S. Hedge, and D. Butler, *Phys. Rev. Lett.* **64**, 84 (1990).

69. J.P. Franck, J. Jung, G. Salamons, W.A. Miner, and M.A-K. Mohamed, *Physica C* **164**, 753 (1989).

70. B. Batlogg, G. Kourouklis, W. Weber, R.J. Cava, A. Jayaraman, A.E. White, K.T. Short, L.W. Rupp, and A.E. Rietman, *Phys. Rev. Lett.* **59**, 912 (1987).

71. H.-C. zur Loye, K.J. Leary, S.W. Keller, T.A. Faltens, W.K. Ham, J.N. Micheals, and A.M. Stacy, *Science* 238, 1558 (1987).

72. M.K. Crawford, M.N. Kunchur, W.E. Farneth, E.M. McCarron, and S.J. Poon, *Phys. Rev. B* **41**, 282 (1990).

73. M. Greeson, M.Sc. Thesis, McMaster University, 1990 (unpublished); E. Schachinger, M. Greeson, and J.P. Carbotte, accepted for publication in *Physical Review B* July (1990).

74. W.A. Little, *Phys. Rev.* **134**, A1416 (1964).

75. V.L. Ginzburg, *Zh. Eksperim. i. Teor. Fiz.* 47, 2318 (1964); V.L. Ginzburg, *Phys. Lett.* 13, 101 (1964).

76. H. Fröhlich, *J. Phys. C* 1, 544 (1968).

77. F. Marsiglio and J.P. Carbotte, *Phys. Rev. B* 36, 3937 (1987).

78. see, for example, *Novel Superconductivity*, edited by S.A. Wolf and V.Z. Kresin (Plenum, New York, 1987).

79. F. Marsiglio, R. Akis, and J.P. Carbotte, *Phys. Rev. B* 36, 5245 (1987).

80. J.M. Daams and J.P. Carbotte, *J. Low Temp. Phys.* 43, 263 (1981).

81. D. Rainer and G. Bergmann, *J. Low Temp. Phys.* 14, 50 (1974).

82. L.N. Bulaevskii, D.V. Dolgov, and M.O. Ptitsyn, *Phys. Rev. B* 38, 11290 (1988).

83. F. Marsiglio, P. Williams, and J.P. Carbotte, *Phys. Rev. B* 39, 9595 (1989).

84. F. Marsiglio, M. Schossmann, E. Schachinger, and J.P. Carbotte, *Phys. Rev. B* 35, 3226 (1987).

85. For finite impurity concentrations, we expect from consideration of the dotted curve in A3.1, which is valid for $\lambda = \infty$, that $h_{c2}(t)$ appears to be a well-behaved function near $t = 0$ for large λ. It is therefore sufficient, to make our point, to compute $h_{c2}(t = 0.1)$, which takes much less computer time, but which should be only slightly smaller than $h_{c2}(t = 0)$.

86. N.E. Phillips, *Phys. Rev.* 114, 676 (1959).

87. Y. Wada, *Phys. Rev.* 135, A1481 (1964).

88. W.L. McMillan and J.M. Rowell, in *Superconductivity*, edited by R.D. Parks (Dekker, New York, 1961) Vol. 1, p. 561.

89. H.K. Leung, J.P. Carbotte, D.W. Taylor, and C.R. Leavens, *J. Low Temp. Phys.* 24, 2534 (1976).

90. F. Marsiglio, J.P. Carbotte, and P.J. Williams, *Phys. Rev. B* **41**, 4484 (1990).

91. P.W. Anderson, *J. Phys. Chem. Solids* **11**, 26 (1959).

92. B.T. Matthias, H. Suhl, and E. Corenzwit, *Phys. Rev. Lett.* **1**, 92 (1958).

93. A.A Abrikosov and L.P. Gorkov, *Zh. Eksperim. i. Teor. Fiz.* **39**, 1781 (1960); Soviet Physics JETP **12**, 1243 (1961).

94. V. Ambegaokar and A. Griffin, *Phys. Rev.* **137**, A1151 (1965).

95. M. Grabowski and L.J. Sham, *Phys. Rev. B* **29**, 6132 (1984).

96. D.B. Kirzhnits, E.G. Maksimov, and D.I. Khomskii, *J. Low Temp. Phys.* **10**, 39 (1973).

97. H. Rietschel and L.J. Sham, *Phys. Rev. B* **28**, 5100 (1983).

98. T. Buche and H. Rietschel, *Phys. Rev. B* **41**, 8691 (1990).

99. J. Hubbard, *Proc. Roy. Soc. (London)* **A276**, 238 (1963); **A277**, 237 (1964); **A281**, 401 (1964).

100. for example, S. Doniach and E.H. Sondheim, in *Green's Functions for Solid State Physicists*, (Benlamin/Cumming, Massachusetts, 1974), Ch. 7.

101. N.F. Berk and J.R. Schrieffer, *Phys. Rev. Lett.* **17**, 433 (1966).

102. S. Doniach and S. Engelsberg, *Phys. Rev. Lett.* **17**, 750 (1966).

103. W.F. Brinkman and S. Engelsberg, *Phys. Rev.* **169**, 417 (1968).

104. for example H.R. Ott *et al.* , *Phys. Rev. Lett.* **52**, 1915 (1984).

105. B. Batlogg *et al.* , *Phys. Rev. Lett.* **55**, 1915 (1985).

106. for example K. Miyake, S. Scmitt-Rink, and C.M. Varma, *Phys. Rev. B* **34**, 6554 (1986).

107. M.R. Norman, *Phys. Rev. B* **37**, 4987 (1988).

108. G. Aeppli, A. Goldman, G. Shirane, E. Bucher, and M.-Ch.Lux-Steiner, *Phys. Rev. Lett.* **58**, 808 (1987).

109. A.B. Migdal, *Zh. Eksperim. i. Teor. Fiz.* **34**, 1438 (1958); Soviet Physics JETP **7**, 762 (1958).

110. D. Bohm and D. Pines, *Phys. Rev.* **109**, 762 (1958).

111. G.R. Stewart, *Rev. Mod. Phys.* **56**, 755 (1984).

112. D.R. Harshman *et al.* , *Phys. Rev. B* **39**, 851 (1989).; S.E. Barret *et al.* , *Phys. Rev. B* **41**, 6283 (1990)..

113. P.A. Lee and N. Read, *Phys. Rev. Lett.* **58**, 2691 (1987).

114. C.T. Rieck, D. Fay, and L. Tewordt, *Phys. Rev. B* **41**, 7289 (1990).